学位申請論文

小原 敬士

DOCTORAL THESIS

# CW and FT Time-Resolved EPR Studies on Spin and Reaction Dynamics of Short-Lived Paramagnetic Species

# ＣＷ及びＦＴ時間分解ＥＰＲによる短寿命常磁性種のスピン及び反応ダイナミクスの研究

Keishi Ohara

Department of Chemistry
Graduate School of Science
Kyoto University

# Contents

# Chapter 1. General Introduction

The spin states of unpaired electrons and nuclei of chemical species play very important roles in chemical reactions, affecting the reaction yield and the selectivity, especially in the existence of an effective external magnetic field.

In the last two decades, the spin and magnetic field effects on chemical reactions have been a subject of great interest and numerous experimental and theoretical investigations have been made.[1-3] The mechanisms of the photoinduced reactions and the interactions and dynamics of radical pairs are of vital importance in such studies. The time-resolved electron paramagnetic resonance (TREPR) technique provides a powerful tool for such investigations, not only because it can detect and identify short-lived intermediate radicals and radical pairs directly, but also because it provide us a method to watch the spin states of electron and nuclei separately in the TREPR spectra. The phenomena of chemically induced dynamic electron polarization (CIDEP) observed in the TREPR spectra often give unique information that is difficult to obtain by other means. Comparison between the CIDEP results and those obtained by other techniques in relation to the magnetic field effects is of considerable interest.

Over the last twenty-five years, the CIDEP phenomena have been investigated extensively by many workers from many different points of view, theoretically and experimentally.[4-6] Several mechanisms producing CIDEP have been proposed so far. Historically, an $ST_0$ mixing radical pair mechanism (RPM)[7-9] was the first to be proposed, then followed by a triplet mechanism (TM)[10,11] and an $ST_{\pm}$ mixing RPM soon after.[12,13] It is rather recent that other mechanisms such as a spin-correlated radical pair (SCRP)[14,15] mechanism and a radical-triplet pair mechanisms (RTPM)[16-18] were suggested. Therefore, analyses of CIDEP spectra can provide detailed information about photochemical reaction mechanisms, interactions in radical pairs, and spin and reaction dynamics of intermediate radicals.

The time-resolved EPR (TREPR) technique is now well-established, it can be used routinely to obtain CIDEP spectra in various media such as solutions, crystals, frozen glasses, micelles, and so on. Most of the CIDEP measurements so far have been carried out in the X-band (9.5GHz, 330mT) microwave (MW) region, because the X-band EPR spectrometer is the most conventional and has a high sensitivity. Technical difficulties in other bands of EPR, that include less sensitivity and a poorer S/N ratio, prevented wide applications of time-resolved measurements in other bands. There have been only a few examples of CIDEP studies at higher or lower MW frequencies.[19-22] However, in order to fully understand the CIDEP phenomena, TREPR experiments at different microwave frequencies are desirable, because CIDEP phenomena strongly depend on the measuring MW frequency and external magnetic field.

High frequency TREPR measurements in the Q-band (35GHz) were reported by Forbes et al.[19,20] They investigated the SCRP in alkyl-chain linked biradical systems comparing the results in the X- and Q-bands, and discussed the merits of multifrequency TREPR measurements. However, at higher frequencies, the TM and $ST_0M$ due to the difference of $g$-factors between a pair of interacting radicals ($\Delta g$) often contribute so effectively that the information about $ST_{\pm}M$ and the weak interacting SCRP might be hidden. Furthermore, in view of the magnetic field effects $ST_{\pm}M$ at low magnetic fields is important, but the high-field limit approximation is already valid in the X-band. Therefore, TREPR measurements at lower MW frequencies may have some advantages in providing new information concerning the CIDEP mechanisms and the magnetic field effects, as indicated by previous reports.[21,22]

Accordingly the author and coworkers have started to study CIDEP phenomena using the time-resolved EPR spectrometers in the S-band (3.0GHz, 100mT) and L-band (1.5GHz, 50mT) MW regions as well as the X-band. This is the first trial of a detailed CIDEP investigation in three different MW frequency regions: X-, S-, and L- bands. In the present thesis, the author report the results of a detailed experimental investigation on

the MW frequency dependence of the CIDEP spectra, paying attention to the TM polarization and the spin correlated radical pairs, descried in chapter 4 and 5, respectively. The comparison between the theory and experimental results confirm the CIDEP mechanisms.

Another theme in this thesis is a quantitative description of the spin and reaction dynamics studied by TREPR. The time evolution of the transient EPR signals is caused by several processes involving CIDEP generation, relaxation, and chemical reactions. Detail studies of the time evolution of EPR signals are important to understand the CIDEP and reaction mechanisms. However, the CW experiments have a limitation in the time and spectral resolution. CW TREPR observes transverse magnetization in a microwave field. The magnetization is treated with the extended Bloch equations. CW TREPR spectra always rise slowly and are broadened in early time regions just after reactions. The time evolution of the signal is different from the actual behavior of the longitudinal magnetization which should be observed to analyze the spin and reaction dynamics. This limitation sometimes prevents a detail study of the CIDEP mechanisms. Detailed analyses require better time and spectral resolution.

Fourier transform EPR ( FT-EPR ) offers superior time-resolution, spectral-resolution, and sensitivity,[6] and therefore, may provide more detailed information about the reaction and spin dynamics of many complicated systems. The recent development of the pulse technique in EPR makes it possible to use an FT-EPR to time-resolved measurements and to study several complicated phenomena more precisely. The time evolution of FT-EPR signals represents the changes in the longitudinal magnetizations and is analyzed more simply.

This thesis presents the results of CW and FT time-resolved EPR investigations on the CIDEP of acetone/triethylamine, the quenching reaction of 2-hydroxypropan-2-yl radical, and the CIDEP of quinoxaline and the related compounds in chapter 6 to 8. A detail

and precise analysis of the time evolution of transient EPR signals provides a clear picture of the spin and reaction dynamics.

Therefore, this thesis represents the following studies about CIDEP development and decay mechanisms.

(1) Magnetic Field Dependence of the Triplet Mechanism CIDEP (Chapter 4).

(2) Magnetic Field Dependence of the Spin-Correlated Radical Pair CIDEP (Chapter 5).

(3) FT-EPR Study of 2-Hydroxypropan-2-yl Radical Produced by the Reaction of Acetone with Triethylamine (Chapter 6).

(4) CW and FT-EPR Investigation of the Quenching Reaction of the 2-Hydroxypropan-2-yl Radical (Chapter 7).

(5) An Analysis of the CIDEP Mechanisms on the Hydrogen Abstraction Reactions of Excited Quinoxaline and Related Compounds (Chapter 8).

# Chapter 2. CW and FT Time-Resolved EPR Experiments

In the present thesis, CW time-resolved EPR spectrometers in three deferent microwave frequency regions and an X-band FT-EPR spectrometer were used.

## 2-1 CW time resolved EPR spectrometers and the data acquisition system

The X-band time resolved EPR measurements were carried out with a modified JEOL FE-3X EPR spectrometer.[23] A conventional cylindrical cavity ( $TE_{011}$ ) whose resonance frequency was around 9.2 GHz was used. The center of the external magnetic field is always around 330mT ( $g = 2.003$ ).

The L-band spectrometer is based on a modified JEOL ES-LB2SX microwave unit. Improvements were made by using components of better qualities for a circulator, an attenuator and an oscillator to achieve better S/N in time resolved experiments.[22] A loop-gap resonator (15mm diameter and 30mm length ) with three slits for light irradiation whose resonance frequency was around 1.5 GHz ( the external magnetic field is around 53mT ) was used. For the S-band measurements modifications were made to the L-band microwave unit.[24] They include replacements of the oscillator, mixer and resonator to appropriate ones for the S-band. The loop-gap resonator for the S-band is of the same size as that of L-band and has four gaps and a window for light irradiation, whose resonance frequency is around 3.0 GHz ( the external magnetic field is around 107mT ). The sensitivities of the S- and L-band spectrometers are much lower than those of the X-band, which is mainly due to the difference in Q-factors and filling factors; the Q-factors of the S- and L-band resonators are less than 500 (unloaded) compared with about 10000 of the X-band, and the filling factors are also small for the S- and L-bands. In the present experiments, the EPR microwave power was about 1.0mW in the X- and L-band and 5.0mW in the S-band, respectively. The dc EPR signals were detected without field modulation and amplified with a wide band preamplifier. For recording

CIDEP spectra, the transient EPR signals were collected by a boxcar integrator ( PAR model 160 or Stanford Research System SR-250 ) whose gate was open for 0.2 μs with several delay times after the laser excitation. The output was digitized by an A/D converter and stored in a personal computer as spectral data. A digital oscilloscope ( Tektronix TDS 520 or 2430A ) was used for recording the time evolution of a transient EPR signal. In recording the time developments of transient EPR signals in X-band, measurements were made at resonance, keeping the microwave power sufficiently low ( 0.2mW or less ) to avoid the effect of nutation. The time evolution curves were accumulated for 64 to 1024 times, and the data were stored and processed in a personal computer.

The sample solutions were deoxygenated by bubbling nitrogen gas before and/or during the experiments. Quartz tubes ( 5mm o.d. for the L- and S-band and 2mm o.d. for the X-band) were used for the experiments on the ZnTPP systems. In the experiments on other systems, the sample solutions were flowed in a quartz flat cell (optical path 0.3mm for X-band experiments of the micellar systems, and 1mm for other experiments ) or a quartz tube ( 5mm o.d. ). The sample temperature was controlled by flowing cold nitrogen gas around the sample cell.

A Nd-YAG laser ( Quanta-Ray DCR-11 or GCR-170, SHG 532nm, 5 or 10 Hz ) was used for photoexcitation of the porphirine systems. A XeCl Excimer laser ( Lumonics Hyper 400, 308nm, 7.5Hz ) was used for the photoexcitation of other systems.

2-2 FT-EPR experiments

In a FT-EPR measurement, there are two ways to obtain time-resolved FT spectra: the two pulse free induction decay (FID) detection and the three pulse stimulated echo detection. The FID detection method is simpler and can achieve higher sensitivities in most systems. However, the dead-time of observation is unavoidable just after the high

power of microwave pulse, then the early stage of FID is unobservable. This leads to an uncertainty in the relative intensities of radicals which have different $T_2$, because FID is damping off with a rate of $1/T_2$. Moreover, if $T_2$ is very short, the radical cannot be observed as in the case of the porphyrin cation. On the other hand, the echo detection method has no dead time and is not influenced by $T_2$, but it requires a long lifetime of a radical compared with the echo detection time. These two methods are usually complementary to each other. In the present thesis, the FID detection method was used.

FT-EPR measurements were carried out with a lab-built spectrometer of the University of Massachusetts at Boston.[6] An excimer laser ( Lambda Phisik EMG 103 MSC ) with XeCl operation ( 308nm, ~30mJ/pulse, pulse width ~15ns, 25Hz ) was used for sample excitation. A high power microwave amplifier ( 1 kW traveling wave tube amplifier ) was used to obtain enough large power of microwave field in a low Q cavity. The sample soutions were circulated through a flow cell with an effective volume of 0.06 ml. Oxygen was removed from solutions by bubbling with argon gas. The FID was measured with a quadrature IF mixer detector and recorded with a sampling rate of 5 ns/point and processed as described in literature.[6,25] A well-known CYCLOPS phase cycling routine was applied to correct for amplitude and phase error introduced by the mixer. The dead-time of observation was about 100ns. In the present study, since the large hyperfine (hf) coupling with six equivalent methyl protons in 2-hydroxypropan-2-yl radical produces a spectrum that far exceeds the spectrometer bandwidth, the time profiles of the $M_I$ = -1, 0 and +1 hf lines were obtained with three separate measurements with the magnetic field set so that the peak of interest was on resonance. The intensities of the signals were obtained by fourier transformation of the FIDs followed by integration of the power spectra. With the magnetic field set to monitor the $M_I$ =0 hf component, the integral of the power spectrum contained contributions from a "dark" signal attributed to paramagnetic centers in the quartz dewar as well as from short lived radicals produced by

hydrogen abstraction from triethylamine. The integrated signal intensities were corrected for these contributions.

The time resolution of the measurements was estimated by determining the rise time of the signal of the 2-hydroxypropan-2-yl radical produced by the hydrogen abstraction reaction of triplet pyrazine with 2-propanol. Here the reaction rate is known to be very fast ( $k_r \sim 10^9\ s^{-1}$ ) [26] and the TM makes the main signal contribution.[23,27] The intrinsic rise time of the signal is expected to be <10 ns. The measured rise time of the EPR signal was ~30ns. It is assumed that this is the time-resolution of the present experiments. The response time is mainly determined by the combined effects of the widths of the microwave (~15ns) and the laser pulses and the laser pulse jitter.

# Chapter 3. CIDEP Generation and Relaxation Mechanisms

In this chapter, the main CIDEP generation and relaxation mechanisms are presented. The detail explanations are available in literature.

## 3-1 The triplet mechanism ( TM )

The spin polarization of the triplet mechanism is often observed on the transient radicals when the rapid reaction occurs from the excited triplet state of a molecule. An anisotropic intersytem crossing (ISC) process from the singlet excited state to the triplet state produces the difference of populations among three spin sublevels of the triplet state in molecular frame. The tumbling or rotation of a triplet molecules in solution leads to provide the spin polarization among the spin sublevels in the laboratory frame. When the radical producing reaction occurs in a time fast enough compared with the spin-lattice relaxation of the triplet state, the TM polarization is conserved in produced radicals. Therefore, the TM polarization is observed as a total emission or enhanced absorption keeping relative line intensities determined by the degeneracies of the nuclear states. A general method to calculate the magnitude of the TM polarization was presented by Atkins and Evans,[10] and Pederesen and Freed,[11] independently using the rotating triplet model. However, there are few studies on quantitative comparison between theory and experimental results, especially in multifrequency regions. The magnetic field dependence of the TM polarization is discussed in detail in Chapter 4.

## 3-2 The radical pair mechanism ( RPM )

The spin polarization of RPM is most frequently observed in the time-resolved EPR experiments. A pair of radicals produced by photochemical or radiation-induced reactions make an interaction with each other. The ST mixing process cause the hyperfine dependent spin-polarization.

(i) $ST_0$ mixing RPM ( $ST_0M$ )

The magnitude of the $ST_0M$ polarization is explained well by the following equation,[4-6)]

$$P^a_{ST_0} \propto \sum_b \mathrm{sign}(Q_{ab}J)\left|Q_{ab}\tau_0\right|^{1/2} \qquad (3\text{-}1)$$

$$Q_{ab} = 1/2\left((g_a - g_b)\mu_B B + \sum_i A^a_i m^a_i + \sum_j A^b_j m^b_j\right) \qquad (3\text{-}2)$$

Here, $g$ is the g-factor, $A$ is the hyperfine coupling constant (hfc) of each radical, $B$ is the strength of the external magnetic field, $J$ is the exchange interaction, and $\tau_0$ is the correlation time of the $ST_0M$ interaction. The subscripts a and b denote the radicals of interest. i and j denote the nuclear spin state of radical a and b, respectively, $m_i$ being the magnetic quantum number of state i.

In these equations, the hyperfine interaction part of $ST_0M$ is not affected by the MW frequency $\omega_0$ (or the external magnetic field $B$ ). Therefore, we can use it as the basis for the comparison of the magnitude of other mechanisms. (see Chapter4)

(ii) $ST_\pm$ mixing RPM ( $ST_\pm M$ )

The ST-M polarization takes place because of the simultaneous flips of electron and nuclear spins and the magnitude is determined by the following equation,[4-6,12,13)]

$$\begin{aligned} P_{ST_\pm} &\propto \left|\langle S, I, m-1 | AS_+ I_- | T_-, I, m\rangle\right|^2 \\ &= \frac{A^2}{8}\left[I(I+1) - m(m-1)\right] \end{aligned} \qquad (3\text{-}3)$$

where $I$ and $m$ are the quantum numbers for the total nuclear spin angular momentum and its z component, respectively. ST-M produces a net emission (E). Therefore, it is often difficult to separate the contributions of the TM and ST-M clearly. The magnitude of the ST-M polarization is proportional to $A^2/B$, and it is considered to become important at a low magnetic field and in a highly viscous solution.

(iii) F-pair RPM

The spin polarization of F-pair RPM is often observed as E/A distortion in a comparatively later time region, more than a few microseconds after the photoexcitation. When free radicals in solution make a collision each other, the $ST_0$ mixing interaction causes the spin polarization. The relative line intensities are represented by the same scheme as that for a triplet geminate-pair RPM. The dynamics and time evolution of signals are discussed in Chapter 7.

### 3-3 The spin-correlated radical pair (SCRP) CIDEP

The CIDEP spectrum of a spin-correlated radical pair (SCRP) was first observed in an SDS micellar solution ten years ago. The SCRP spectra are known to be observed in the cases of chain-linked biradicals, radical pairs in viscous media and in micellar media. The specific E/A phase pattern of the SCRP CIDEP is explained by the energy diagram of mixed states of three triplet sublevels and a singlet level.[6,14,15] The characteristic E/A phase lines ( when the SCRP is produced from a triplet precursor and $J < 0$ ) are observed for the transitions between these four levels. A lot of studies on the SCRP has been progressed in many points of view, but there are few studies on the magnetic field dependence of the SCRP CIDEP. This is an important subject, and will be discussed in Chapter 5.

### 3-4 The radical-triplet pair mechanism ( RTPM )

The spin polarization due to RTPM is produced through the interaction between doublet radicals and triplet state molecules. The generation mechanism of the RTPM polarization is explained on the basis of the doublet-quartet mixing in a radical-triplet pair. Recent studies suggested that the RTPM includes two mechanisms, one generating a net polarization and the other producing a hyperfine dependent polarization, which resemble the $ST_-$ and $ST_0$ mixing in the RPM, respectively.[17,18] Detailed studies of the RTPM may provide useful information not only about the interactions in radical-triplet pairs but also

the quenching processes of excited states by radicals which have not been studied in detail by other methods. Most of the published reports on RTPM, however, have been concerned with the spin polarization generated by the interaction between stable radicals such as nitroxides and excited triplet state molecules. The importance of the RTPM polarization in the CIDEP spectra of reaction intermediate radicals has not been shown clearly except the case of benzil and 1-naphthol.[16,18] The RTPM polarization dynamics is discussed in Chapter 8.

The magnetic field effect on the RTPM polarization is a quite important and interesting subject. It is considered to resemble that of ST-M and $ST_0M$.

## 3-5. Relaxation Mechanisms

The spin polarization of a radical decays to the thermal equilibrium with the spin-lattice relaxation time. The relaxation is considered to be caused by several processes, and an important subject in magnetic resonance. In EPR experiments, the relaxation of radicals or triplet molecules in non-viscous and isotropic solution is usually considered to be caused mainly by the rotational motion. The fluctuation of anisotropic magnetic energy such as g-factor, hyperfine coupling (hfc), and zero field splitting (zfs) cause the relaxation. The spin-lattice relaxation time ( $T_1$) is in general given by;[4-6,20]

$$\frac{1}{T_1} = \frac{B_{loc}^2 \tau_c}{2\left(1+\omega_0^2 \tau_c^2\right)} \qquad (3\text{-}4)$$

Here, $B_{loc}$ is the value of the local magnetic field including the relaxation transition, and $\tau_c$ is the correlation time of the effective fluctuation. The spin-spin relaxation time ( $T_2$) is always less than $T_1$. The spin-lattice relaxation time of triplet state ( ${}^3T_1$ ) is discussed more detail in Chapter 4.

# Chapter 4. Magnetic Field Dependence of the Triplet Mechanism CIDEP

## 4-1. Introduction

In this chapter, the author report the results of a detailed experimental investigation on the MW frequency dependence of the CIDEP spectra, paying attention to the TM polarization. The TM is one of the most important and basic CIDEP mechanisms and has been treated theoretically in early works [10,11] and discussed in many experimental works involving photochemical reactions. Nevertheless, it appears that detailed comparisons between the theoretical predictions and the experimental results have been scarce. A precise understanding of the TM is also needed before we study the $ST_{\pm}M$ and the SCRP at lower frequencies.

The TM contribution in a CIDEP spectrum is predicted to be strongly affected by the MW frequency as well as several parameters of the precursor triplet molecule such as the rotational correlation time ($\tau_R$), the zero field splittings ($D$, $E$ ), and the quenching reaction rate ($k_T$). [10,11] Then it may be expected that the MW frequency dependence of the TM provides a good check of the theory. To our knowledge, this is the first report of a detailed CIDEP investigation in three different MW frequency regions, X-, S-, and L-bands.

The experimental systems studied here are well-known and simple reaction systems which have large signal intensities and large TM contributions in the X-band spectra. They are zinc tetraphenylporphyrin (ZnTPP) and p-benzoquinone (p-BQ) in alcohols as an example of a photoinduced electron transfer reaction, and pyrazine / 2-propanol and maleic anhydride (MA) / 2-propanol systems as typical examples of hydrogen abstraction reactions from alcoholic solvents. The CIDEP results on these systems in the X-band [23,27-31] suggest that the triplet precursors provide large initial polarizations and that their reactions are rapid enough to produce large TM.

4-2. Experimental

ZnTPP, pyrazine, and MA were commercially available special grade reagents (Wako Pure Chemical Industries) used as received. Special grade solvents (Nakalai tesque) were used without further purification. p-BQ was purified by recrystallization from ethanol.

4-3. Spin Polarization of the TM

The TM occurs when a triplet precursor is scavenged by a fast chemical reaction before relaxing to the thermal equilibrium in the three spin sublevels. The magnitude of the initial spin polarization produced by the TM was estimated theoretically in the early works of Atkins and Evans,[10] Pedersen and Freed.[11] When a fast rotating triplet molecule is quenched by a fast reaction and produces a pair of radicals in a high magnetic field, the magnetization produced by TM is given by the following equations,[10]

$$P_{TM}^{0} = \left(\frac{k_T {}^3T_1}{1+k_T {}^3T_1}\right)\frac{4}{15}\left(D\hat{K}+3E\hat{I}\right)\left\{\frac{\omega_0}{\omega_0^2+\tau_R^{-2}}+\frac{4\omega_0}{4\omega_0^2+\tau_R^{-2}}\right\} \qquad (4\text{-}1)$$

$$\frac{1}{{}^3T_1} = \frac{2}{15}\left(D^2+3E^2\right)\left\{\frac{\tau_R^{-1}}{\omega_0^2+\tau_R^{-2}}+\frac{4\tau_R^{-1}}{4\omega_0^2+\tau_R^{-2}}\right\} \qquad (4\text{-}2)$$

$$\hat{K} = \tfrac{1}{2}\left(w_x+w_y\right)-w_z,\ \hat{I} = \tfrac{1}{2}\left(w_y-w_x\right),\ w_i = k_i/k_{total}$$

Here, $\omega_0$ is the microwave angular frequency, $\tau_R$ is the rotational correlation time which is assumed to be isotropic, $D$ and $E$ are the zero field splitting (zfs) constants of the triplet state, $k_T$ is the rate of the quenching reaction, ${}^3T_1$ is the spin-lattice relaxation time of the precursor triplet state, and $k_i$ is the intersystem crossing rate to triplet sublevel i, $w_i$ being its relative populating rate. These equations clearly indicate that the magnitude of the spin polarization due to the TM depends on the several parameters of the triplet molecule, i.e. the zfs constants ($D$ and $E$ ), $\tau_R$ , and $k_T$. As is well-known, ${}^3T_1$ has a minimum value around $\omega_0\tau_R \approx 1$. Then, when $\omega_0\tau_R << 1$, the system is called to be in the fast motion region, and when $\omega_0\tau_R >> 1$ it is called to be in the slow motion region. The TM should

show different MW frequency (or magnetic field) dependence in each region, but the distinction between the fast and slow motion regions is not so clear, because the condition $\omega_0\tau_R \approx 1$ is satisfied with different $\tau_R$ for each frequency. When $k_T^3 T_1 \ll 1$, eq.4-1 is simplified to the following approximate equations in two limiting cases:

(a) fast motion limit ( $\omega_0\tau_R \ll 1$ )

$$P_{TM}^0 = \frac{k_T \omega_0 \tau_R \left(D\hat{K} + 3E\hat{I}\right)}{\left(D^2 + 3E^2\right) + \left(3k_T / 2\tau_R\right)} \qquad (4\text{-}3)$$

In this limit, the magnitude of the TM is simply proportional to the MW frequency, but the absolute magnitude of $P_{TM}$ is considered to be small compared with the polarization in the thermal equilibrium. Then the spin polarization would not be observed under the normal CIDEP experimental conditions.

(b) slow motion limit ( $\omega_0\tau_R \gg 1$ )

$$P_{TM}^0 = \frac{k_T \omega_0 \tau_R \left(D\hat{K} + 3E\hat{I}\right)}{\left(D^2 + 3E^2\right) + \left(15k_T \tau_R \omega_0^2 / 4\right)} \qquad (4\text{-}4)$$

In this limit, the magnitude of the TM is proportional to $\omega_0/(1+\alpha\omega_0^2)$. Then the polarization may decrease or increase with the increase of the MW frequency (magnetic field) depending on the various parameters involved.

In this work we compare the TM polarization with respect to the $ST_0M$ polarization. The magnitude of the $ST_0M$ polarization is explained well by the following equation,[4-6)]

$$P_{ST_0}^a \propto \sum_b \mathrm{sign}(Q_{ab} J) \left| Q_{ab} \tau_0 \right|^{1/2} \qquad (4\text{-}5)$$

$$Q_{ab} = 1/2 \left( \left(g_a - g_b\right)\mu_B B + \sum_i A_i^a m_i^a + \sum_j A_j^b m_j^b \right) \qquad (4\text{-}6)$$

Here, $g$ is the g-factor, $A$ is the hyperfine coupling constant (hfc) of each radical, $B$ is the strength of the external magnetic field, $J$ is the exchange interaction, and $t_0$ is the correlation time of the $ST_0M$ interaction. The subscripts a and b denote the radicals of

interest. i and j denote the nuclear spin state of radical a and b, respectively, $m_i$ being the magnetic quantum number of state i.

In these equations, the hyperfine interaction part of $ST_0M$ is not affected by the MW frequency $\omega_0$ (or the external magnetic field $B$ ). Therefore, we can use it as the basis for the comparison of the magnitude of the TM. When the contributions of the $\Delta g = g_a - g_b$ term, ST_M and the SCRP are small, $ST_0M$ produces a simple anti-symmetric phase pattern of the polarization, which can be easily separated out from the symmetrical net polarization of the TM. However, the contribution due to ST_M has to be considered in the present work.

The ST_M polarization takes place because of the simultaneous flips of electron and nuclear spins and the magnitude is determined by the following equation,[12,13]

$$\begin{aligned} P_{ST_\pm} &\propto \left|\langle S,I,m-1|AS_+I_-|T_-,I,m\rangle\right|^2 \\ &= \frac{A^2}{8}\left[I(I+1)-m(m-1)\right] \end{aligned} \qquad (4\text{-}7)$$

where $I$ and $m$ are the quantum numbers for the total nuclear spin angular momentum and its z component, respectively. ST_M produces a net emission (E). Therefore, it is often difficult to separate the contributions of the TM and ST_M clearly. The magnitude of the ST_M polarization is proportional to $A^2/B$, and it is considered to become important at a low magnetic field and in a highly viscous solution. Neglect of this contribution is probably a good approximation in the ZnTPP/p-BQ system because of a small hfc, but it may make a significant contribution in the pyrazine/2-propanol and MA/2-propanol systems, especially at low temperatures.

## 4-3. Results and Discussion

In the following we discuss the MW frequency (magnetic field) dependence of the TM in three different systems. Comparison of the absolute magnitudes of the spin polarizations in different MW frequency regions is not possible, because it is difficult to make the required experimental conditions the same at different frequencies. Therefore,

we compare the relative magnitude of the TM polarizations with respect to those due to $ST_0M$ at different MW frequencies.

(1) ZnTPP and p-BQ in alcohols

Figure 4-1 shows the CIDEP spectra of the system of ZnTPP (0.80mM) and p-BQ (0.010M) in ethanol observed in the X-, S-, and L-bands at several temperatures. The photoinduced electron transfer from the triplet state of ZnTPP to p-BQ produces the ZnTPP cation radical and the p-BQ anion radical.[28-30)]

$$^3\text{ZnTPP}^* + \text{BQ} \xrightarrow{\text{ET}} \text{ZnTPP}^{+\cdot} + \text{BQ}^{-\cdot}$$

The main CIDEP mechanisms are considered to be the TM and $ST_0M$ due to hyperfine interaction and $\Delta g$.[30)] Five sharp hf lines with four equivalent protons ( $a_H$ = 0.236mT ) are assigned to the p-BQ anion and one broad signal is assigned to the ZnTPP cation. The center positions of the spectra of the two radicals are clearly different, especially in the X-band, because of the $\Delta g$ between the ZnTPP cation and the p-BQ anion radicals. The p-BQ anion spectrum in the X-band is an overall absorption with an E/A ( emission on the low field side and absorption on the high field side) distortion at higher temperatures, but it changes to E/A* (* indicates a net excess polarization ) at lower temperatures. The broad spectrum due to the ZnTPP cation shows an absorptive signal gaining more intensity at lower temperatures. This spectral change with temperature is caused by the changes in the reaction rate and the stability of the radical pair, which usually make $ST_0M$ more effective than the TM at lower temperatures. As seen from Figure 4-1 the spectra in the S- and L-bands are different from those in the X-band at low temperatures. The spectra are net absorptive at all temperatures in the S- and L-bands, indicating that the relative contribution of the TM is enhanced at lower frequencies compared with the X-band. However, the difference between the S- and L-band spectra is comparatively small, and it is difficult to see the difference without a careful analysis.

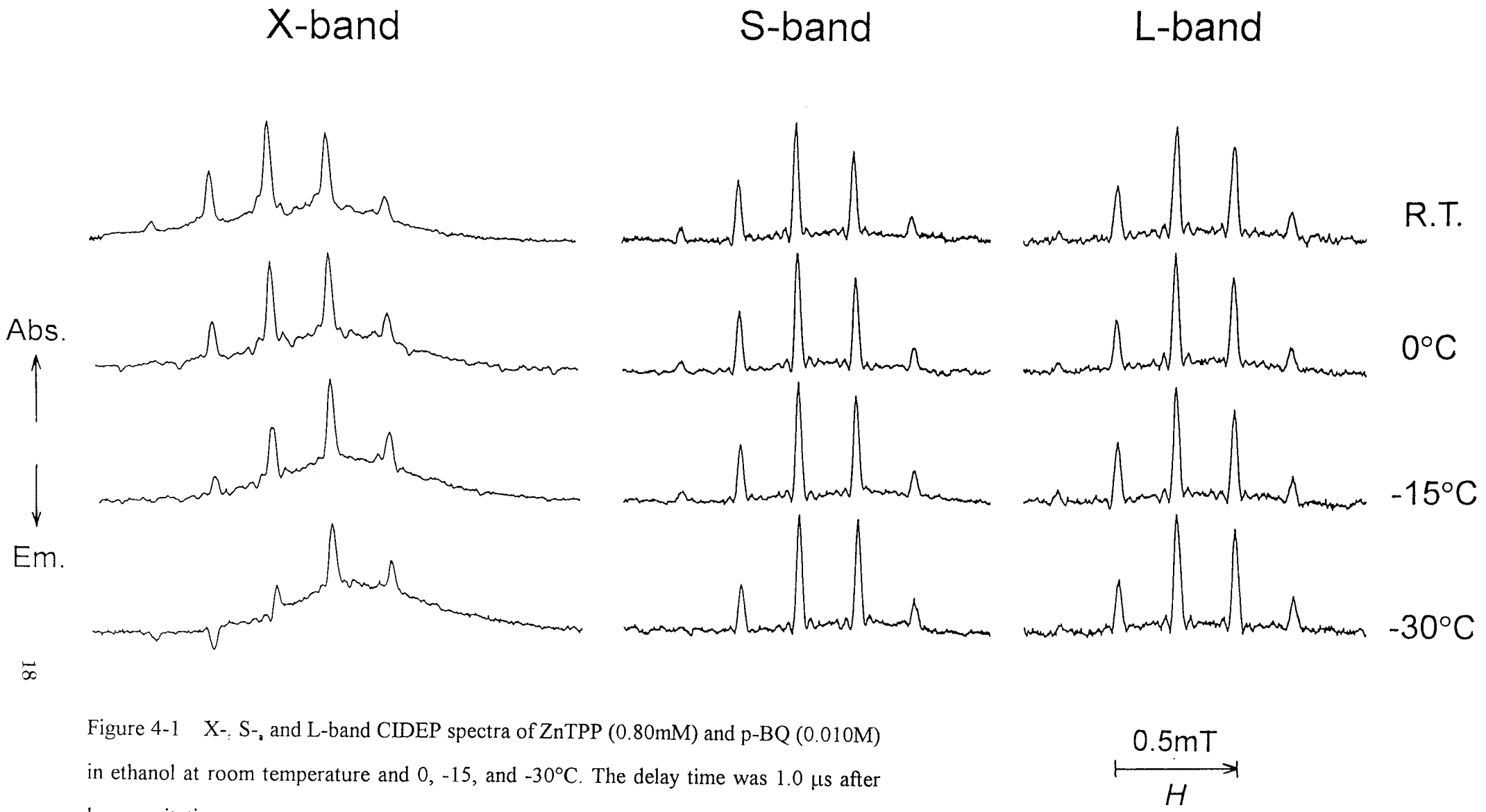


Figure 4-1 X-, S-, and L-band CIDEP spectra of ZnTPP (0.80mM) and p-BQ (0.010M) in ethanol at room temperature and 0, -15, and -30°C. The delay time was 1.0 μs after laser excitation.

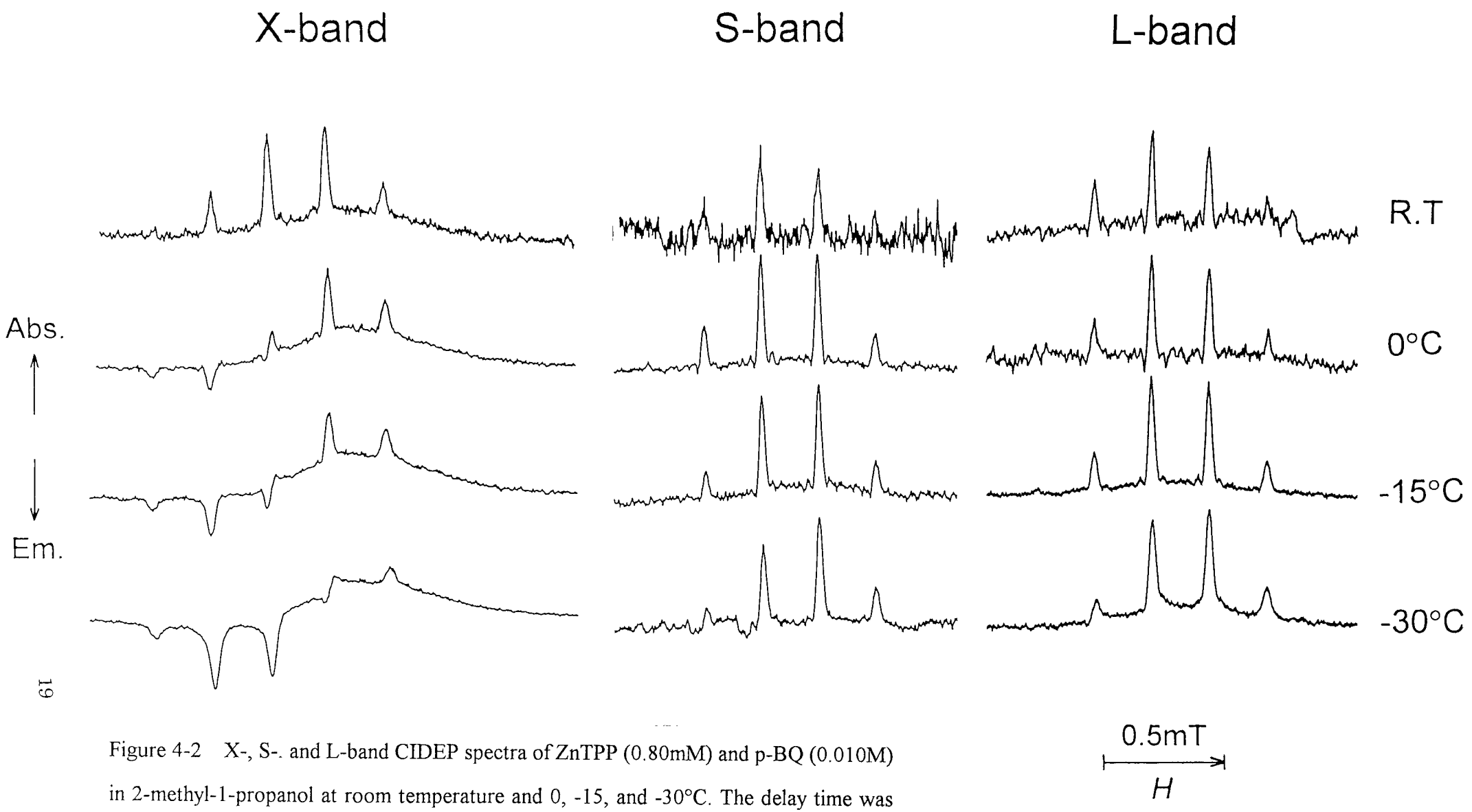


Figure 4-2 X-, S-. and L-band CIDEP spectra of ZnTPP (0.80mM) and p-BQ (0.010M) in 2-methyl-1-propanol at room temperature and 0, -15, and -30°C. The delay time was 1.0 μs after laser excitation.

Figure 4-2 shows the CIDEP spectra of the system of ZnTPP and p-BQ in 2-methyl-1-propanol observed in the X-, S-, and L-band regions at different temperatures. Though the overall feature is similar to that in ethanol, the MW frequency dependence of the TM contribution is simpler, i.e., the TM contribution increases with a decrease of the MW frequency. The results suggest that the system would be in the slow-motion region ( $\omega_0\tau_R >> 1$ ). The SCRP signals are also observed within 1.0 μs at lower temperatures at all of the three MW frequencies, but they will be discussed in more detail in another report.

In order to see the MW frequency dependence more closely, we have made a detailed analysis of the TM contribution in the spectra obtained in ethanol and 2-methyl-1-propanol at different temperatures using spectral simulation. Since $\Delta g$ between the ZnTPP cation ( $g$ = 2.0025) and the p-BQ anion ( $g$ = 2.0040) radicals is rather large, total magnitude of the $ST_0M$ polarization is strongly dependent on the MW frequency. Therefore, the relative contribution of the TM must be compared on the basis of the normalized magnitude of the $ST_0M$ polarization corrected for the $\Delta g$ difference. The correction factor is provided by dividing the total magnitude of the $ST_0M$ polarization at each MW frequency by the value obtained from the only hyperfine interaction part. The obtained relative TM contributions ($P_{TM}^{rel}$) at different MW frequencies are given in Table 4-1. Here, it should be noticed that $P_{TM}^{rel}$ values are independent of the *absolute magnitude* of $ST_0M$. Important results are summarized as follows.

(i) In ethanol the TM contribution increases on going from the X-band to the S-band at all temperatures. At lower temperatures it increases on going from the S- to the L-band, but an opposite trend is found at temperatures higher than 0°C.

(ii) In 2-methyl-1-propanol the TM contribution increases with a decrease of the MW frequency at temperatures lower than 0°C. The increase is larger at lower temperatures.

We now examine whether we can explain these results on the basis of the

Atkins-Evans theory. In Figure 4-3 we show the calculated values of ${}^3T_1$ of the triplet ZnTPP and $P_{TM}$ versus rotational correlation time at different MW frequencies. In these calculations, the zfs's of the triplet ZnTPP are taken to be $D$ = 0.8814GHz and $E$ = 0.2938GHz.[32] These values are rather small as the zfs of the excited triplet states of organic molecules and consequently ${}^3T_1$, which are reported to be about 28ns in ethanol [6] and 81ns in 2-butanol [33] in the X-band at room temperature, become relatively long,. The calculated values obtained using the rotational correlation times listed in Table 4-1 are close to these values. Because of the relatively large size of the ZnTPP molecule, $\tau_R$ is also very long, being on the order of $10^{-10}$~$10^{-9}$ s in ethanol and $10^{-9}$~$10^{-8}$ s in 2-methyl-1-propanol, respectively. Then the system is in the slow rotational motion region at all three MW frequencies, except in ethanol at higher temperature in the L-band. The electron transfer reaction rate ($k_T$) is estimated to be ~5x$10^7$ $s^{-1}$ for ethanol at room temperature from the reported rate constant [6] and the concentration of p-BQ (0.01M), though this value is considered to have a considerable uncertainty, because the rate constant has been reported to be concentration dependent.

In Figure 4-3 values of $P_{TM}$ calculated for (b) $k_T$ = 5x$10^7$ $s^{-1}$ and (c) 1x$10^8$ $s^{-1}$ are shown as functions of the rotational correlation time. The calculation shows that $P_{TM}$ increases with a decrease of the MW frequency for large $\tau_R$. For example, the $P_{TM}$ versus $\tau_R$ curves given in Figure 4-3b show that $P_{TM}$ increases with a decrease of the MW frequency for $\tau_R \geq$ 1x$10^{-9}$ s. It also predicts that the $P_{TM}$ versus $\tau_R$ curves for the L- and S-bands cross each other at $\tau_R \approx$ 1x$10^{-9}$ s. It is further predicted that at the L- and S-bands $P_{TM}$ increases with an increase of $\tau_R$ provided that the reaction rate is kept the same. These predictions seem to be qualitatively in good agreement with the observation. Quantitatively, the results in ethanol are somewhat different. The TM contribution decreases on going from the S-band to the L-band at temperatures higher than 0°C in ethanol where $\tau_R \leq$ 2.5x$10^{-10}$ s. Figure 4-3b predicts such a trend at $\tau_R$ = 5x$10^{-10}$ ~ 1x$10^{-9}$ s, but this corresponds to a much lower temperature region. However, the TM

Table 1. The MW frequency dependence of the relative TM polarization in the system of ZnTPP and p-BQ in ethanol and 2-methyl-1-propanol $P_{TM}$ / $P_{ST0M}$ is the relative amount of TM and $ST_0M$ RPM contributions in the experimental spectra, obtained from the spectral simulation $P_{TM}^{rel}$ is the value obtained correcting for the $\Delta g$ contribution. $\tau_R$ is rotational correlation time of the triplet molecure calculated from the molecular volume and the solvent viscosity $\nu$ represent the MW frequency.

| Temp. | Room temperature | | | 0°C | | | -15°C | | | -30°C | | |
|---|---|---|---|---|---|---|---|---|---|---|---|---|
| | X-Band | S-Band | L-Band | X-Band | S-Band | L-Band | X-Band | S-Band | L-Band | X-Band | S-Band | L-Band |
| | | | | | | ethanol | | | | | | |
| $\nu$ / GHz | 9.271 | 2.992 | 1.474 | 9.270 | 2.974 | 1.470 | 9.270 | 2.971 | 1.458 | 9.271 | 2.972 | 1.454 |
| $P_{TM}/P_{ST0M}$ | 81 / 19 | 90 / 10 | 85 / 15 | 71 / 29 | 86 / 14 | 84 / 16 | 67 / 33 | 81 / 19 | 86 / 14 | 56 / 44 | 77 / 23 | 81 / 19 |
| $P_{TM}^{rel}$ | 1 | 1.69 | 1.00 | 1 | 2.01 | 1.61 | 1 | 1.68 | 2.27 | 1 | 2.10 | 2.51 |
| $\tau_R$ / s | | $1.5 \times 10^{-10}$ | | | $2.5 \times 10^{-10}$ | | | $3.2 \times 10^{-10}$ | | | $5.6 \times 10^{-10}$ | |
| | | | | | | 2-methyl-1-propanol | | | | | | |
| $\nu$ / GHz | 9.270 | 2.987 | 1.510 | 9.270 | 2.980 | 1.484 | 9.271 | 2.973 | 1.470 | 9.271 | 2.970 | 1.454 |
| $P_{TM}/P_{ST0M}$ | 76 / 24 | 87 / 13 | 87 / 13 | 55 / 45 | 75 / 25 | 81 / 19 | 46 / 54 | 71 / 29 | 77 / 23 | 15 / 85 | 64 / 36 | 70 / 30 |
| $P_{TM}^{rel}$ | 1 | 1.64 | 1.54 | 1 | 2.02 | 2.61 | 1 | 2.30 | 3.03 | 1 | 8.05 | 9.90 |
| $\tau_R$ / s | | $5.1 \times 10^{-10}$ | | | $1.2 \times 10^{-9}$ | | | $2.4 \times 10^{-9}$ | | | $5.5 \times 10^{-9}$ | |

Table 2. The MW frequency dependence of the relative TM polarization in the pyrazine / 2-propanol system. Notations are the same as in table1.

| Temperature | | -30°C | | | -60°C | |
|---|---|---|---|---|---|---|
| | X-Band | S-Band | L-Band | X-Band | S-Band | L-Band |
| $\nu$ / GHz | 9.262 | 2.959 | 1.405 | 9.263 | 2.978 | 1.365 |
| $\omega_{SL}$ / $\omega_X$ | 1 | 0.320 | 0.152 | 1 | 0.322 | 0.147 |
| $P_{TM}^{rel}$ | 1 | 0.39 | 0.17 | 1 | 0.37 | 0.11 |
| $\tau_R$ / s | | $4.6 \times 10^{-10}$ | | | | |

Table 3. The MW frequency dependence of the relative TM polarization in the MA / 2-propanol system. Notations are the same as in table 1

| Temp. | 0°C | | | -10°C | | | -20°C | | |
|---|---|---|---|---|---|---|---|---|---|
| | X-Band | S-Band | L-Band | X-Band | S-Band | L-Band | X-Band | S-Band | L-Band |
| $\nu$ / GHz | 9.238 | 2.976 | 1.485 | 9.238 | 2.973 | 1.482 | 9.239 | 2.959 | 1.476 |
| $\omega_{SL}$ / $\omega_X$ | 1 | 0.322 | 0.161 | 1 | 0.322 | 0.160 | 1 | 0.320 | 0.160 |
| $P_{TM}^{rel}$ | 1 | 0.42 | 0.25 | 1 | 0.40 | 0.29 | 1 | 0.50 | 0.32 |
| $\tau_R$ / s | | $9.0 \times 10^{-11}$ | | | $1.5 \times 10^{-10}$ | | | $2.1 \times 10^{-10}$ | |

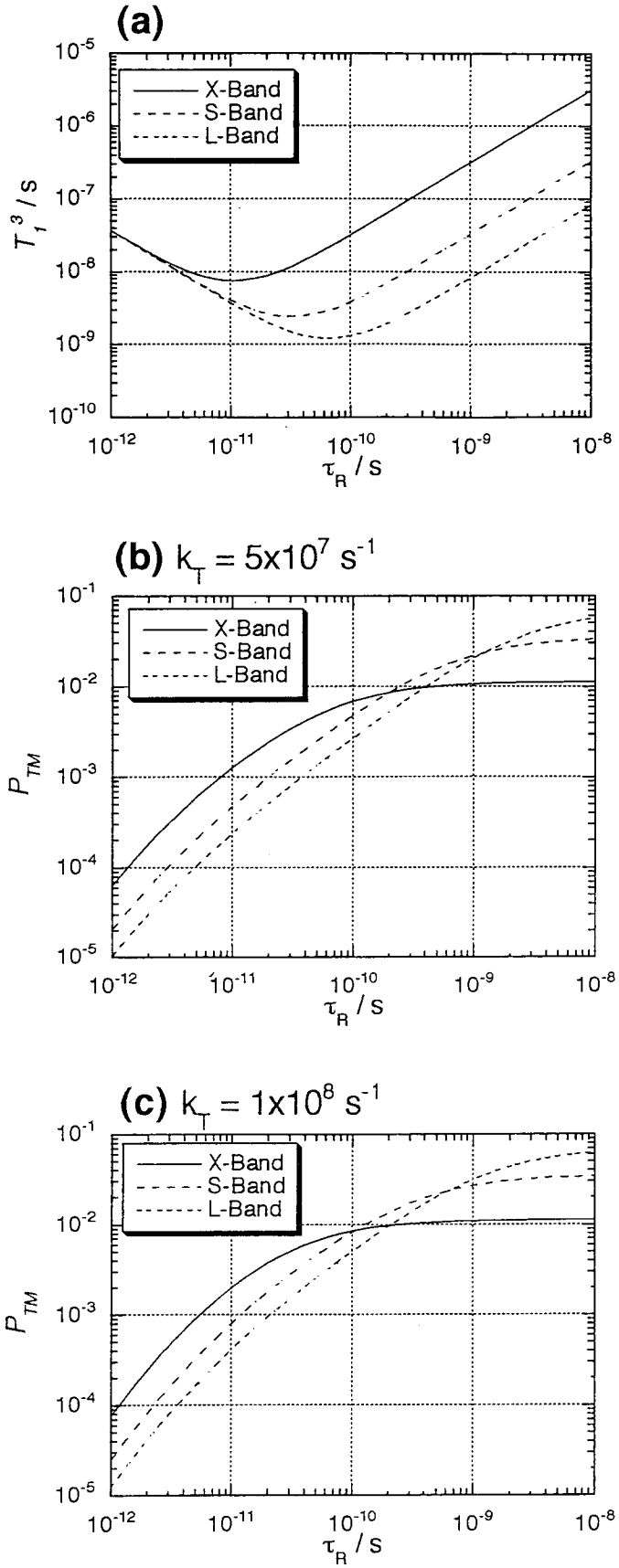


Figure 4-3 Calculated values of (a) ${}^3T_1$, (b) $P_{TM}$ at $k_T = 5x10^7$ s$^{-1}$, and (c) $P_{TM}$ at $k_T = 1x10^8$ s$^{-1}$ versus $\tau_R$ in the X-, S-, and L-bands for the ZnTPP and p-BQ system obtained from eq.5-1 and 2. $D = 0.8814$GHz and $E = 0.2938$GHz were used (see text).

polarization is strongly dependent on the reaction rate as seen from the difference between parts b and c of Figure 4-3. If $k_T$ = 1x10$^8$ M$^{-1}$ s$^{-1}$, the calculated results become much closer to the observed ones in ethanol.

The results obtained in 2-methyl-1-propanol are in agreement with the predicted result in the slow rotation region; for example, $\tau_R \geq$ 1x10$^{-9}$ s in Figure 4-3b. However, $P_{TM}^{rel}$ for the S- and L- bands at -30°C are very large. This may be due to the errors introduced by the contributions due to the SCRP and ST_M mechanisms. Also at low temperatures, the validity of eq. 4-5 becomes questionable because of very slow rotation. To sum up, we may conclude that the observed results given in Table 4-1 are well-explained on the basis of the Atkins-Evans theory, at least qualitatively. However, for a more accurate comparison the reaction rates in different solvents at different temperatures have to be known accurately. It should also be noted that the Atkins-Evans formula is based on the isotropic rotation. In the case of TPP the rotational motion is expected to be anisotropic and the correlation time effective in the relaxation process may be slower than the calculated ones for isotropic rotation.

(2) Pyrazine / 2-propanol system

Figure 4-4 shows the CIDEP spectra of the pyrazine (Py, 0.10M)/ 2-propanol system observed in the X-, S-, and L-band regions. The hydrogen abstraction reaction of the excited triplet state of pyrazine from 2-propanol produces the pyrazinyl radical (·PyH, $g$ = 2.0034) and the 2-hydroxypropan-2-yl radical ( $g$=2.00315, $a_{II}$=1.97mT).[23,27]

$$^3Py^* + (CH_3)_2CHOH \xrightarrow{HA} \cdot PyH + (CH_3)_2\dot{C}OH$$

The second-order hyperfine splittings of the 2-hydroxypropan-2-yl radical are observed more clearly in the S- and L-band spectra.[21,22] The spectral pattern in the X-band is absorption over the entire spectrum with a slight distortion to an E/A type as reported before.[23,27] This result indicates that the contribution of TM ( it gives a net A character to the spectra ) is dominant over that of $ST_0M$ ( it gives an E/A character ) in

the X-band. On the other hand, the spectra in the S- and L-bands show an E/A* pattern, which indicates dominant $ST_0M$ character. Since $\Delta g$ between the pyrazinyl and 2-hydroxypropan-2-yl radicals is quite small, the magnitude of the $ST_0M$ polarization is considered to be independent of the MW frequency, when all other experimental conditions except the MW frequency were kept the same. Then the result shows that the contribution of the TM decreases with a decrease of the MW frequency. This is the opposite trend to that found in the case of ZnTPP / p-BQ. The relative signal intensity of the pyrazinyl radical is much weaker in the S- and L-bands. This is also due to the decrease of the TM contribution at the low MW frequencies, because the small hfc of the pyrazinyl radical compared with that of the 2-hydroxypropan-2-yl radical makes the $ST_0M$ contribution small.

An attempt to make a more quantitative analysis of the frequency dependence is made in the following way. When the polarization due to ST_M is neglected, CIDEP spectra can be simulated with only the TM and $ST_0M$. The TM and $ST_0M$ produce symmetric and antisymmetric polarizations, respectively. Therefore the hf lines on the low and high magnetic field sides corresponding to $M_I$ and $-M_I$ ( for example, lines with $M_I$ = -1 and 1, $M_I$ represents the total quantum number of hyperfine coupling nuclei.) have the same amount of TM polarization but an opposite amount of $ST_0M$ polarization. The sum and the difference of the intensities ($I_h$ and $I_l$ ) of these corresponding hf lines give the amounts of the TM and $ST_0M$ polarizations, respectively. The relative contribution of the TM with respect to that of $ST_0M$ is given by dividing the sum by the difference ( $(I_h + I_l)/(I_h - I_l)$ ). We use this value to examine the frequency dependence of the relative TM polarization. In Table 4-2, the MW frequency dependence of the TM contribution with respect to that in the X-band ($P_{TM}^{rel}$) is given. It is seen that the TM polarization appears to increase almost in proportion to the MW frequency. In the present calculation the contribution of ST_M is neglected. It was, however, shown that ST_M makes a significant contribution in the acetone /2-propanol system at a low MW frequency.[22] Since the sign

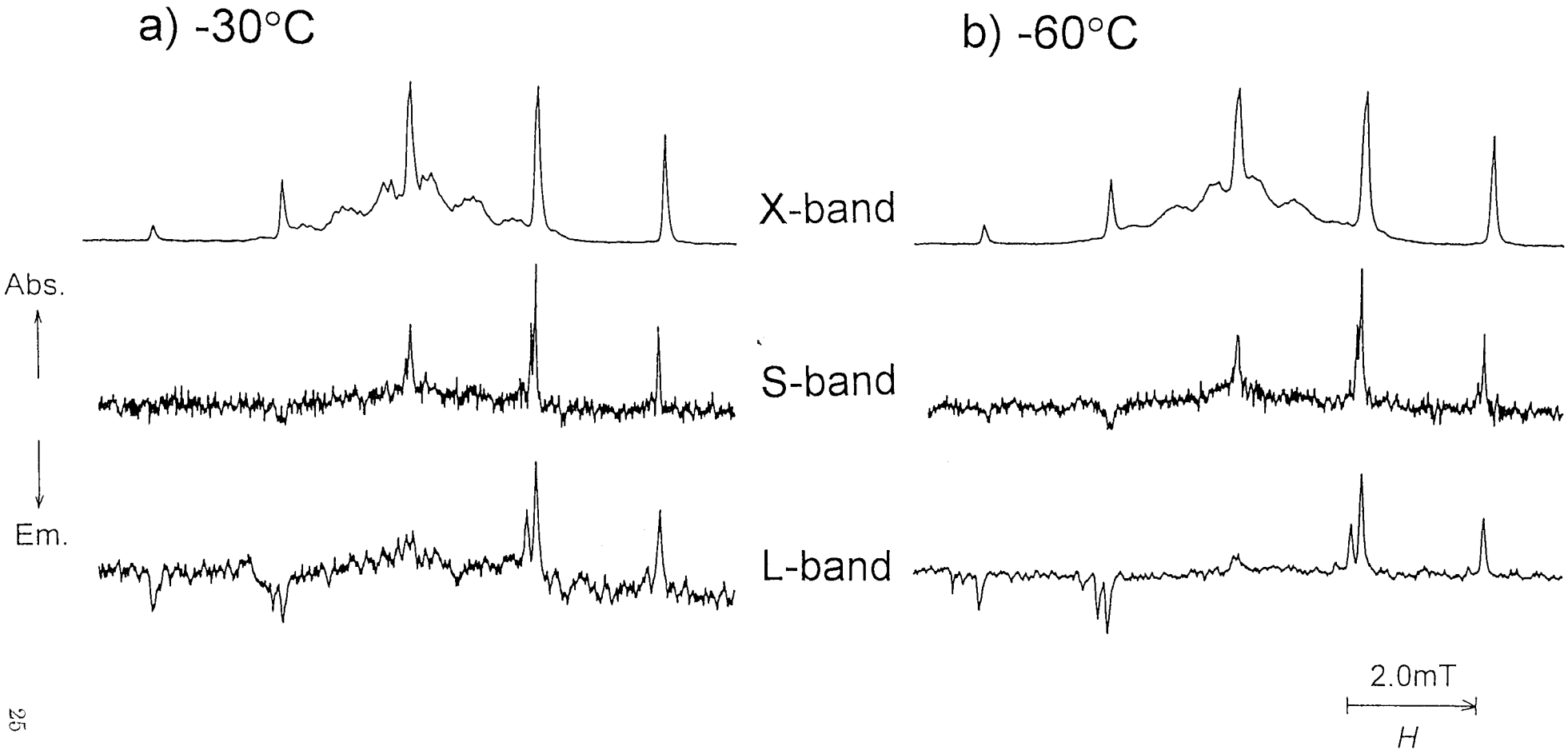


Figure 4-4 X-, S-, and L-band CIDEP spectra of the pyrazine (0.10M) / 2-propanol system at (a) -30 and (b) -60°C. The delay time was 0.5 μs after laser excitation.

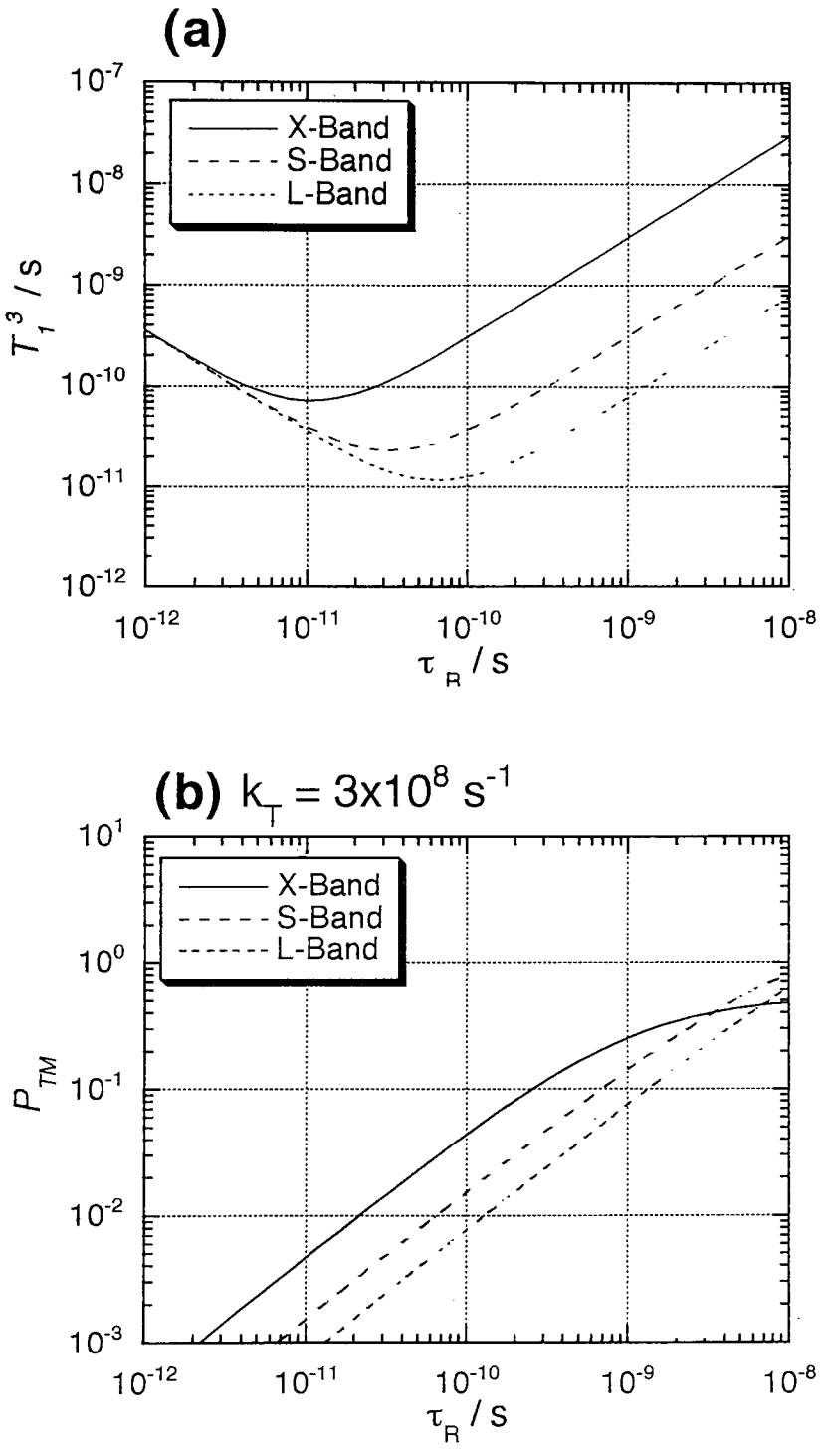


Figure 4-5 Calculated values of (a) $^3T_1$ and (b) $P_{TM}$ versus $\tau_R$ in the X-, S-, and L-bands for the pyrazine / 2-propanol system obtained from eq.1 and 2. $D$ = 4.860GHz and $E$ = -5.283GHz, $k_T = 3x10^8$ s$^{-1}$ were used (see text).

of the ST_M contribution is opposite to that of the TM, it reduces the calculated value of $P_{TM}$. Therefore the calculated value becomes smaller than the true value, when the ST_M contribution is significant. The small value of $P_{TM}$ in the L-band at low temperatures may be due to this cause.

Using eq. 4-1 and 2 we have calculated the dependence of the spin-lattice relaxation time of the triplet pyrazine ($^3T_1$) and the magnitude of the initial polarization ($P_{TM}$) on the rotational correlation time of the triplet molecule ($\tau_R$) at different MW frequencies. In these calculations, the values of the zfs of triplet pyrazine are taken to be $D$ = 4.860GHz and $E$ = -5.283GHz, as reported in the literature.[34] Because of the large $D$ and $E$ values a deviation from the high-field approximation in deriving eq.4-1 and 2 would be serious at low MW frequencies. Nevertheless, it seems worthwhile to compare the experimental results with the calculated ones. On the basis of the reported rate constant, $k_T$ is estimated to be $1.7 \times 10^9$ $s^{-1}$ at room temperature [26] and on the order of $10^8$ $s^{-1}$ at lower temperatures. The rotational correlation time is estimated to be $4.6 \times 10^{-10}$ s at -30°C from the solvent viscosity and the molecular volume. This means that the system is in the slow rotation region at low temperature (Figure 4-5a). However, the MW frequency dependence is now predicted to be different from the case of TPP In this region the calculation predicts that the TM polarization is approximately proportional to the MW frequency, as shown in Figure 4-5b. The observed frequency dependence seems to be in good agreement with this prediction. Though the system is not in the fast motion limit, the MW frequency dependence is similar to that expected for the fast limit, because of the large zfs and shorter $\tau_R$.

(3) MA / 2-propanol system

Figure 4-6 shows the CIDEP spectra of the MA (0.10M)/ 2-propanol system observed in the X-, S-, and L-band regions. The excited triplet state of MA abstracts a hydrogen of a solvent to attach it to the C=C double bond. The produced solvent radical

is added quickly to the C=C double bond of the ground state MA, and the spin adduct radical (·MAR) is produced by the following scheme:

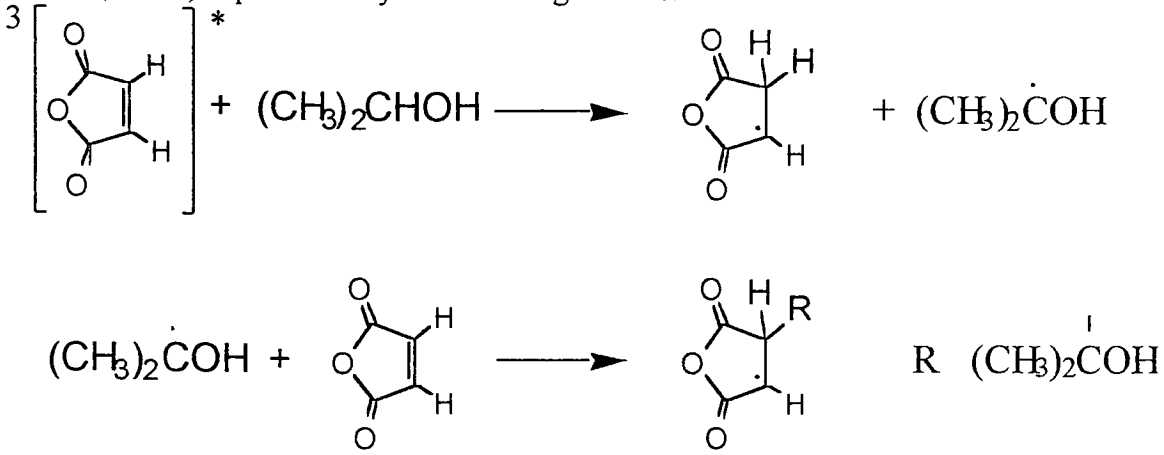

This scheme is similar to that of the photosensitized reaction of MA with xanthone,[31] but in the present case the TM polarization is produced by the intersystem crossing of excited MA itself. The spin polarization of the secondary spin adduct radical (·MAR) whose spectrum has four hyperfine (hf) lines with two unequivalent protons ($a_{Ha}$ = 2.0mT, $a_{Hb}$ = 3.33mT), is complicated because it involves the polarization transfer process and the secondary $ST_0M$.[31] Therefore, it is excluded from the present discussion. In the spectrum of the primary radical (·MAH), there are six hf lines with one ($a_{Ha}$ = 2.07mT) and two ($a_{Hb}$ = 3.50mT) equivalent protons, and the second-order splittings are clearly observed at low MW frequencies. The spectral patterns of ·MAH are all E with an E/A distortion in the X-band but E*/A in the S- and L-bands. The contribution of TM ($P_{TM}$) decreases with a decrease of the MW frequency, as in the case of the pyrazine/2-propanol system. Table 4-3 gives the changes of $P_{TM}^{rel}$ at different frequencies and temperatures. The decrease of $P_{TM}$ on going from the X-band to the L-band is not so large as in pyrazine.

The calculation of the initial polarization of TM shows a difference between MA and pyrazine. The zfs of triplet MA has not been determined, but we take $D$ = 3.0GHz and $E$ = 1.0GHz which are reasonable for an ordinary $\pi\pi^*$ organic triplet. The triplet reaction rate is assumed to be $k_T = 3\times10^8$ $s^{-1}$, as in the case of pyrazine. The rotational correlation time of MA is estimated to be $\sim10^{-10}$ s at 0°C. The calculated results of ${}^3T_1$ of

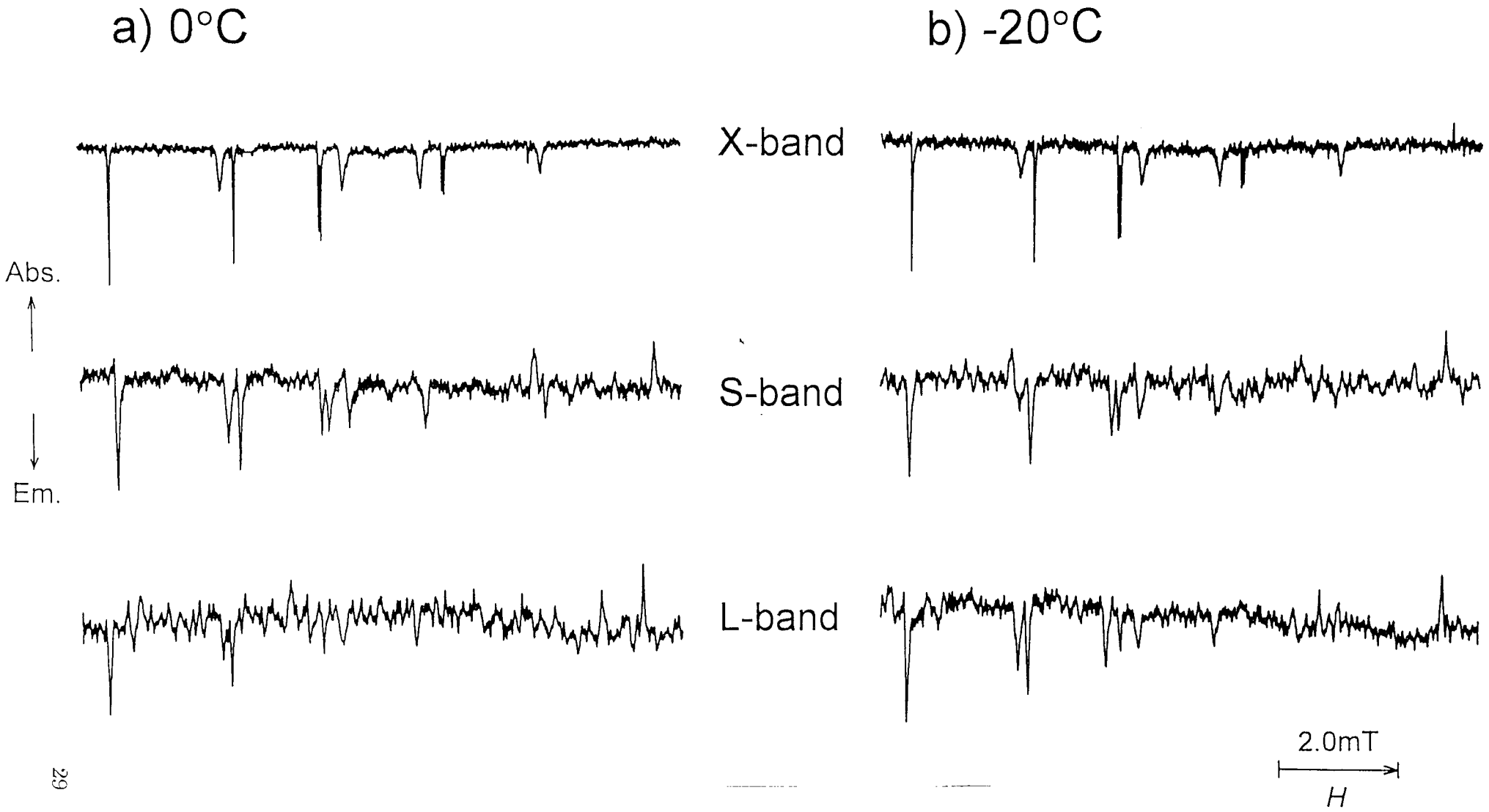


Figure 4-6 X-, S-, and L-band CIDEP spectra of the MA (0.10M) / 2-propanol system at (a) 0 and (b) -20°C. The delay time was 0.5 μs after laser excitation.

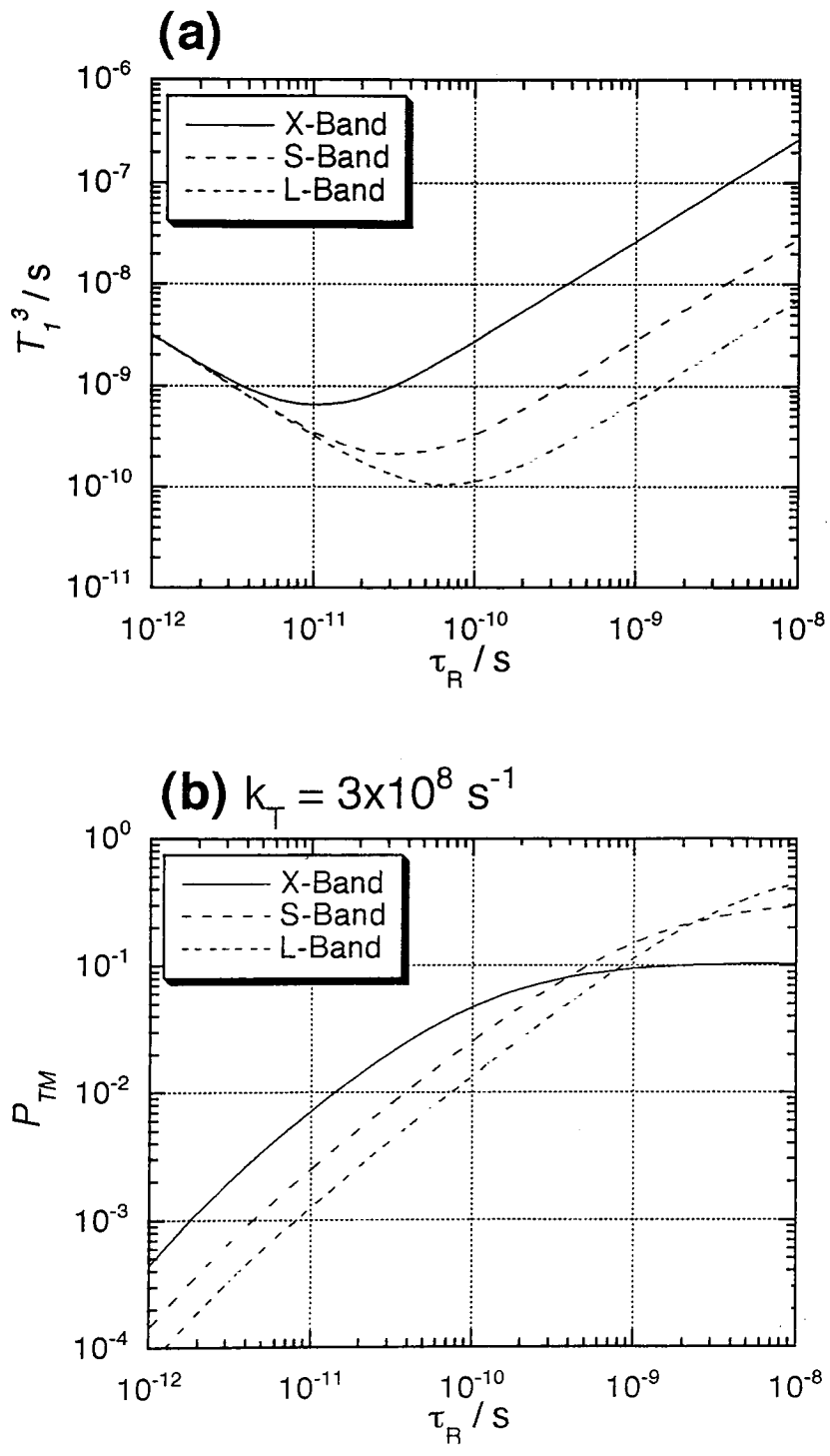


Figure 4-7 Calculated values of (a) ${}^3T_1$ and (b) $P_{TM}$ versus $\tau_R$ in the X-, S-, and L-bands for the MA/ 2-propanol system obtained from eq.1 and 2. $D$ = 3.0GHz, $E$ = 1.0GHz, and $k_T$ =3x10$^8$ s$^{-1}$ were used (see text).

the triplet MA and $P_{TM}$ are shown in Figure 4-7. ${}^3T_1$ varies with $\tau_R$ as in the pyrazine triplet, but its value is about 10 times larger at the same $\tau_R$ because of much smaller $D$ and $E$. In the region around $\tau_R \approx 10^{-10}$ s, the relative contributions of the TM are predicted to increase with the MW frequency, but it is not proportional to the MW frequency as in the fast motion limit. This prediction is indeed in agreement with the observation. However, the observed smaller changes of the TM contribution with the MW frequency may be partly due to the ST_M contribution, particularly at low temperatures, because both TM and ST_M give rise to emissive polarizations. We should also note that the MA / 2-propanol system is considered to be a typical case of the MW frequency dependence of the TM, because many organic molecules have similar values of zfs, $\tau_R$, and $k_T$. For example, benzophenone which is a typical aromatic carbonyl compound, has $D$ = 4.179GHz, $E$ = 1.042GHz,[35] $k_T = 10^8 \sim 10^9$ s$^{-1}$ with appropriate quenchers, and $\tau_R \approx 10^{-10}$ s in alcoholic solvents at room temperature. Therefore, its TM contribution is considered to behave in a similar way as in MA. It is considered that neither the fast nor the slow motion limit is applicable in this case.

## 4-5. Concluding remarks

In conclusion, this work presents a CIDEP investigation of the MW frequency dependence of the TM in the three typical examples. In the first ZnTPP/p-BQ systems, they are in the slow rotational motion region and the spin polarization of the TM decreases with an increase of MW frequency. On the contrary, in the pyrazine/2-propanol system, the spin polarization of the TM increases with an increase of the MW frequency, though the system is still in the slow motion region. The difference is mainly due to the differences in the zfs and the rotational correlation times. In MA/2-propanol the TM contribution also increases with an increase of the MW frequency, as in pyrazine, but the system is likely to be in neither the fast nor the slow motion region. The observed results are explained reasonably well on the basis of the Atkins-Evans theory, but for more

thorough comparison between the experimental results and the theoretical predictions accurate data on the reaction rates are needed. Also the validities of the high-field approximation in the systems of large zfs and the assumption of isotropic rotation must be examined carefully.

The MW frequency dependence of the TM contribution is very sensitive to the rotational correlation time of the triplet molecule. Therefore, the MW frequency dependence may be useful for studying the environments of the radicals in heterogeneous media, such as micelles, vesicles, and so on. The MW frequency dependence of the TM may also give an insight into the unresolved problems of the spin polarization mechanism, for example, the main polarization mechanism in the case of SCRP [36-39] and the system for which a strangely large contribution of $ST_{\pm}M$ was reported.[40] Consequently, the multifrequency TREPR experiments provide a new possibility in investigating CIDEP mechanisms.

# Chapter 5. Magnetic Field Dependence of the Spin Correlated Radical Pair CIDEP

## 5-1. Introduction

In this chapter, the magnetic field dependence of the SCRP CIDEP is discussed. SCRP spectra were observed in the photolysis of acetone in 2-propanol, xanthone and 2,6-di-tert-butylphenol (2,6-DBP) in a sodium dodecylsulfate (SDS) micellar solution, and zinc tetra(4-sulfonatophenyl)porphyrin ( ZnTPPS ) and p-benzoquinone (p-BQ) in a cetyltrimethylammonium chloride (CTAC) micellar solution at three different external magnetic fields, i.e. X-, S-, L-band microwave regions. The obtained spectra are compared in detail, and the spin polarization and relaxation mechanisms, as well as the interaction in the SCRP are discussed.

## 5-2. Experimental

Acetone, 2-propanol ( Nakalai tesque ), acetone-$d_6$, and 2-propanol-$d_8$ (Aldrich) were used as received.

Xanthone, 2,6-DBP, p-BQ and DQ were commercially available special grade reagents ( Nakalai tesque ) used as received. ZnTPPS was synthesized from $H_2$TPPS ( meso-tetra(4-sulfonatatophenyl)porphine ) dihydrochloride ( porphyrine products, inc.) in ethanol. SDS and CTAC were special grade reagents ( Nakalai tesque ) used as received. The micellar solutions were prepared with the concentration of 0.1M in distilled water. As the critical micelle concentrations (CMC) were 8mM and 1.4mM, and aggregation numbers were 62 and 105 for SDS and CTAC, respectively. The micelle concentration were about 1mM in both cases.

## 5-3. Results and discussion

### (a) The SCRP CIDEP of Acetone / 2-propanol system

Figure 5-1 shows the CIDEP spectra in the X-, S-, and L-band microwave

regions observed in the photolysis of acetone in 2-propanol at several temperatures. The spectra are assigned to the 2-hydroxypropan-2-yl radical.[6,14,41] The seven hyperfine lines in the X-band spectra are explained by six equivalent protons, and the second order splittings are observed clearly in the S and L-band spectra.[21,22] The spectral pattern changes with temperature, from E/A at higher temperatures to E*/A at lower temperatures. The net E character increases with a decrease of temperature. This is mainly due to an increase of the ST$_-$ mixing RPM. The external magnetic field dependence of the spectra was discussed in detail in previous report.[21,22] Here only the magnetic field dependence of the SCRP spectra is discussed. The E/A phase-pattern signal of the SCRP was clearly observed in the central part of the spectrum in the X-band at lower temperatures ( $\leq$-45°C ). On the other hand, it was not observed in the spectra in the S- and L-band. The second order splittings and the increased net polarization of the ST$_-$M may disturb the observation of the E/A signals.

Figure 5-2 shows the CIDEP spectra in the X-, S-, and L-band microwave regions observed in the photolysis of acetone-$d_6$ in 2-propanol-$d_8$ at several temperatures. The spectra are simpler compared with those of the protonated one because of a diminution of the second order splittings and ST$_-$M, since the hfc is rather small compared with the protonated radical. The spectral pattern is almost the same as that of the protonated one. The E/A lines of the SCRP were observed in the X-band at lower temperatures. In particular at -88°C, all of the hf lines have the E/A distortion.[42] On the other hand, in the S- and L-band spectra, the E/A lines could be observed only in the center hf line even at -90°C. The SCRP signal was much weaker compared with the signal due to the $ST_0M$ RPM which is independent of the magnetic field. The results seem to indicate that the SCRP signals decrease with a decrease of the magnetic field.

The SCRP interactions in the geminate cage is considered to be independent of the magnetic field. The SCRP polarization is explained by the interaction similar to that in the case of the $ST_0M$; the correlation time and the reaction rate in the singlet manifold are

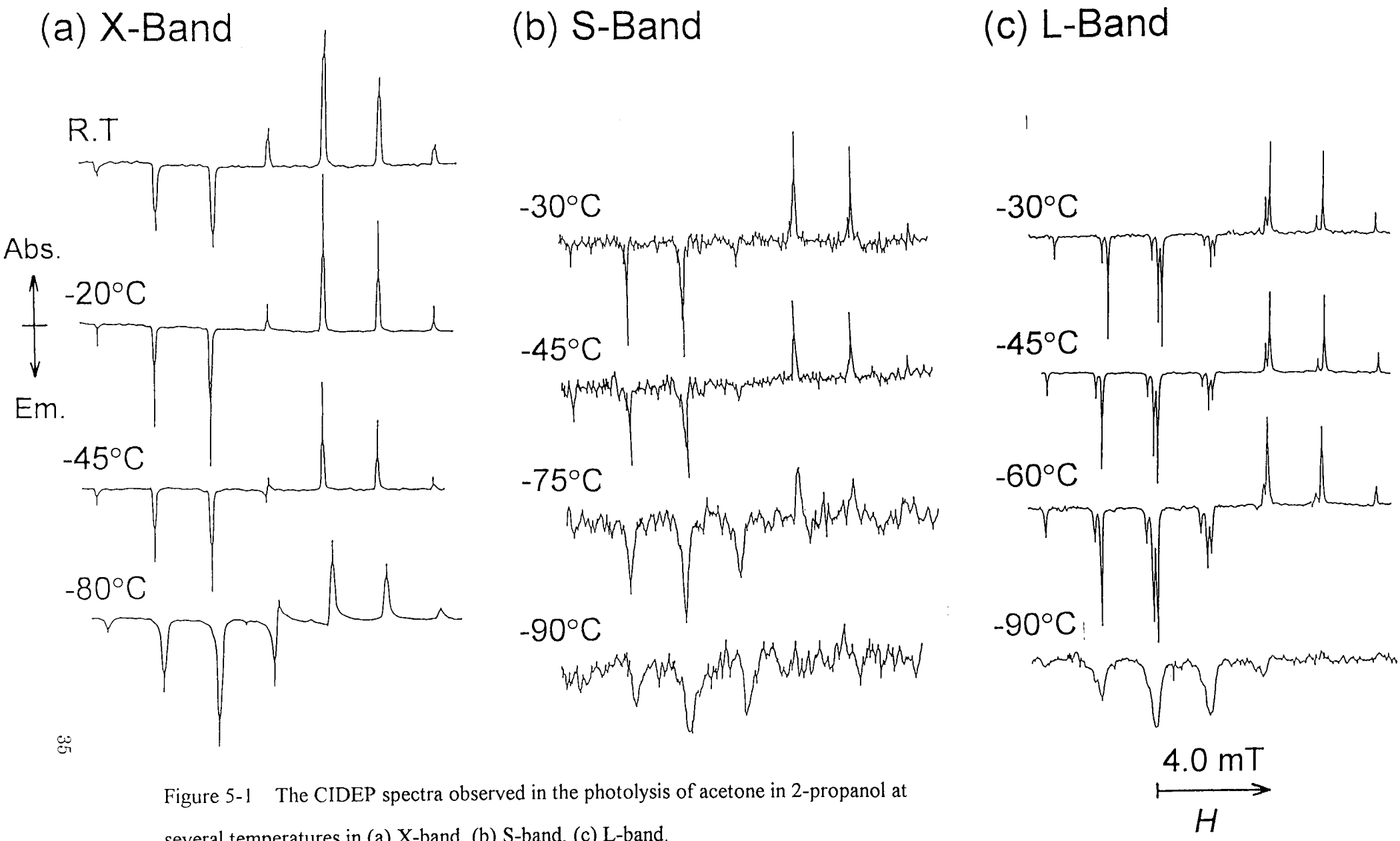


Figure 5-1 The CIDEP spectra observed in the photolysis of acetone in 2-propanol at several temperatures in (a) X-band, (b) S-band, (c) L-band.

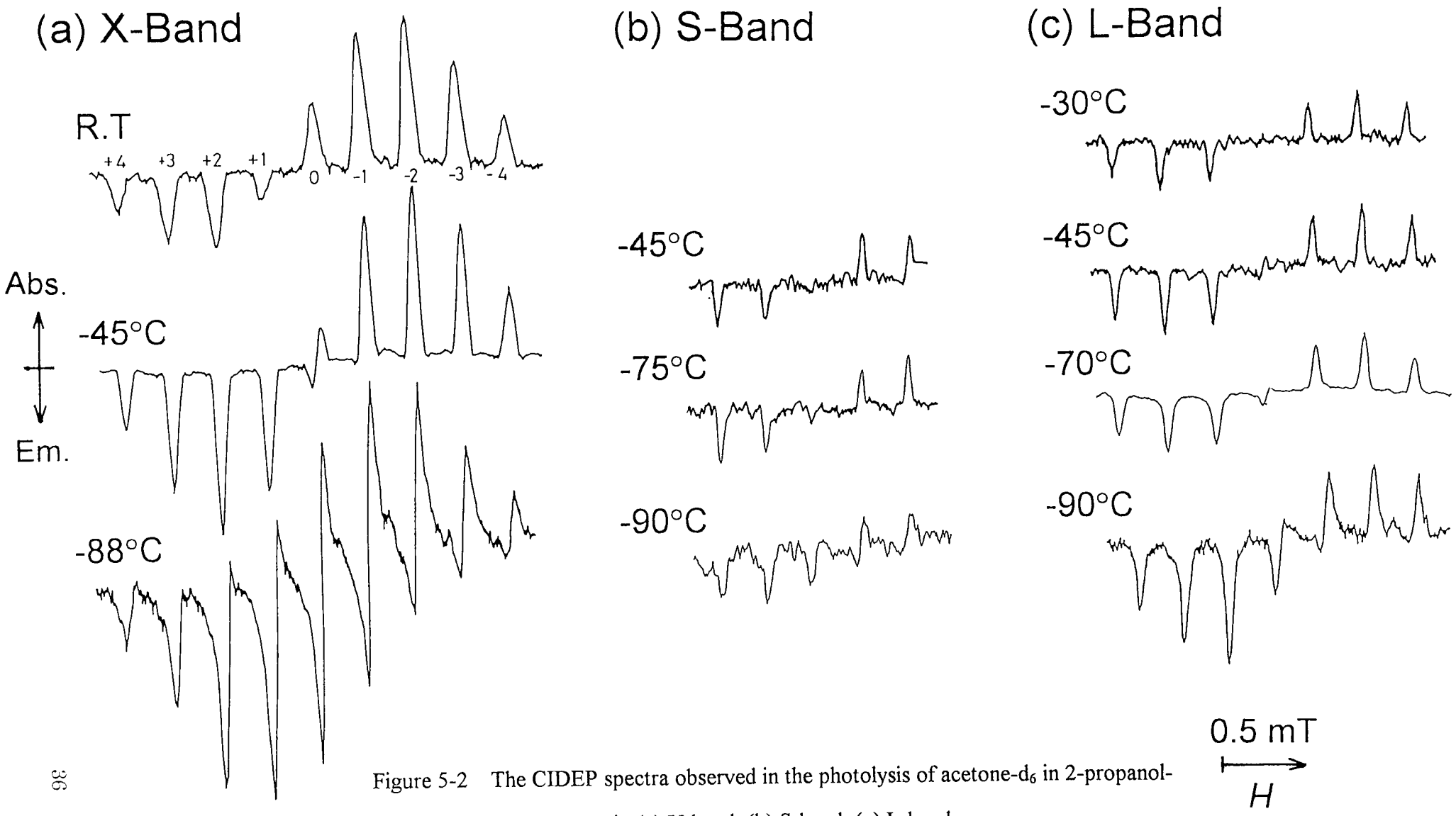


Figure 5-2 The CIDEP spectra observed in the photolysis of acetone-$d_6$ in 2-propanol-$d_8$ at several temperatures in (a) X-band, (b) S-band, (c) L-band.

mainly determined by the diffusion constants of the solvents, which are independent of the magnetic field. The TM polarization and the ST_M parts depend on the magnetic field. Then, the net polarization increases or decreases with a change of the magnetic field strength.[22,24] However, the E/A phase component is considered to be independent of the magnetic field.

Though the relaxation process of the SCRP CIDEP has not been clearly understood, it is considered that the rotational motion and/or the fluctuation of the exchange or dipole interaction in the SCRP cause the relaxation.[6,20] The magnetic field dependence of the relaxation has been scarcely investigated in the CIDEP studies.[20]

Spin-lattice relaxation processes in radicals and triplets in non-viscose solutions are usually explained by the rotational relaxation model in EPR. In this case, the spin-lattice relaxation time ( $T_1$ ) is given by,[4-6,20]

$$\frac{1}{T_1} = \frac{B_{loc}^2 \tau_c}{2\left(1+\omega_0^2 \tau_c^2\right)} \qquad (5\text{-}1)$$

Here, $B_{loc}$ is the value of the local magnetic field that induces the relaxation transition, and $\tau_c$ is the correlation time of the fluctuation. The spin-spin relaxation time ( $T_2$) is always less than $T_1$. Figure 5-3 shows a plot of the calculated $T_1$ versus the correlation time. The relaxation times determined by the fluctuation of the exchange and dipole interactions are explained by a similar equation.[20] The magnetic field dependence of $T_1$ is considered to consist of two typical cases: In the fast motion (fluctuation) region, $T_1$ is independent of the external magnetic field. In the slow motion region, $T_1$ always decreases with decreasing the external magnetic field.

In the acetone/2-propanol system, the SCRP signals were observed only at very low temperatures ( $\leq$ -45°C). The correlation time of the SCRP in the geminate cage is comparatively long because the solvent viscosity is very high. This case is considered to be in the slow motion region; $T_1$ decreases with decreasing the external magnetic field.

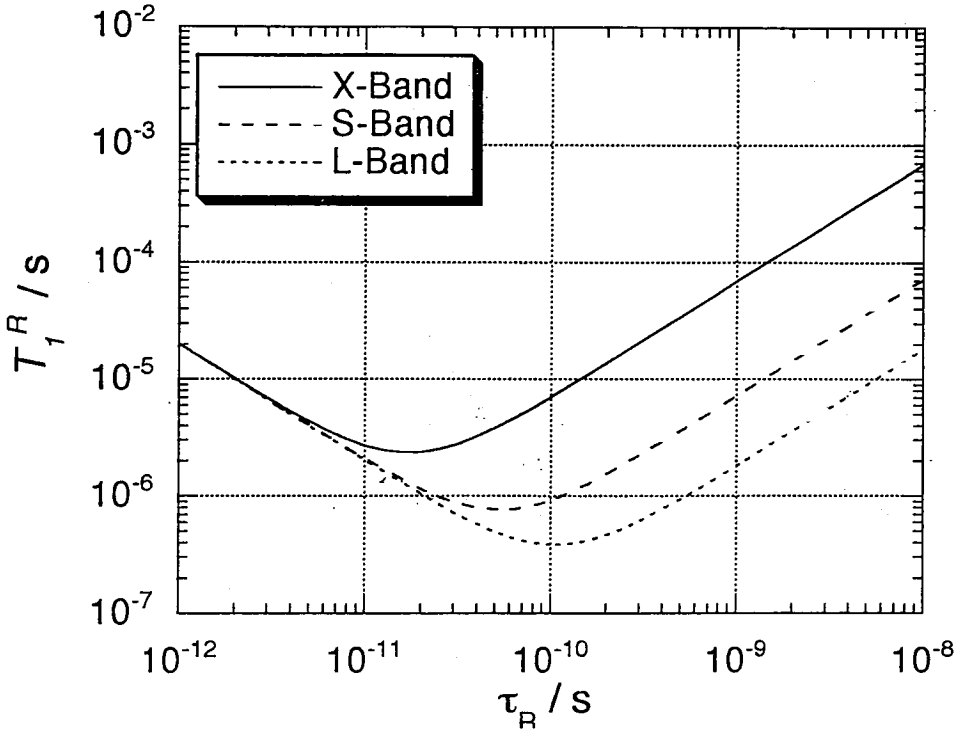


Figure 5-3 A plot of the calculated spin-lattice relaxation time ${}^{R}T_1$ versus the correlation time. $B_{loc}$ = 0.05GHz is used. ( see eq.5-1 )

The SCRP signals are weakened by faster $T_1$ in the S- and L-bands compared with the X-band. This is a reasonable explanation qualitatively.

(b) Xanthone / 2,6-DBP in SDS micelle

Figure 5-4 shows the CIDEP spectra in the X, S, and L-bands observed in the photolysis of xanthone and 2,6-DBP in a SDS micellar solution at room temperature and 0°C. The spectra show characteristic E/A/E/A pattern assigned to the SCRP of the xanthone ketyl and the phenoxyl radical produced by the hydrogen abstraction reaction of xanthone triplet from 2,6-DBP [40] The spectrum changes clearly with the observing MW frequency. In the X-band the spectrum has an additional net emission with an E/A/E/A pattern, but in the S-band the net E character was much weaker compared with the X-band, and in the L-band the net E character was not observed. The results show that the net E polarization decreases with decreasing the MW frequency. Such MW frequency dependence is shown in the net polarization due to the TM in the pyrazine/2-propanol and maleic anhydride/2-propanol systems.[24] In Chapter 4, the magnetic field dependence of the TM polarization is discussed in detail. The result can be explained by assuming that the net E polarization of the SCRP spectra is due to the TM. It is considered that xanthone and 2,6-DBP in the SDS micelle reacts quickly enough to conserve the TM polarization to the produced SCRP The magnetic field dependence of the TM suggests that the triplet xanthone in the micelle has a correlation time of $10^{-11}$ to $10^{-10}$ $s^{-1}$ [24] This value is reasonable in the case of a small molecule such as pyrazine in a non-viscose solvent such as benzene at room temperature. However, it was reported in literature [6,43] that the triplet state molecule is generally more restricted in a micelle compared with the case in solutions. On the other hand, the E/A/E/A component of the SCRP spectra is scarcely affected by the MW frequency. The interaction between radical pairs, shown as the exchange integral $J$ in the spectra, seems to be independent to the external magnetic field. This is considered to be reasonable, but more detailed analyses and experiments are

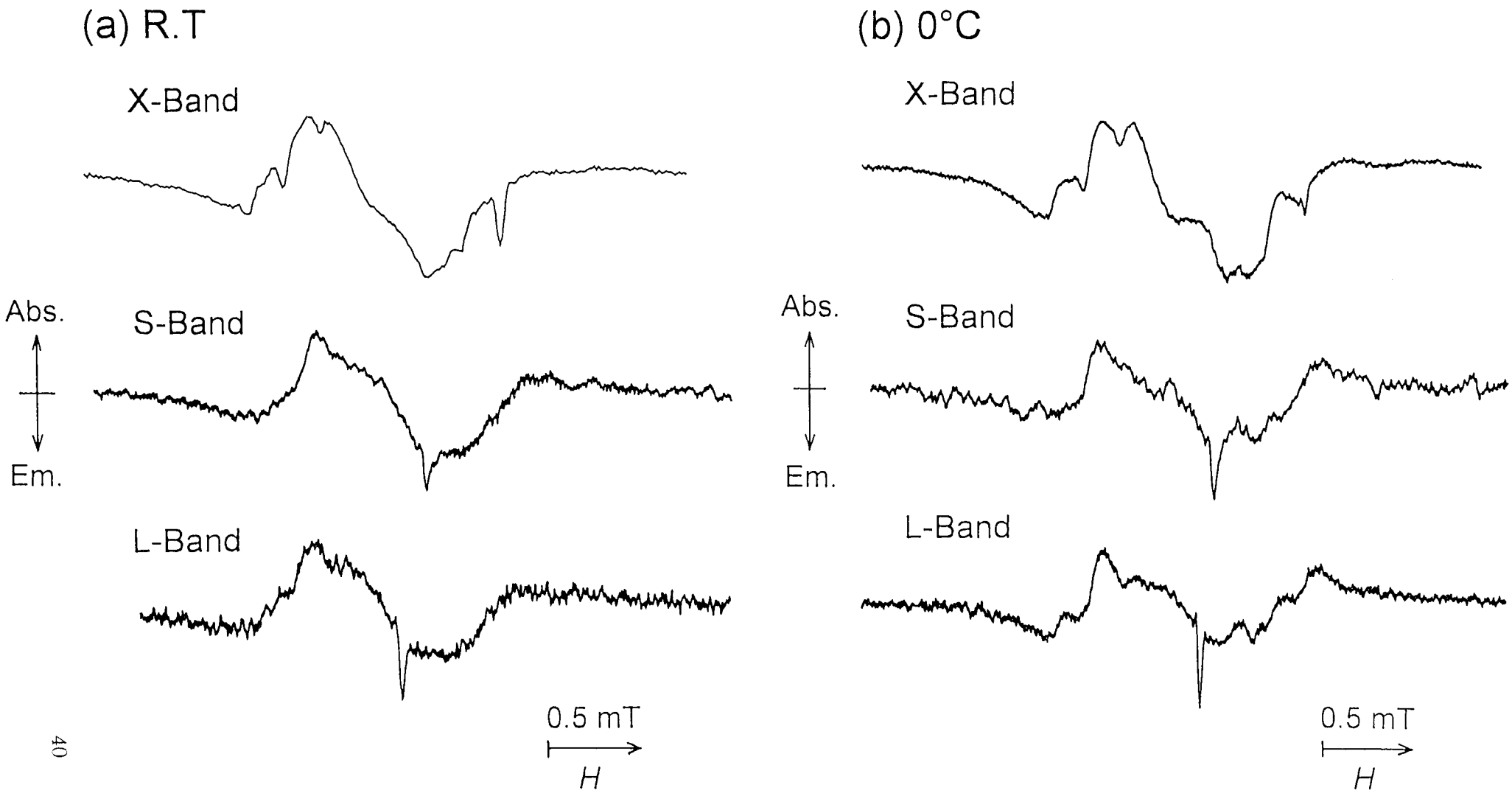


Figure 5-4 The CIDEP spectra in the X-, S-, and L-bands observed in the photolysis of xanthone and 2,6-DBP in SDS micellar solution at (a) room temperature and (b) 0°C.

required.

Figure 5-5 shows the time evolution of the SCRP signals in the X and L-bands observed in xanthone and 2,6-DBP at 0°C. The decay curves are explained by a single exponential decay, the decay rates determined by a least squares fits of data being 3.0μs in the X-band, and 2.0μs in the L-band. The relaxation time decreases with decreasing the external magnetic field, this is reasonable when $\tau_c \approx 10^{-11}$ $s^{-1}$ on the basis of eq.5-1. This value of $\tau_c$ is reasonable in the case of a small molecule such as pyrazine in a non-viscose solvent such as benzene at room temperature, as described above. This value is too small for the rotation of the SCRP as a whole in the SDS micelle. It is generally considered that the chemical species are more restricted in the micelle compared with the cases in solutions. The relaxation of the SCRP is possibly caused by the fast rotation of each radical of the SCRP The magnetic field dependence of $T_1$ would be useful in clarifying the relaxation mechanisms of the SCRP

(c) ZnTPPS / p-BQ or DQ in CTAC micelle

Figure 5-6 shows the CIDEP spectra of ZnTPPS and p-BQ in a CTAC micellar solution at room temperature and 5°C. The spectra are assigned to the SCRP signals of p-BQ anion radical ( $a_H$ = 0.236mT ).[6,28-30,43] The reaction is considered to occur according to the following scheme,[43]

$$^3ZnTPPS^{4-} + BQ \xrightarrow{ET} ZnTPPS^{3-}\cdot + BQ^{-}\cdot$$

A broad spectrum of the $ZnTPPS^{3-}$ radical is observed in the X-band, but not in the S- and L-bands. The $ZnTPPS^{3-}$ and p-$BQ^-$ anion radicals are trapped by the CTAC cationic micelle, and interact each other. The E/A phase-lines of the SCRP are almost the same in the X, S, and L-band. A slight distortion of E/A type over the entire spectrum in the X-band is mainly due to the $ST_0M$ RPM of the $ZnTPPS^{3-}$ radical because of the difference of the g-factors ( $\Delta g$ ) between $ZnTPPS^{3-}$ ( $g$ = 2.0025 ) and p-BQ anion ( $g$ = 2.0040 ) radicals. The net polarization of the TM and ST_M is considered to be weak in all of the

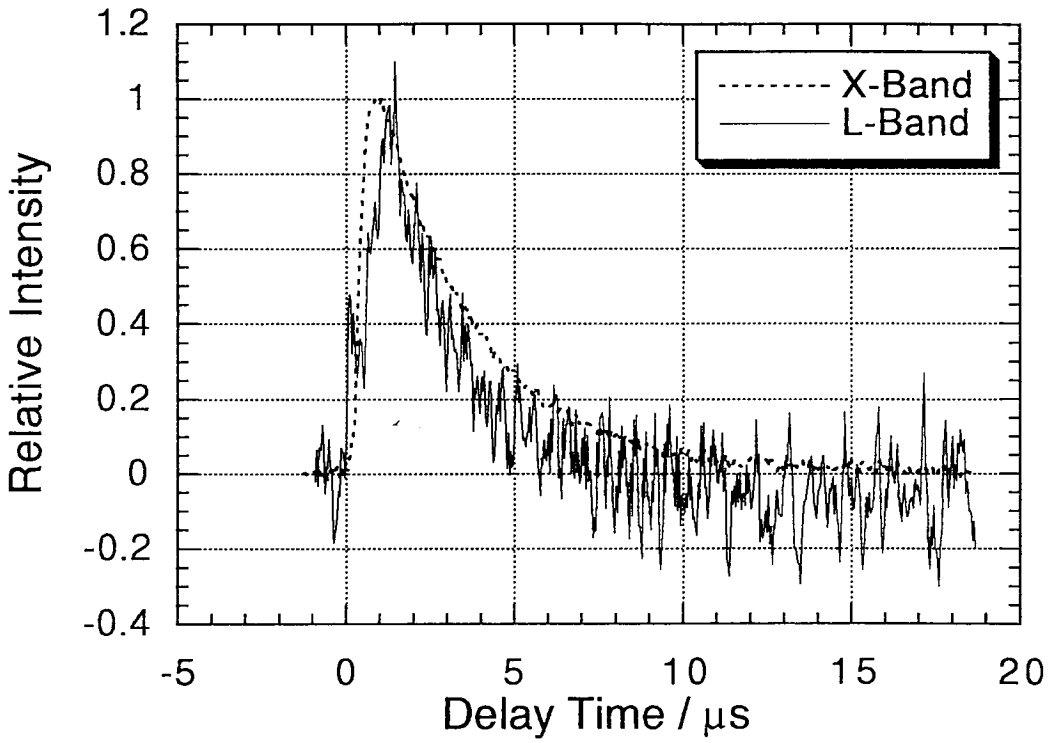


Figure 5-5 The time evolution of the transient EPR signals in the X-, and L-bands observed in the photolysis of xanthone and 2,6-DBP in SDS micellar solution at 0°C.

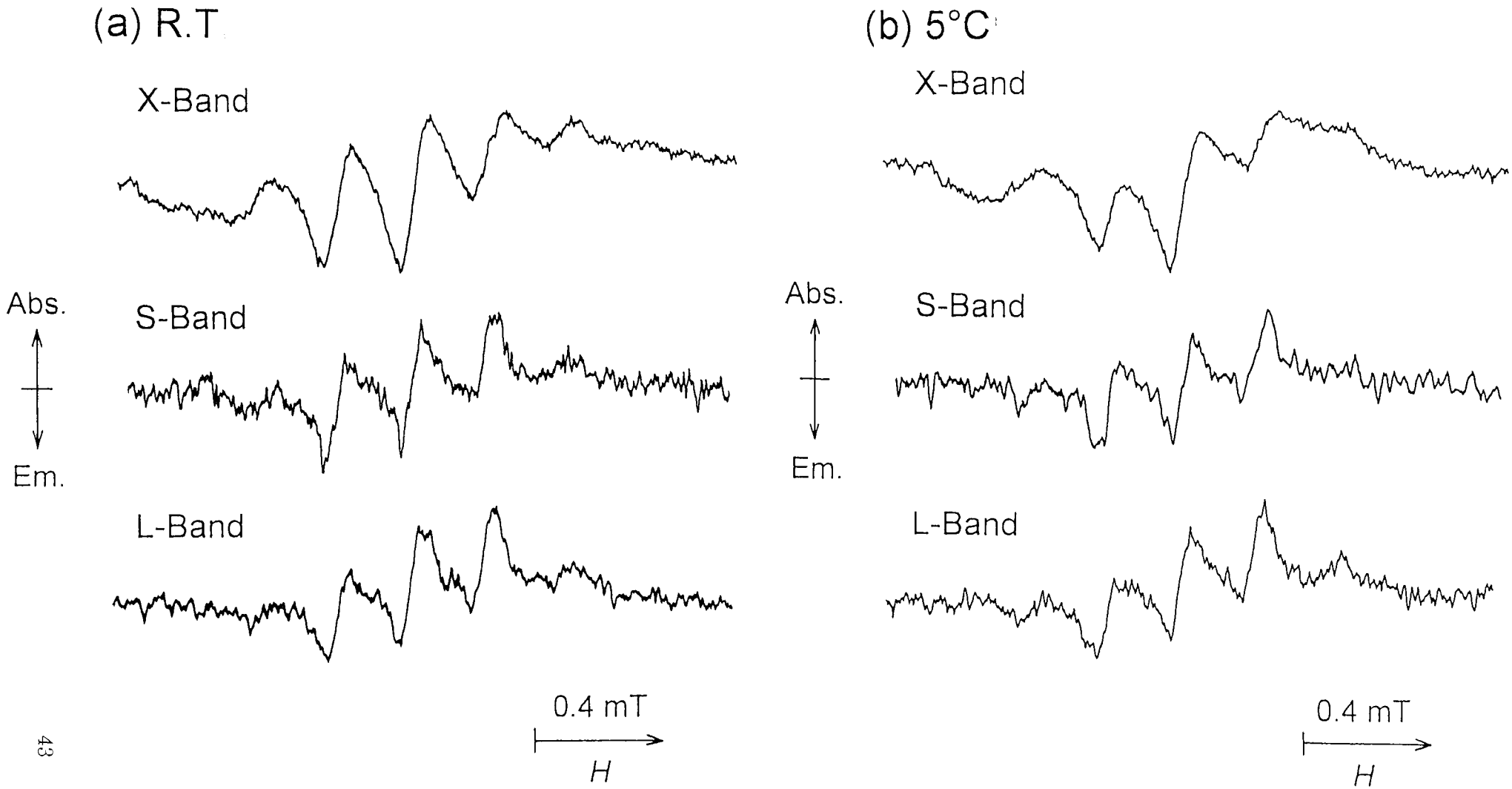


Figure 5-6 The CIDEP spectra in the X-. S-, and L-bands observed in the photolysis of ZnTPPS and p-BQ in CTAC micellar solution at (a) room temperature and (b) 5°C.

X-, S-, and L-bands. In the S- and L-band, $\Delta g$ component of the $ST_0M$ is negligible, so the spectrum becomes symmetric with decreasing the magnetic field. The spectrum of the $ZnTPPS^{3-}$ radical is very weak in the S- and L-bands. This is, probably, because the spin-lattice relaxation time of the $ZnTPPS^{3-}$ radical decreases with a decrease of the magnetic field. The magnetic field dependence of the relaxation time represented by eq.5-1 shows that the correlation time is around $10^{-10}$ $s^{-1}$ or more in the case of the $ZnTPPS^{3-}$ radical. This is reasonable considering the size of ZnTPPS and the viscosity in the micellar media. On the other hand, the magnetic field dependence of the relaxation time of the SCRP seems to be not so obvious compared with the case of the $ZnTPPS^{3-}$ radical. The results suggest the relaxation process of the SCRP is not determined by the rotation of the SCRP as a whole, but by the rotation of each radical of the SCRP or other fluctuation processes. This point is very important, but more detailed investigation is required to confirm this.

## 5-4. Conclusion

The magnetic field dependence of the SCRP CIDEP was investigated in acetone/2-propanol, xanthone and 2,6-DBP in SDS micelle, and ZnTPPS and p-BQ in CTAC micelle. In acetone/2-propanol system, the SCRP signals were much weakened in S- and L-band compared with the X-band. The result can be explained by the magnetic field dependence of the spin-lattice relaxation time of the SCRP. On the other hand, in xanthone and 2,6-DBP in SDS micellar solution, the SCRP signal is not influenced by the magnetic field, except for the net emissive component which decreases with decreasing the magnetic field. The net component is explained well by the TM. The relaxation time of the SCRP decreases a little with decreasing the magnetic field. The result can also be explained by the magnetic field dependence of the spin-lattice relaxation time. The magnetic field dependence of the SCRP CIDEP would be useful to understand the relaxation process and the interaction of the SCRP

# Chapter 6. FT-EPR Study of the CIDEP of 2-Hydroxypropan-2-yl Radical Produced by the Reaction of Acetone with Triethylamine

## 6-1. Introduction

The CIDEP of 2-hydroxypropan-2-yl radical produced by photochemical reactions of acetone has attracted considerable attention.[6,14,21,22,25,41,42,44-47] Photolysis of acetone in 2-propanol produces an E/A* (low-field emission/high-field absorption with net absorptive character) type spectrum at temperatures higher than -30°C. This was originally interpreted in terms of contributions from the $ST_0$ mixing of the radical pair mechanism(RPM) and the triplet mechanism(TM).[41,42,47] However, the involvement of TM was questioned and alternative interpretations have been suggested.[25,48,49] A comparison of the time profiles of the net absorptive signal and RPM signal contributions led Levstein and van Willigen to the conclusion that the absorptive signal cannot be due to TM.[25] They suggested that the transfer of polarization from triplet precursors at thermal equilibrium to doublet radical products gives rise to the absorptive signal. McLauchlan and coworkers also concluded that the TM contribution is negligible.[48] These authors proposed that an, as yet unidentified mechanism is responsible for the absorptive component. Very recently, however, McLauchlan's group favored the TM involving the secondary reaction following bond breaking as well as the hydrogen abstraction reaction.[50] On the other hand, Wan et al. attributed the net absorption to a TM contribution originating in the triplet state of the enol tautomer.[49] It appears that further investigations are needed to settle this question completely.

In previous work, Tominaga et al. studied CIDEP of the 2-hydroxypropan-2-yl radical produced by the photolysis of acetone in various amines.[51] It was found that the spectrum in triethylamine (TEA) at room temperature is of A*/E (low-field absorption/high-field emission with net absorptive character) type as opposed to the E/A* pattern observed in 2-propanol. This indicates that the hydrogen abstraction reaction in this case occurs predominantly from the singlet excited state of acetone. On the other hand, in

the solutions of acetone and TEA in benzene, the polarization pattern depends upon the TEA concentration; $A^*/E$ at a higher concentration (4M) and $E/A^*$ at a lower concentration (<2M). These results were explained in terms of the competition between reactions involving singlet and triplet excited states of acetone. At lower TEA concentrations intersystem crossing (ISC) to the triplet state becomes dominant, so that the reaction goes predominantly via the triplet excited state. The time evolution of the cw time-resolved EPR (TREPR) CIDEP spectra given by acetone in TEA was interpreted qualitatively in terms of geminate-pair RPM, F-pair RPM and TM of CIDEP. However, the time resolution and sensitivity of the TREPR measurement was not good enough to analyze the dynamics quantitatively.

FT-EPR offers superior time resolution and sensitivity, [6] and, therefore, may provide more detailed information on the reaction and spin dynamics of the acetone-amine system. Since the relative magnitude of singlet and triplet excited state contributions to the reaction of acetone with TEA can be varied by varying the TEA concentration, the reaction appears to be ideally suited for an investigation of the origin of the net absorptive character of TREPR and FT-EPR spectra of the photogenerated 2-hydroxypropan-2-yl radical. It is noted that the reaction of triplet acetone with TEA is much faster than the hydrogen abstraction reaction involving 2-propanol so that the system lends itself better for observation of TM CIDEP.

## 6-2. Experimental

Acetone, TEA and benzene from Aldrich were used as received. Solutions of acetone (1M) in TEA and acetone (1M) with TEA (1M) in benzene were used as samples. The solutions were circulated through a flow EPR cell with an effective volume of 0.06 ml. Oxygen was removed from the solutions by bubbling with argon gas.

6-3. Results and Discussion

The TREPR spectrum of the 2-hydroxypropan-2-yl radical produced by laser excitation of acetone (1M) in TEA measured 0.5 μs after the laser pulse is shown in Figure 6-1. The Figure also displays the time profiles of the $M_I$ = +1, 0 and -1 hf lines measured with FT-EPR. Figure 6-2 gives a similar presentation of results obtained with a solution of acetone (1M) and TEA (1M) in benzene. The results are qualitatively in agreement with the previous TREPR measurements.[51] A notable feature of both systems is that, whereas the intensities of the -1 and +1 hf lines show a strong time dependence in the time regime from 50 ns to 10 μs due to CIDEP effects, the $M_I$ = 0 hf line intensity shows only minor changes.

Following the procedure discussed previously,[25] we study the time developments of spin polarization (SP) due to different mechanisms by examining the time profiles of $\Delta S_M$, the difference in intensities of the +1 and -1 hf lines, $\Sigma S_M$, the sum of the intensities of the +1 and -1 hf lines, and $S_0$, the intensity of the $M_I$ =0 resonance. $\Delta S_M$ represents SP due to RPM, while $\Sigma S_M$ and $S_0$ represent the net absorption or emission contributions. The results are discussed in terms of the following reaction scheme.[6,51]

(A) Radical formation reactions of acetone with TEA

$$(CH_3)_2CO \xrightarrow{h\nu} {}^1(CH_3)_2CO^* \xrightarrow{ISC} {}^3(CH_3)_2CO^*$$

$${}^1(CH_3)_2CO^* + N(C_2H_5)_3 \xrightarrow{{}^1k_{HA}} (CH_3)_2\dot{C}OH + (C_2H_5)_2N\dot{C}HCH_3$$

$${}^3(CH_3)_2CO^* + N(C_2H_5)_3 \xrightarrow{{}^3k_{HA}} (CH_3)_2\dot{C}OH + (C_2H_5)_2N\dot{C}HCH_3$$

(B) A radical quenching reaction

$$2\,(CH_3)_2\dot{C}OH \xrightarrow{k_{2r}} \text{products}$$

Then, the time-evolution of the radical concentration ($N_R$) and SP ($P$) should be given by the following equations.[6]

(1) Radical concentration

$$N_R = \frac{N_0}{(k_{2r}N_0t + 1)}$$

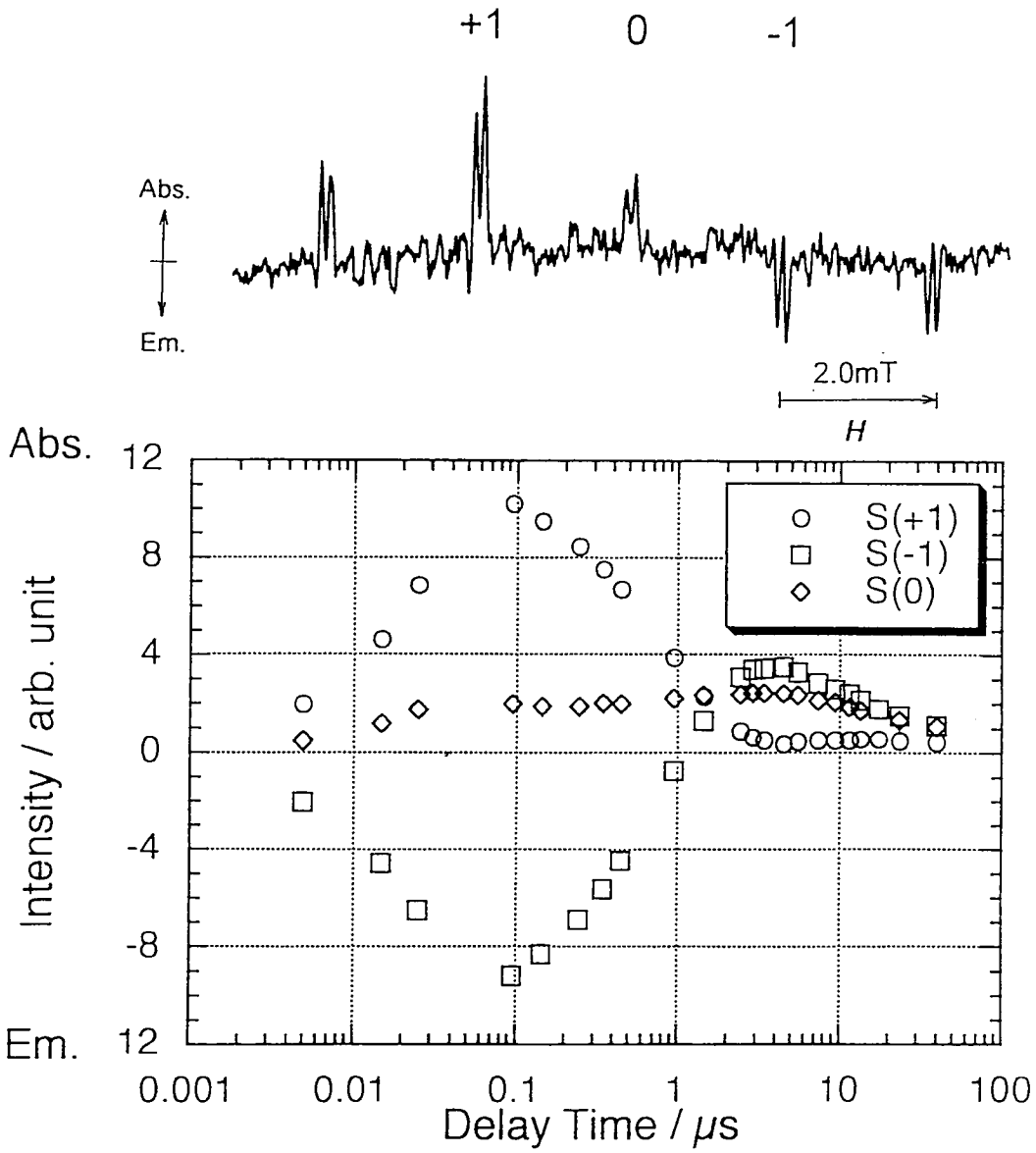


Figure 6-1. TREPR spectrum at 0.5μs and the time profiles of the intensities of the $M_I$ =+1,0,-1 hf lines measured by FT-EPR, of the 2-propanolyl radical in the TEA solution of 1M acetone.

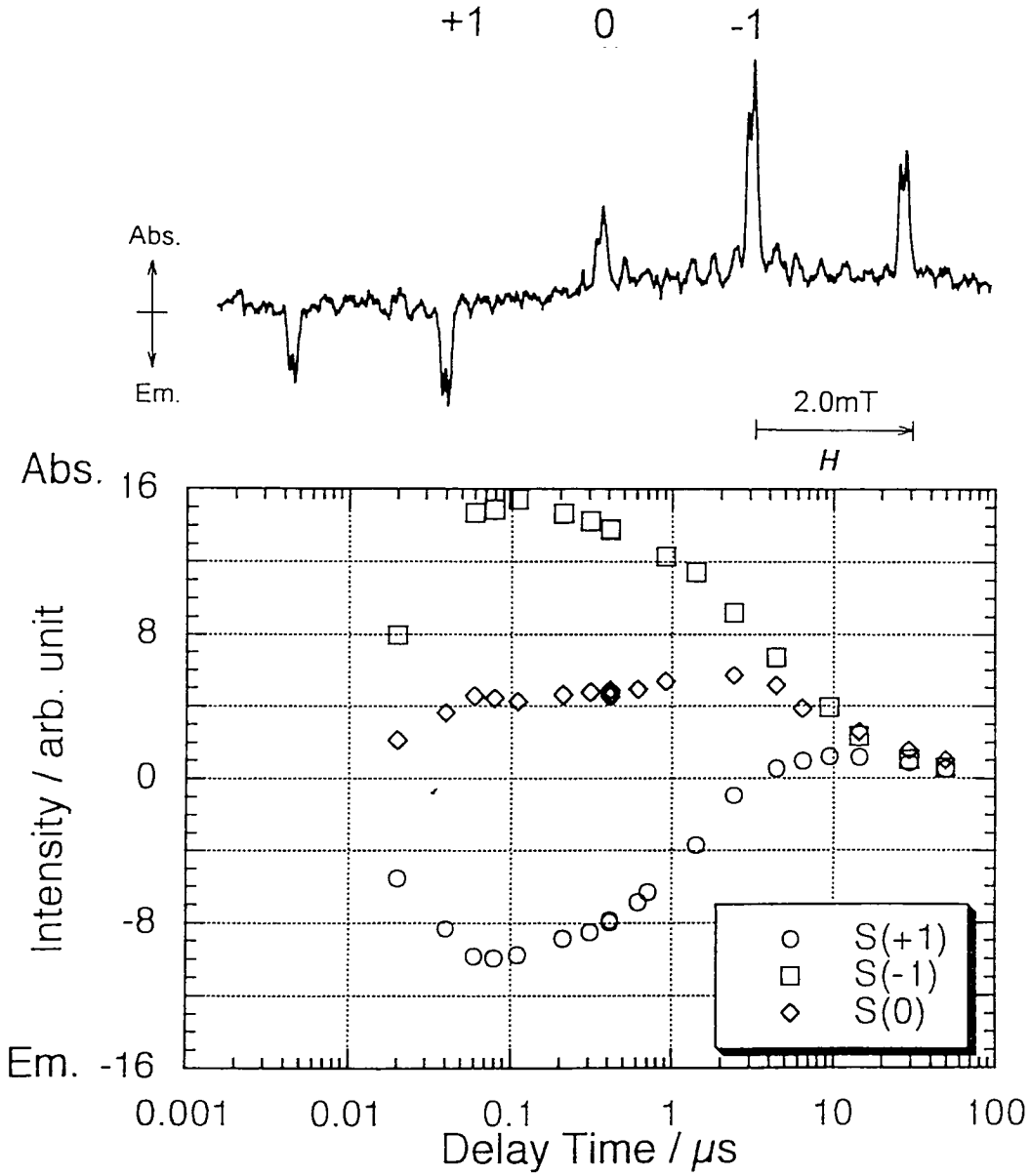


Figure 6-2. TREPR spectrum at 0.5μs and the time profiles of the intensities of the $M_I$ =+1,0,-1 hf lines measured by FT-EPR, of the 2-propanolyl radical in the benzene solution of 1M acetone and 1M TEA.

Here, $k_{2r}$ is the rate constant of the second order radical decay. The equation takes into account that, with the TEA concentrations used in the study, the rates of radical formation are fast compared to the instrument response time so that the initial radical concentration (t=0) is set equal to $N_0$ and the time dependence is determined by chemical decay only.

(2) Geminate-pair RPM

$$P_{RPM} = P^0_{RPM}\left\{\exp(-t/T_1^R) - \exp(-k_f t)\right\} + P^\infty_{RPM}\left\{1 - \exp(-t/T_1^R)\right\}$$

Here, $P^0_{RPM}$ and $P^\infty_{RPM}$ are the initial polarization and the polarization at thermal equilibrium of the geminate-pair RPM, respectively. $T_1^R$ is the spin-lattice relaxation time of the 2-hydroxypropan-2-yl radical. $kf$ is the growth rate constant of the signal due to the geminate-pair RPM. $kf >> 1/T_1^R$ is also assumed.

(3) F-pair polarization

The time development of the F-pair polarization is given by the following equation.

$$\frac{dP_{FRPM}}{dt} = ak_F\left(N_R\right)^2 - \frac{P_{FRPM}}{T_1^R}$$

Here, $k_F$ is the second order rate constant of the development of F-pair RPM. Since the exact solution of this equation is complicated, we use the following approximate solution.

$$P_{FRPM} = ak_F\left(N_0\right)^2 \; T_1^R\left\{\frac{1}{(k_{2r}N_0 t + 1)^2} - \exp(-t/T_1^R)\right\}$$

This equation is considered to be appropriate, as long as the condition, $2k_{2r}N_0T_1^R >> k_{2r}N_0$ t +1, is satisfied. This condition is satisfied in the present case as shown later.

(4) TM

$$P_{TM} = P^0_{TM}\left\{\exp(-t/T_1^R) - \exp\left[-({}^3k_{HA} + 1/T_1^T)t\right]\right\} + P^\infty_{TM}\left\{1 - \exp(-t/T_1^R)\right\}$$

Here, $P^0_{TM}$ and $P^\infty_{TM}$ is the initial polarization and the polarization at thermal equilibrium of TM. $T_1^T$ is the spin-lattice relaxation times of acetone triplet state. ${}^3k_{HA}$ is the rate constant of the hydrogen abstraction reaction. $({}^3k_{HA} + 1/T_1^T) >> 1/T_1^R$ is also assumed.

$\Delta S_M$, $\Sigma S_M$ and $S_0$ should be given by the combinations of the above equations for $P$ and $N_R$. We first discuss the results obtained with the solution of acetone in TEA. In this case, the hydrogen abstraction reaction of acetone in the singlet excited state is considered to be

faster than the ISC process, making the singlet reaction dominant. As shown in Figure 6-3a, $\Delta S_M$ rises quickly reaching its maximum value within 100 ns, it then decays through zero, signifying an inversion from an A/E to an E/A polarization pattern, reaching a minimum around 3 μs. On the other hand, $\Sigma S_M$ and $S_0$, shown in Figure 6-3b, rise slowly reaching a maximum at 2 μs. The measured time profiles are fit in the following way. $\Delta S_M$ reflects contributions from two mechanisms: RPM due to *singlet* geminate-pairs (A/E polarization pattern) and RPM due to *triplet* F-pairs (E/A pattern). Then the time-development of $\Delta S_M$ should be given by the equation,

$$\Delta S_M = \frac{A\{\exp(-t/T_1^R) - \exp(-k_f t)\}}{(k_{2r}N_0 t + 1)} + B\left\{\frac{1}{(k_{2r}N_0 t + 1)^2} - \exp(-t/T_1^R)\right\} \qquad (6\text{-}1)$$

The first term represents the evolution of SP of the geminate-pair RPM, the second the F-pair RPM. The signs of $A$ and $B$ are positive and *negative*, respectively, reflecting the opposite phase of SP. The least-squares fit of the data to eq.6-1 is shown as a solid line in Figure 6-3a. An excellent fit is obtained with the following values of the parameters: $kf = 4.0 \times 10^7$ s$^{-1}$; $T_1^R$ = 0.89 μs and $k_{2r}N_0 = 5.9 \times 10^4$ s$^{-1}$. $T_1^R$ is somewhat smaller than that obtained for 2-hydroxypropan-2-yl radical in 2-propanol. $kf$ is close to that found for the pyrazine/2-propanol system and is likely determined by the time resolution of the experiment. The decay of initial polarization and inversion of the polarization pattern are accounted for very well by the inclusion of the F-pair RPM. It should be also noted that $2\,k_{2r}N_0T_1^R$ is about $10^{-1}$, which satisfies the condition for eq. 6-1 to be appropriate.

$\Sigma S_M$ and $S_0$ represent net absorptive signals. Since their rise time is slow (cf. Figure 6-3b), the contribution of the TM can be neglected. If signal growth and decay are due to relaxation of the spin system to thermal equilibrium and second order chemical decay, respectively, the time profile of these signals is expected to be given by,

$$\Sigma S_M = \frac{A\{1 - \exp(t/T_1^R)\}}{(k_{2r}N_0 t + 1)} \qquad (6\text{-}2)$$

The observed time evolution of $\Sigma S_M$ and corrected $S_0$ can be fit reasonably well to eq.6-2. The least-squares fits, shown by the solid lines in Figure 6-3b, give a rise time of 0.91 μs, which is in

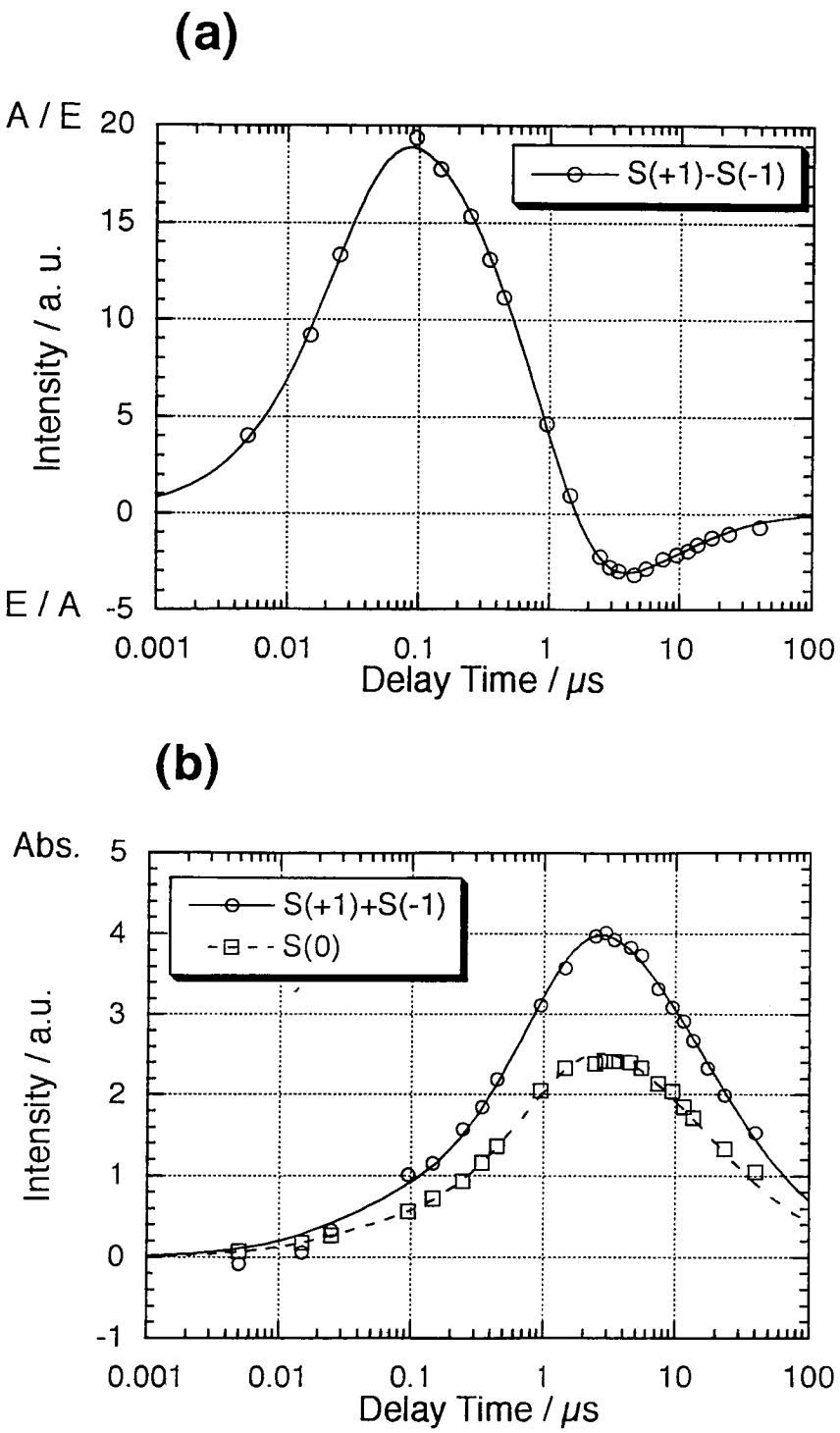


Figure 6-3. (a) The time evolution of $\Delta S_M$ in the TEA solution. The solid line represents the result of a least-squares fit of the data points to eq.6-1.

(b) The time evolutions of $\Sigma S_M$ (O) and the center hf line($M_I = 0$, □ ) in the TEA solution. The time evolution of the intensity of the center hf line has been corrected for contributions from a dewar signal and a signal from the radicals derived from triethylamine. The lines represent the results of least-squares fits of the data points to eq.6-2.

close agreement with $T_1^R$ derived from the time dependence of $\Delta S_M$. Therefore, it can be concluded that the absorptive signal contribution is generated by relaxation of the spin system, born with zero net spin polarization, to thermal equilibrium. The decay of $\Sigma S_M$ and $S_0$ is well explained by second order chemical decay of the radical with $k_{2r}N_0 = 5.9 \times 10^4\ s^{-1}$

The results obtained with the solution in benzene can be interpreted in a similar way. In this case, ISC is faster than the reaction involving singlet excited state acetone so that the triplet state reaction becomes dominant. The time-profile of the $\Delta S_M$ signal is shown in Figure 6-4a. The mechanisms that produce SP are the RPM due to *triplet* geminate pair initially and F-pair at later times. In this case the time dependence of $\Delta S_M$ is also given by eq.6-1, but $A$ and $B$ now have equal signs since both mechanisms give rise to the same (E/A) SP pattern. The growth of the signal can be fit with $kf = 4.0 \times 10^7\ s^{-1}$ However, $T_1^R$ and $k_{2r}N_0$ cannot be determined accurately from the $\Delta S_M$ data alone, since the first and the second terms of eq.6-1 are comparable. Therefore, we tried to determine the values of these parameters using $\Sigma S_M$ and $S_0$ data.

As shown in Figure 6-4b, $\Sigma S_M$ and $S_0$ show a fast rise during the first 100 ns which is followed by a more gradual increase with the signals reaching a maximum at 1.5 μs. Since the reaction of triplet acetone with TEA is fast, the initial rise is likely to be due to TM.[1] We try to fit the data by assuming that the first rise is due to TM CIDEP and that the slow increase is produced by the relaxation of the spin system to thermal equilibrium. The time-developments of $\Sigma S_M$ and $S_0$ are given by ,

$$\Sigma S_M = \frac{A\left\{\exp(-t/T_1^R) - \exp(-k_{TM}t)\right\} + B\left\{1 - \exp(-t/T_1^R)\right\}}{(k_{2r}N_0 t + 1)} \qquad (6\text{-}3)$$

---

[1] This may also include the polarization transferred from the triplet precursor at thermal equilibrium. In the present study, this contribution could not be distinguished from that of TM.

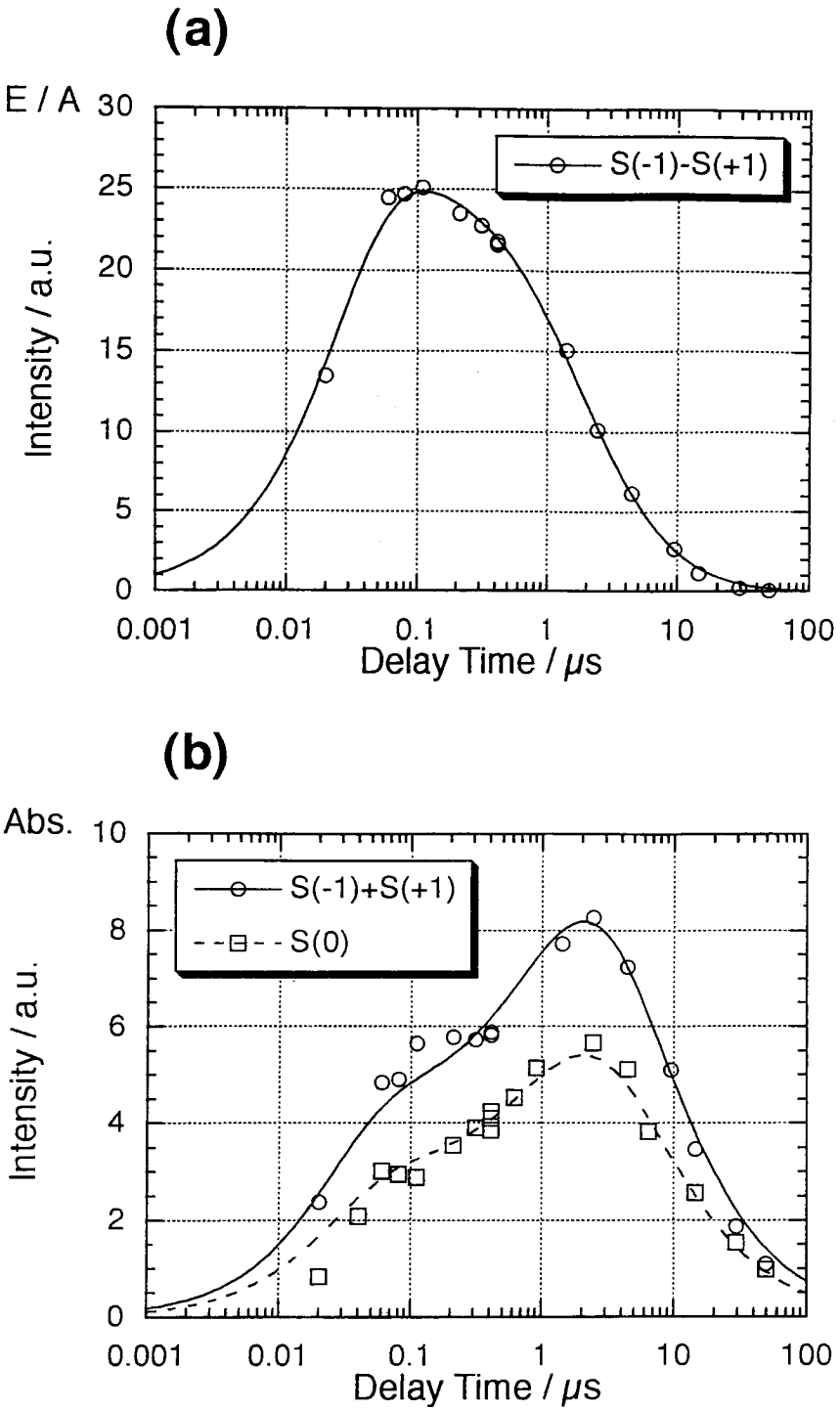


Figure 6-4. (a) The time evolution of $\Delta S_M$ in the benzene solution. The line represents the result of a least-squares fit of the data points to eq.6-1.

(b) The time evolutions of $\Sigma S_M$ (O) and the center hf line($M_I = 0$, □ ) in the benzene solution. The time evolution of the intensity of the center hf line has been corrected for contributions from a dewar signal and a signal from the radicals derived from triethylamine. The lines represent the results of least-squares fits of the data points to eq.6-3.

Here, $k_{TM}$ is the apparent growth rate constant of the polarization due to TM. The first term of eq.6-3 represents the evolution of SP of TM, and the second the relaxation to thermal equilibrium of SP due to both TM and the geminate-pair RPM. The experimental data of $\Delta S_M$, $\Sigma S_M$ and $S_0$ are fitted quite well with $k_{TM} = kf = 4.0 \times 10^7\ s^{-1}$, $T_1^R = 0.77\ \mu s$, $k_{2r}N_0 = 1.6 \times 10^5\ s^{-1}$, as is shown in Figure 6-4a and 4b. The results are consistent with those obtained from the acetone/TEA system. The value obtained for $k_{TM}$ and $kf$ apparently reflect the instrument response time.

On the basis of the present results, we now make two comments with regards to the CIDEP of 2-hydroxypropan-2-yl radical. First, judging from the fast rise time of the $\Sigma S_M$ and center line signals given by the acetone/TEA solution in benzene, the rate of the hydrogen abstraction reaction is much faster than in the acetone/2-propanol system. Nevertheless, the TM contribution to the SP must be less than the thermal equilibrium polarization since a large fraction of the signal intensity develops over a period of 1.5 μs (cf. Figure 6-4b) due to spin-lattice relaxation. This observation lends support to the conclusion that TM CIDEP is negligible in the reaction of acetone with 2-propanol.[25] In a previous TR-EPR study it was established that population differences between top and bottom sublevels of triplet states of aliphatic ketones are rather small.[52] Therefore, even under optimum conditions, the contribution of the TM is expected to be small. Second, the experiments show that the F-pair RPM contribution is very significant in both systems, it represents 25-35 % of that of the geminate-pair RPM. Though the contribution due to F-pairs is not so evident in the decay of $\Delta S_M$ for acetone/TEA in benzene, a careful analysis nevertheless shows that it must be significant. It is not possible to determine the spin-lattice relaxation time accurately without taking account of the F-pair contribution.

## 6-4. Conclusion

The time profiles of the FT-EPR signals of 2-hydroxypropan-2-yl radical produced by the photochemical reaction of acetone with TEA can be explained satisfactorily

assuming that the reaction can occur via the acetone singlet and/or triplet excited state depending on TEA concentration as previously proposed. They established that the spin polarization is generated by the singlet and/or triplet geminate pairs RPM and triplet F-pairs RPM. The net absorptive character of the FT-EPR spectra is mainly due to the relaxation to Boltzmann equilibrium. The contribution of TM CIDEP is small compared to the thermal equilibrium spin polarization even in the case where the triplet reaction may be fast enough to compete with relaxation of the triplet spin system. The F-pair RPM is found to make a significant contribution to the spin polarization.

# Chapter 7 CW and FT-EPR Investigation of the Quenching Reaction of the 2-Hydroxypropan-2-yl Radical

## 7-1. Introduction

Hydrogen abstraction reactions of nitrogen heterocyclic molecules (azaaromatics) such as pyrazine and quinoxaline have been investigated by using both laser photolysis [26,53] and time-resolved EPR (TREPR).[23,27] It has been shown that these molecules in the excited triplet states abstract hydrogen from alchohols and other hydrogen donors. When pyrazine in 2-propanol is photolyzed, pyrazinyl and 2-hydroxypropan-2-yl radicals are formed to give CIDEP (Chemically Induced Dynamic Electron Polarization) spectra. Likewise quinoxalinyl and 2-hydroxypropan-2-yl radicals are produced by the photolysis of quinoxaline in 2-propanol, but the CIDEP spectrum of 2-hydroxypropan-2-yl was not observed in previous EPR work.[23,27] It was concluded that the 2-hydroxypropan-2-yl radical is quickly quenched by ground state quinoxaline. The same conclusion was reached in laser photolysis studies.[26,53] It is assumed that the quenching reaction of the 2-hydroxypropan-2-yl radical by pyrazine is too slow to be observed by laser photolysis and TREPR.

In the present chapter the author investigates the time evolution of the CIDEP signals of the pyrazine/2-propanol system measured with CW- and FT-EPR methods in more detail. We show that the CIDEP spectrum of the 2-hydroxypropan-2-yl radical is strongly dependent on the pyrazine concentration and that quenching of the 2-hydroxypropan-2-yl radical by pyrazine can be studied with TREPR. Similar quenching reactions take place with quinoxaline and p-benzoquinone. With an analysis of the concentration dependences of the CIDEP signals, we determine the quenching rate constants. The information on the stability of the 2-hydroxypropan-2-yl radical is also needed for a detailed analysis of radical diffusion by the transient grating technique.[54,55]

Since the pyrazinyl radical is also produced by the reaction of the 2-hydroxypropan-2-yl radical with pyrazine, this system is suited to study the dynamics of spin polarization produced by the secondary reaction. Superior time resolution of the FT-EPR technique enables us to observe time development of the spin system in the first 10~500 ns time region of the reaction. Therefore, it is studied that the time profiles of the CIDEP signals of both pyrazinyl and 2-hydroxypropan-2-yl radicals by FT-EPR.

## 7-2 Experimental

Pyrazine, quinoxaline were commercially available special grade reagents used as received. p-BQ was recrystallized in ethanol.

## 7-3. Results and Discussion

### 7.3.1 CW-TREPR

Figure 7-1 shows the CIDEP spectra of the pyrazine / 2-propanol system at room temperature obtained with different delay times. The spectra consist of sharp well resolved peaks separated by 1.98 mT assigned to the 2-hydroxypropan-2-yl radical and a broad peak in the center of the spectrum assigned to the pyrazinyl radical. The spectral pattern is net absorption with a slight E/A ( low field emission and high field absorption ) type distortion. The result indicates that the hydrogen abstraction reaction of triplet pyrazine occurs very rapidly, so that the triplet mechanism (TM) polarization ( net A) is dominant with a small contribution of the $ST_0$ mixing radical pair mechanism (RPM, E/A).[26,53] The reaction to produce these radicals is,

$$\text{(I)} \qquad {}^3Py^* + (CH_3)_2CHOH \longrightarrow \cdot PyH + (CH_3)_2\dot{C}OH$$

The time evolution of the spectrum is affected sensitively by the pyrazine concentration. When the pyrazine concentration is 0.10 M (Figure 7-1a), the spectrum of the 2-hydroxypropan-2-yl radical almost disappears within 1 μs. On the other hand, when the concentration of pyrazine is 0.01M (Figure 7-1b), the 2-hydroxypropan-2-yl radical

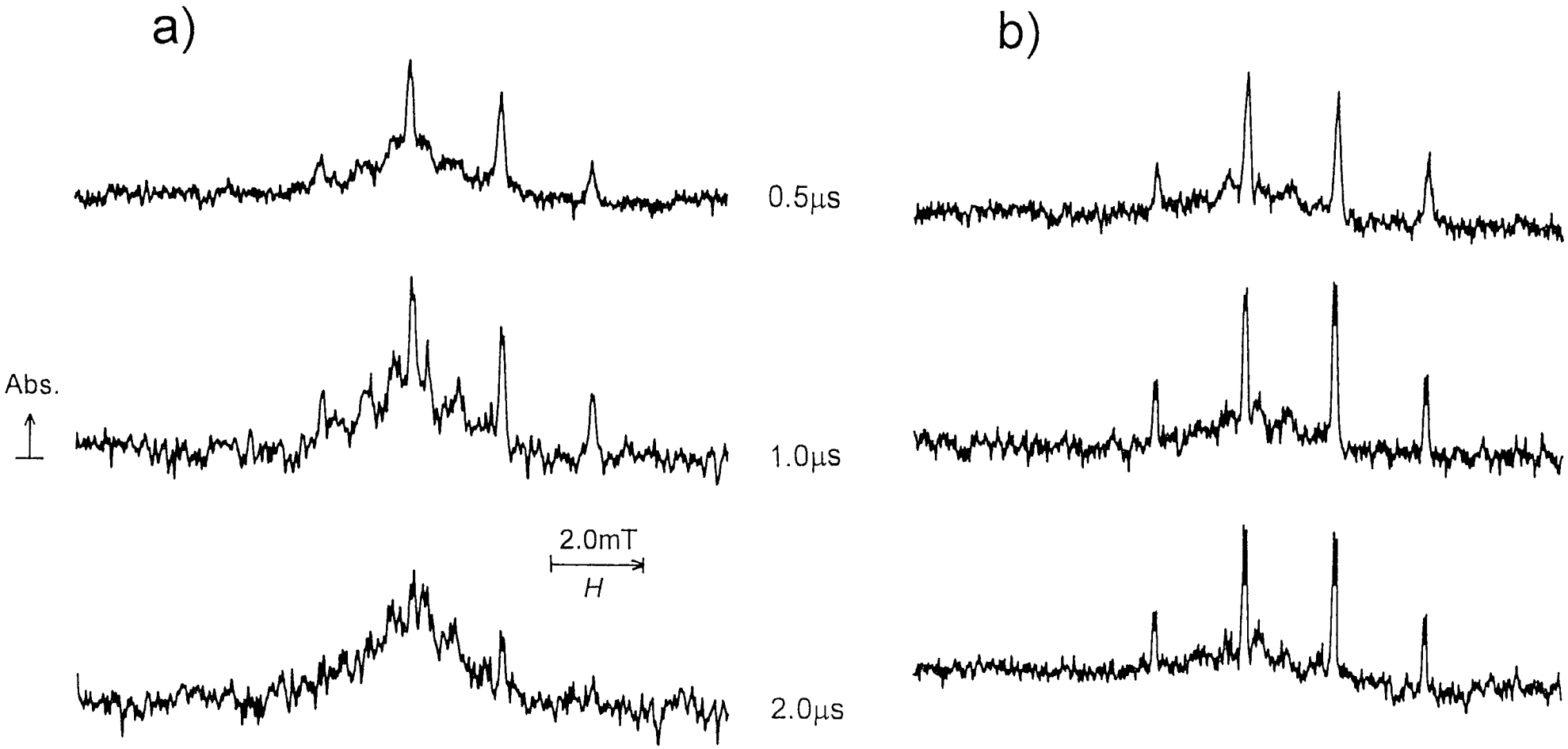




Figure 7-1 Time evolutions of CIDEP spectra given by the pyrazine / 2-propanol system at room temperature. The concentrations of pyrazine were (a) 0.10 M and (b) 0.010M.

spectrum remains strong even at more than 2 μs after excitation. By contrast the decay of the pyrazinyl radical spectrum is not affected by the pyrazine concentration. Figure 7-2 shows the time profiles of the transient EPR signals of (a) the pyrazinyl and (b) 2-hydroxypropan-2-yl radicals at several pyrazine concentrations measured by CW-TREPR at 0°C. The decays of the signals are approximately given by single exponential curves. The time evolution of the pyrazinyl radical signal is independent of the pyrazine concentration within the time resolution of our CW-TREPR system, and is determined by the spin-lattice ($T_1$) and spin-spin ($T_2$) relaxation times. On the other hand, the decay of the 2-hydroxypropan-2-yl radical signal clearly depends on the pyrazine concentration. The decay rate increases with increasing of the pyrazine concentration. This concentration dependence suggests that the 2-hydroxypropan-2-yl radical is quenched by pyrazine according to the following scheme,

$$\text{(II)} \qquad \text{Py} + (\text{CH}_3)_2\dot{\text{C}}\text{OH} \xrightarrow{k_q'} \cdot\text{PyH} + (\text{CH}_3)_2\text{CO}$$

In a precise analysis the time development of the transient EPR signal in a CW experiment can be obtained by solving a modified Bloch equation, but the solution is a complex function of $T_1$, $T_2$, and the effective microwave power. When $T_1 >> T_2$, in the limit of low microwave power and in the absence of quenching, the signal at resonance is expected to decay exponentially with $k_d^0 = 1/T_1$.[56] The decay time of the 2-hydroxypropan-2-yl signal in the presence of pyrazine is shorter than $1/k_d^0$ presumably because of the chemical quenching. Then, the signal decay is determined by $(k_q[\text{Py}] + k_d^0)$, where $k_q$ is the second order rate constant of the quenching reaction of the 2-hydroxypropan-2-yl by pyrazine. In Figure 7-3a, the observed decay rate $(k_q[\text{Py}] + k_d^0)$ of 2-hydroxypropan-2-yl is plotted against the pyrazine concentration ([Py]). In making the analysis of the decay, the initial part of the decay was omitted to avoid the effect of the bimolecular recombination reaction. The plot gives the quenching rate constant $k_q = 6.6 \times 10^6\ \text{M}^{-1}\,\text{s}^{-1}$ The linear relation between rate of signal decay ($k_d$) and [Py] supports our

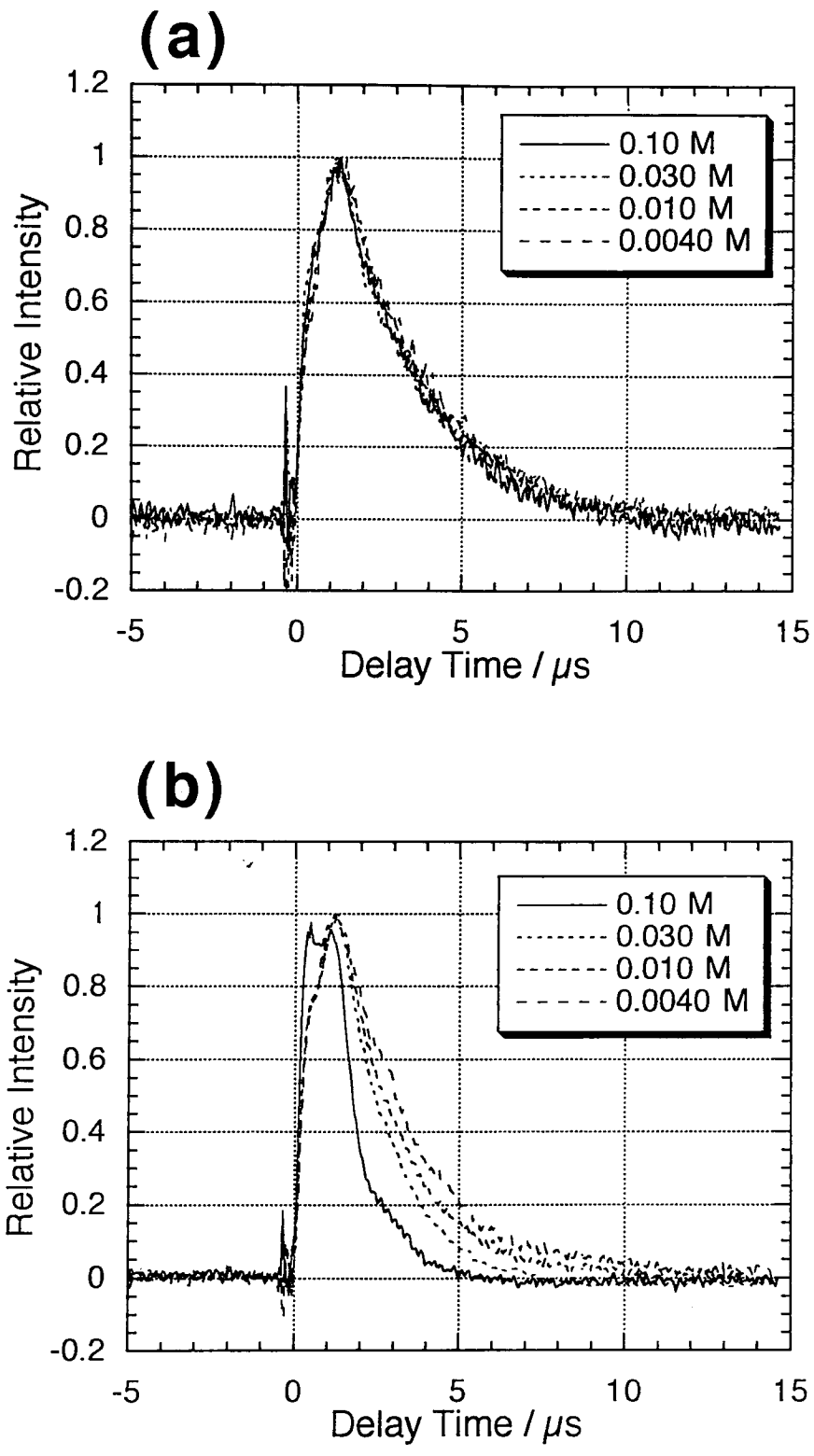


Figure 7-2 Time evolutions of EPR signals (a) pyrazinyl radical (·PyH) and (b) 2-hydroxypropan-2-yl radical measured by CW TREPR at 0°C.

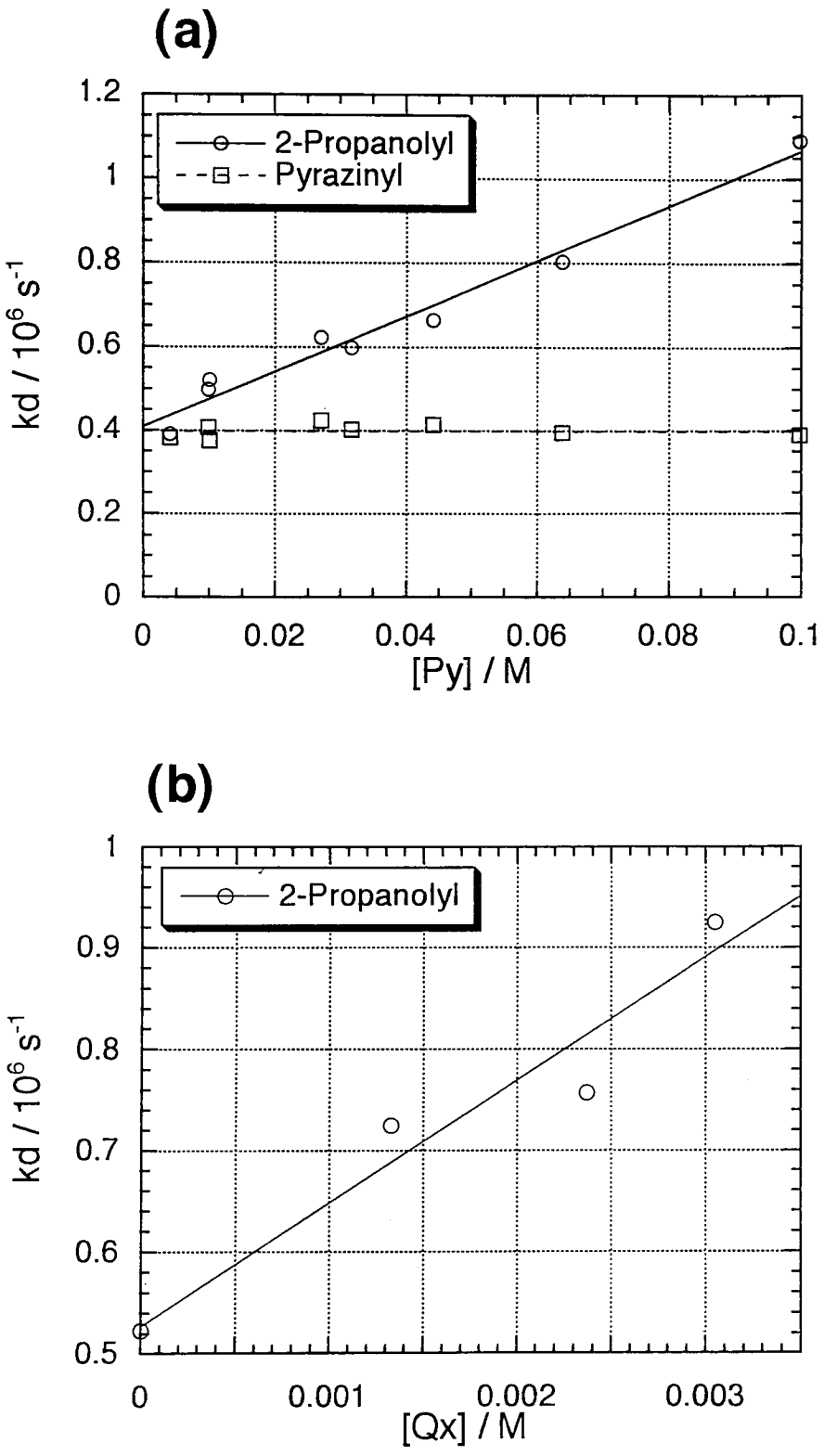


Figure 7-3 (a) The observed decay rate ( $k_d=k_q[Py]+k_d^0$) of 2-hydroxypropan-2-yl at 0°C is plotted against the pyrazine concentration ([Py]). (b) A similar plot for the system of 0.01M pyrazine solution containing quinoxaline, tempertature 0°C.

scheme. Extrapolation of the linear relation to [Py] = 0 gives $1/k_d^0$ = 2.4 μs, which is in good agreement with the reported value of $T_1^{R1}$ = 2.7 μs.[6,47]

Other azaaromatics are expected to quench the 2-hydroxypropan-2-yl radical similarly. For example, in the case of quinoxaline, the hydrogen abstraction reaction rate of triplet quinoxaline is much slower ($k_T = 1.4 \times 10^4 M^{-1} s^{-1}$ ) than that of pyrazine,[26,53] but quinoxaline is believed to be a good quencher of the 2-hydroxypropan-2-yl radical.[23,26,27,53] Though the photolysis of a dilute solution of quinoxaline in 2-propanol shows a weak 2-hydroxypropan-2-yl signal, it is too weak for a kinetic study. Therefore we studied pyrazine solutions containing small amounts of quinoxaline to determine the rate constant of quenching by quinoxaline. If quinoxaline quenches the 2-hydroxypropan-2-yl radical effectively, the time evolution of the 2-hydroxypropan-2-yl signal should show a pronounced quenching effect.

Results of CIDEP measurements on a 0.010M pyrazine solution containing quinoxaline at concentrations ranging from 0.001M to 0.003 M at 0°C presented in Figure 7-3b show that the decay rates of the 2-hydroxypropan-2-yl signals are markedly increased. From the plot of decay rate versus quinoxaline concentration we derive $k_q = 1.2 \times 10^8 M^{-1} s^{-1}$. By comparison, $k_q$ was previously estimated to be $1.6 \times 10^8 M^{-1} s^{-1}$ by laser photolysis at room temperature.[26,53] Considering the uncertainties involved in both measurements, the agreement is considered to be good. It is thus shown that the quenching rate by pyrazine is about 20 times slower than that by quinoxaline.

It seems worthwhile to examine whether or not such a quenching reaction commonly takes place with different types of molecules. CIDEP studies have been carried out frequently with quinone and carbonyl compounds in alcohols, but little attention has been paid to such a quenching reaction. We have studied the concentration dependence of time-resolved EPR spectra obtained by the photolysis of p-benzoquinone(p-BQ)/2-propanol. Figure 7-4 shows the CIDEP spectra obtained 1.0 μs after laser excitation at 0°C. The spectra consist of three pairs of hf lines due to the p-BQ semiquinone radical

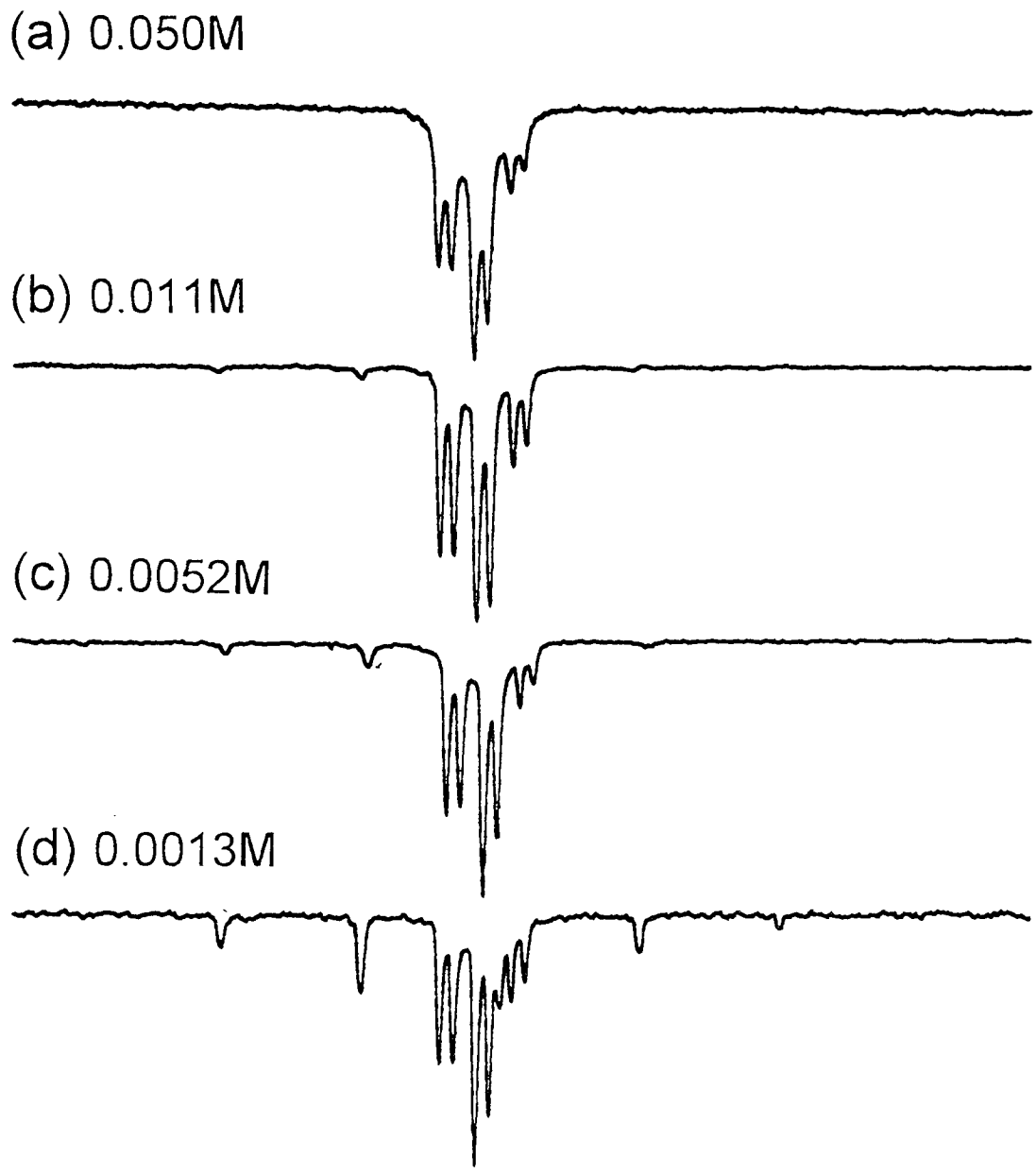


Figure 7-4 The concentration dependence of the CIDEP spectra given by the p-BQ / 2-propanol system at 0°C. p-BQ concentrations (a) 0.050M, (b) 0.011M, (c) 0.0052M, (d) 0.0013M.

and widely separated peaks coming from 2-hydroxypropan-2-yl. It is seen that the relative intensity of the 2-hydroxypropan-2-yl spectrum is strongly dependent on p-BQ concentration. It increases with decreasing the p-BQ concentration. The result clearly established that 2-hydroxypropan-2-yl is quenched by p-BQ as is the case for pyrazine and quinoxaline. A Stern-Volmer type plot of the relative intensities of 2-hydroxypropan-2-yl gives a quenching rate constant $k_q \approx 10^8 M^{-1} s^{-1}$. This value is much larger than that of pyrazine and a bit smaller than that of quinoxaline. The quenching reaction of the 2-hydroxypropan-2-yl radical may occur commonly with many other molecules.

7.3.2. FT-EPR studies of pyrazine/2-propanol

Since the quenching reaction of the 2-hydroxypropan-2-yl radical produces the pyrazinyl radical, this should affect the time profile of the pyrazinyl signal. Figure 7-4 shows the time evolutions of the transient EPR signals of the pyrazinyl and the 2-hydroxypropan-2-yl ( $M_I = \pm 1$ peak) radicals measured by FT-EPR technique at room temperature. The concentration of pyrazine is 0.1M. The time evolution of the pyrazinyl signal shows a peculiar behavior, a fast rise in the first 80ns, followed by a nearly constant intensity during the next 1μs, and then a decay. This feature could not be observed clearly with CW-TREPR. We try to rationalize this behavior in terms of two radical generation steps, one fast ($\sim 10^8 s^{-1}$) and one slow ($\sim 10^6 s^{-1}$), and an exponential signal decay step. Signal decay is attributed to spin-lattice relaxation, as in the analysis of the CW-TREPR data. The hydrogen abstraction rate involving triplet pyrazine (reaction I) is believed to be larger than $10^9 s^{-1}$. Therefore the fast rise component is determined by the time resolution of the experiment which is estimated to be about 30ns.[57] The slow rise component is considered to be due to the polarization development produced by the secondary reaction of the 2-hydroxypropan-2-yl radical with pyrazine (reaction II) in which spin polarization is transferred from the 2-hydroxypropan-2-yl radical to the pyrazinyl radical. On the other

hand, the time evolution of the 2-hydroxypropan-2-yl signal can be accounted for in terms of single exponential signal generation and decay steps.

When the pyrazinyl radical is produced by reaction II, the spin polarization of the 2-hydroxypropan-2-yl radical must be conserved and transferred to the pyrazinyl radical formed in this reaction. However, because the reaction is not selective with respect to the nuclear spin states of pyrazine, only the *net* polarization of the 2-hydroxypropan-2-yl radical is conserved.[31,58,59)]

In the following we try to fit the obtained time profiles. The signal intensity is given by the product of spin polarization and radical concentration. For simplicity, we assume that the signal intensity at thermal equilibrium is negligibly small. This is a good approximation in the present case because the initial CIDEP intensity is much larger than the signal at thermal equilibrium. Then the time development of the EPR signals can be described in the following way.

(a) 2-hydroxypropan-2-yl radical

The time development of the spin polarization due to different CIDEP mechanisms are differentiated by taking the difference in intensities between the $M_I = +1$ and -1 hf lines ($\Delta S_M$), or the sum of the intensities of the +1 and -1 hf lines ($\Sigma S_M$)[8] $\Delta S_M$ represents the spin polarization due to RPM, while $\Sigma S_M$ represents the net absorption or emission mainly due to TM. They decay by both the spin-lattice relaxation and the chemical quenching. Then, $\Sigma S_M$ and $\Delta S_M$ are given by the following equations:

$$\Sigma S_M = A \cdot \left[ \exp\left\{ -\left( k_q' + 1/T_1^{R1} \right) t \right\} - \exp\left( -k_{TM} t \right) \right] \qquad (7\text{-}1)$$

$$\Delta S_M = B \cdot \left[ \exp\left\{ -\left( k_q' + 1/T_1^{R1} \right) t \right\} - \exp\left( -k_f t \right) \right] \qquad (7\text{-}2)$$

Here, $T_1^{R1}$ is the spin-lattice relaxation time of the 2-hydroxypropan-2-yl radical, $k_{TM}$ and $kf$ are the rate constants of the TM and the geminate pair RPM CIDEP generation, which are considered to be much larger than $k_q'$. $k_q' = k_q[\mathrm{Py}]$ is the rate of quenching of 2-hydroxypropan-2-yl by pyrazine. The intrinsic $k_{TM}$ is given by the sum of the primary hydrogen abstraction reaction rate ($k_{HA}$) and the spin-lattice relaxation rate of triplet

pyrazine ($T_1^T$), $k_{TM}=k_{HA}+1/T_1^T$ In the present case both $1/k_{TM}$ and $1/kf$ are much shorter than the instrumental response time($1/k_i$), so that $k_i$ is the rate of signal generation of both $\Sigma S_M$ and $\Delta S_M$. The spin-lattice relaxation times of $\Sigma S_M$ and $\Delta S_M$ are assumed to be the same. This is normally a good approximation except for special cases in which spin exchange or chemical exchange processes take place effectively. Consequently, the time dependence of $\Sigma S_M$ and $\Delta S_M$ are the same with apparent rise rate $k_i$ and decay rate $k_q'+1/T_1^{R1}$ Here we also assume that second order decay of the 2-hydroxypropan-2-yl radical is much slower than the quenching reaction and can be ignored. Since the rate constant of the bimolecular recombination reaction is $10^9\,M^{-1}\,s^{-1}$, this assumption is valid when the radical concentration is much lower than $10^{-4}$ M. The fact that the experimental results are well reproduced by eq.7-2 supports the validity of this assumption. The least squares fits to the data shown in Figure 7-5b as solid and broken lines give $k_i=3.7\times10^7\,s^{-1}$, $k_q'+1/T_1^{R1}=0.88\times10^6\,s^{-1}$

(b) pyrazinyl radical

There are two processes that give rise to the pyrazinyl radical, the primary hydrogen abstraction reaction of triplet pyrazine and the secondary reaction of the 2-hydroxypropan-2-yl radical with pyrazine. In the primary reaction spin polarization is produced by TM and RPM and its time evolution is given by,

$$P_1^{R2}=C\cdot\left[\exp(-t/T_1^{R2})-\exp(-k_i t)\right] \qquad (7\text{-}3)$$

Here, $T_1^{R2}$ is the spin-lattice relaxation time of the pyrazinyl radical and $1/k_i$ is the instrumental responce time. In reaction II spin polarization is transferred from the 2-hydroxypropan-2-yl radical and decays by spin-lattice relaxation. Then the time evolution is described by the following differential equation.

$$\frac{dP_2^{R2}}{dt}=f\;P_{net}^{R1}-\frac{P_2^{R2}}{T_1^{R2}} \qquad (4)$$

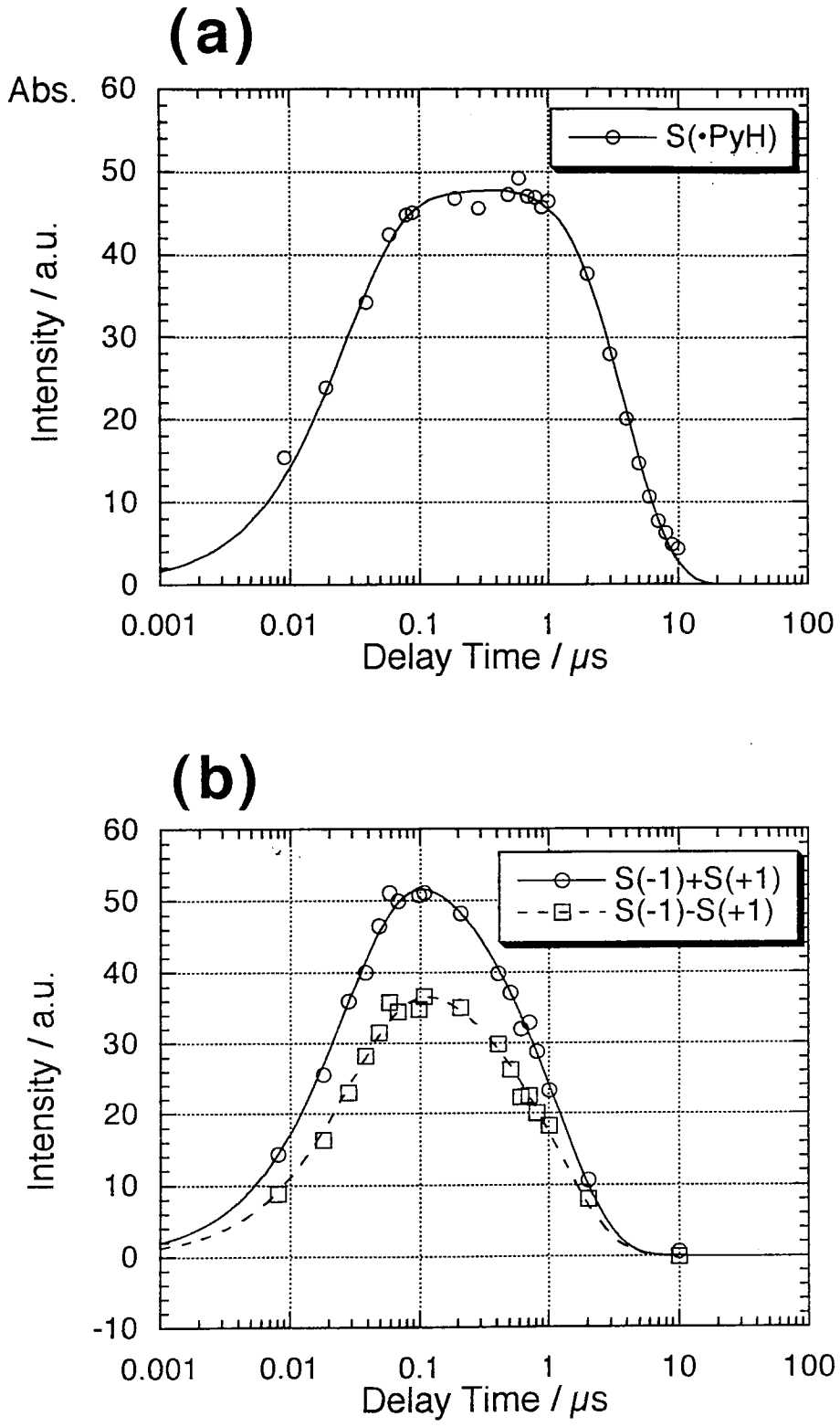


Figure 7-5 Time evolutions of the EPR signals of (a) pyrazinyl radical and (b) 2-hydroxypropan-2-yl radical measured by FT-EPR at room temperature.

Here, $P_{net}^{R1}$ represents the *net* polarization of the 2-hydroxypropan-2-yl radical, $f$ represents the rate constant of spin polarization transfer. $P_{net}^{R1}$ is given by eq.7-1 with $k_{TM} = k_i$. The polarization generated by reaction II, obtained by solving eq.7-4, is given by

$$P_2^{R2} = A \cdot f \cdot \left[ \frac{e^{-k_i t} - e^{-t/T_1^{R2}}}{k_i - 1/T_1^{R2}} - \frac{e^{-(k_q' + 1/T_1^{R1})t} - e^{-t/T_1^{R2}}}{k_q' + 1/T_1^{R1} - 1/T_1^{R2}} \right] \quad (7\text{-}5)$$

We further assume that the lifetime of the pyrazinyl radical is long compared with the spin-lattice relaxation time. The total polarization of the pyrazinyl radical is obtained by adding eq.7-3 and 7-5. Then the time evolution of the transient EPR signal of the pyrazinyl radical is given by

$$S(\cdot\mathrm{PyH}) = D \cdot \left[ \exp(-t/T_1^{R2}) - r \cdot \exp\left\{ -(k_q' + 1/T_1^{R1})t \right\} - (1-r) \cdot \exp(-k_i t) \right] \quad (7\text{-}6)$$

The signal rises with fast and slow rate constants, $k_i$ and ($k_q' + 1/T_1^{R1}$), respectively, and then decays with $T_1^{R2}$ The parameter $r$ represents the contribution of the secondary spin polarization relative to the total spin polarization.

The least squares fit of the data with eq.7-6 is shown in Figure 7-5a as a solid line. An excellent fit is obtained with values: $k_i = 3.7 \times 10^7\ s^{-1}$, $T_1^{R2} = 2.86\mu s$, $k_q' + 1/T_1^{R2} = 0.88 \times 10^6\ s^{-1}$ ( obtained from the analysis of the data shown in Figure 5b ), and r = 0.52. Using the reported value of $T_1^{R1}$ = 2.7μs of the 2-hydroxypropan-2-yl radical and [Py]=0.1M, the quenching rate constant $k_q$ is found to be $5.1 \times 10^6\ M^{-1} s^{-1}$ This values is in reasonable agreement with that obtained from the CW-TREPR measurements. $r$ = 0.52 means that half of the signal intensity from the pyrazinyl radical is due to the quenching reaction.

## 7-4. Conclusion

It is found that the 2-hydroxypropan-2-yl radical is quenched effectively by pyrazine, quinoxaline and p-benzoquinone. CW-EPR measurements show that the quenching rate constants are $6.6 \times 10^6$, $1.2 \times 10^8$, and $\sim 10^8\ M^{-1} s^{-1}$ for pyrazine, quinoxaline, and p-benzoquinone, respectively. The time profiles of the EPR signals of the pyrazinyl

and 2-hydroxypropan-2-yl radicals measured by the FT-EPR technique are analyzed in detail. They are satisfactorily explained in terms of the reaction schemes involving the primary hydrogen abstraction reaction and a subsequent secondary quenching reaction of the 2-hydroxypropan-2-yl radical by pyrazine. It is shown that half of the signal intensity of the pyrazinyl radical in 0.1M pyrazine solution arises from the polarization transfer from the 2-hydroxypropan-2-yl radical. The results indicate that the quenching of the 2-hydroxypropan-2-yl radical is a reaction that may take place with many compounds.

# Chapter 8. An Analysis of the CIDEP Mechanisms in the Hydrogen Abstraction Reactions of Excited Quinoxaline and Related Compounds

## 8-1. Introduction

CIDEP spectra of some azaaromatic compounds (azaaromatics) such as quinoxaline and phenazine are among such cases. These compounds were investigated in early TREPR studies.[23,27] In the photolysis of quinoxaline and phenazine in 2-propanol totally emissive CIDEP spectra were observed and assigned to the quinoxalinyl and phenazinyl radicals, respectively, which were produced by hydrogen abstraction reactions of the triplet states from 2-propanol. It is known that the excited triplet states of most of azaaromatics, including quinoxaline and phenazine undergo hydrogen abstraction reactions in the presence of appropriate hydrogen donors.[23,26,27,53] Since the intersystem crossing favorably populates the top spin sublevels of these $^3\pi\pi^*$ azaromatics,[23,27,60,61] the net emissive (E) spin polarization was ascribed to TM. However, the reaction rate of triplet quinoxaline in 2-propanol was estimated to be $1.8\times10^5 s^{-1}$ by the transient absorption method.[26,53] This rate is far too slow to produce an effective TM polarization, because the spin-lattice relaxation rate of an organic triplet state molecule is usually on the order of $10^8$~$10^9$ $s^{-1}$ This situation is different from the case of pyrazine where the hydrogen abstraction rate of $^3n\pi^*$ pyrazine is very fast and the involvement of TM is well established.[23,26,27,53,62] Thus the origin of the net emissive polarization of $^3\pi\pi^*$ azaaromatics is uncertain. Considering a relatively long lifetime of triplet quinoxaline in 2-propanol, the RTPM appears to be a possible candidate of the emissive polarization.

The spin polarization due to RTPM is produced through the interaction between doublet radicals and triplet state molecules. The generation mechanism of the RTPM polarization is explained on the basis of the doublet-quartet mixing in a radical-triplet pair. Recent studies suggested that the RTPM includes two mechanisms, one generating a net polarization and the other producing a hyperfine dependent polarization, which resemble

the $ST_-$ and $ST_0$ mixing in the RPM, respectively.[17,18] Detailed studies of the RTPM may provide useful information not only about the interactions in radical-triplet pairs but also the quenching processes of excited states by radicals that have not been studied in detail by other methods. Most of the published reports on RTPM, however, have been concerned with the spin polarization generated by the interaction between stable radicals such as nitroxides and excited triplet state molecules. The importance of the RTPM polarization in the CIDEP spectra of reaction intermediate radicals has not been clearly recognized except in the cases of benzil and 1-naphthol.[16,18] The main reason for this is the difficulty to satisfy the condition under which collisions between radicals and triplet molecules are sufficiently frequent with long correlation times required for effective RTPM interactions. This requires relatively long lifetimes of triplet molecules and enough concentrations of both radicals and triplet molecules.

In this chapter, the author has investigated the CIDEP spectra obtained by the photolysis of quinoxaline, phenazine and quinoline in 2-propanol in detail. Both TREPR and transient absorption experiments have been made on these systems at various concentrations and temperatures. Time dependent changes of the CIDEP spectra show involvement various CIDEP mechanisms. Relatively long-lived triplet states of these molecules satisfy the condition to observe the polarization due to the RTPM. We have tried to clarify the CIDEP mechanisms and dynamics of spin polarization from an analysis of the time evolution of the transient EPR signals. It is shown that the observed net E polarization is consistently explained by the RTPM.

## 8-2. Experimental

Transient absorption experiments were carried out with a lab-built spectrometer of conventional design. A 150W Xe lamp was used as a reference light source operating with a flash. A light transmitted through a sample was analyzed by a monochrometer and detected by a photomultiplier tube (Hamamatsu Photonics). Time evolution signals were

recorded with a digital oscilloscope and data were stored and processed by a personal computer.

Quinoxaline, phenazine and quinoline were commercially available special grade reagents ( Nakalai tesque ) used as received. Special grade solvents were used without further purification.

## 8-3. Results and discussion

### 8.3.1. CIDEP spectra under different conditions

First, we show the CIDEP results in the photolysis of quinoxaline, phenazine, and quinoline in 2-propanol under different conditions.

In the photolysis of quinoxaline (Qx) in 2-propanol the photochemical reaction is believed to proceed by the following scheme.[23,26,27,53)]

(I) $^3Qx^* + (CH_3)_2CHOH \rightarrow \cdot QxH + (CH_3)_2\dot{C}OH$

(II) $(CH_3)_2\dot{C}OH + Qx \rightarrow \cdot QxH + (CH_3)_2CO$

Triplet state quinoxaline produced by photoexcitation abstracts a hydrogen atom from 2-propanol, and produces quinoxalinyl and 2-hydroxypropan-2-yl radicals. The 2-hydroxypropan-2-yl radical is quickly quenched by ground state quinoxaline and produces another quinoxalinyl radical as reported before. [23,26,27,53,62)] Other azaaromatics such as phenazine, quinoline, are known to react via similar reaction schemes ( reaction I and II ).

(a) Concentration dependence of the CIDEP spectra

Figure 8-1 shows the concentration dependence of the CIDEP spectra obtained in the photolysis of quinoxaline in 2-propanol at 0°C. Broad spectra with partially resolved hyperfine structures were assigned to the quinoxalinyl radical as reported before. [23,27)] The spectrum of the 2-hydroxypropan-2-yl radical was not observed at higher concentrations ( Figures. 8-1a and b ), but observed weakly at a low concentration ( Figure 8-1c ). This is because the 2-hydroxypropan-2-yl radical was quenched quickly

( $k_q$=1.1x10$^8$M$^{-1}$s$^{-1}$ ) by ground state quinoxaline as represented by reaction (II).[62] The CIDEP spectrum in Figure 8-1a shows a total emission CIDEP In a previous report,[23] the net E polarization was ascribed to TM. However, on the basis of the slow rate constant ( 1.4x10$^4$M$^{-1}$s$^{-1}$ ) determined by the transient absorption, it is difficult to justify this assignment. As shown in Figure 8-1, the spectral pattern changed remarkably with the concentration of quinoxaline. At a high concentration of quinoxaline(0.022M) the spectral pattern was total emission as reported before, whereas at a low concentration (0.0027M) the pattern changed to E/A. The spectral change is explained by the change in the relative contributions of the total E and the E/A components. The E/A polarization is obviously due to the $ST_0$ mixing of RPM with triplet geminate pair and/or F-pair. The net E polarization decreases drastically with decreasing the quinoxaline concentration. This observation cannot be compatible with the assignment that the emissive polarization is due to TM.

Figure 8-2 shows the concentration dependence of the CIDEP spectrum obtained in the photolysis of phenazine in 2-propanol at 0°C. The photoreaction of phenazine progresses by the scheme similar to that of quinoxaline. Observed spectra are assigned to the phenazinyl radical. [23,27] The 2-hydroxypropan-2-yl radical was not observed also because of quenching by ground state phenazine. The concentration dependence is similar to that of quinoxaline, but the extent of the change is not so drastic. The net E polarization decreases with decreasing the phenazine concentration, but remains to be dominant even at a low concentration ( 0.00336M ).

(b) Excitation power dependence of the CIDEP spectra

Figure 8-3 shows the excitation laser power dependence of the CIDEP spectrum in the photolysis of phenazine ( 0.010M ) in 2-propanol at 0°C. The net E polarization decreases with decreasing the excitation power. However, the dependence was weaker compared with the concentration dependence. The result suggests that the concentrations

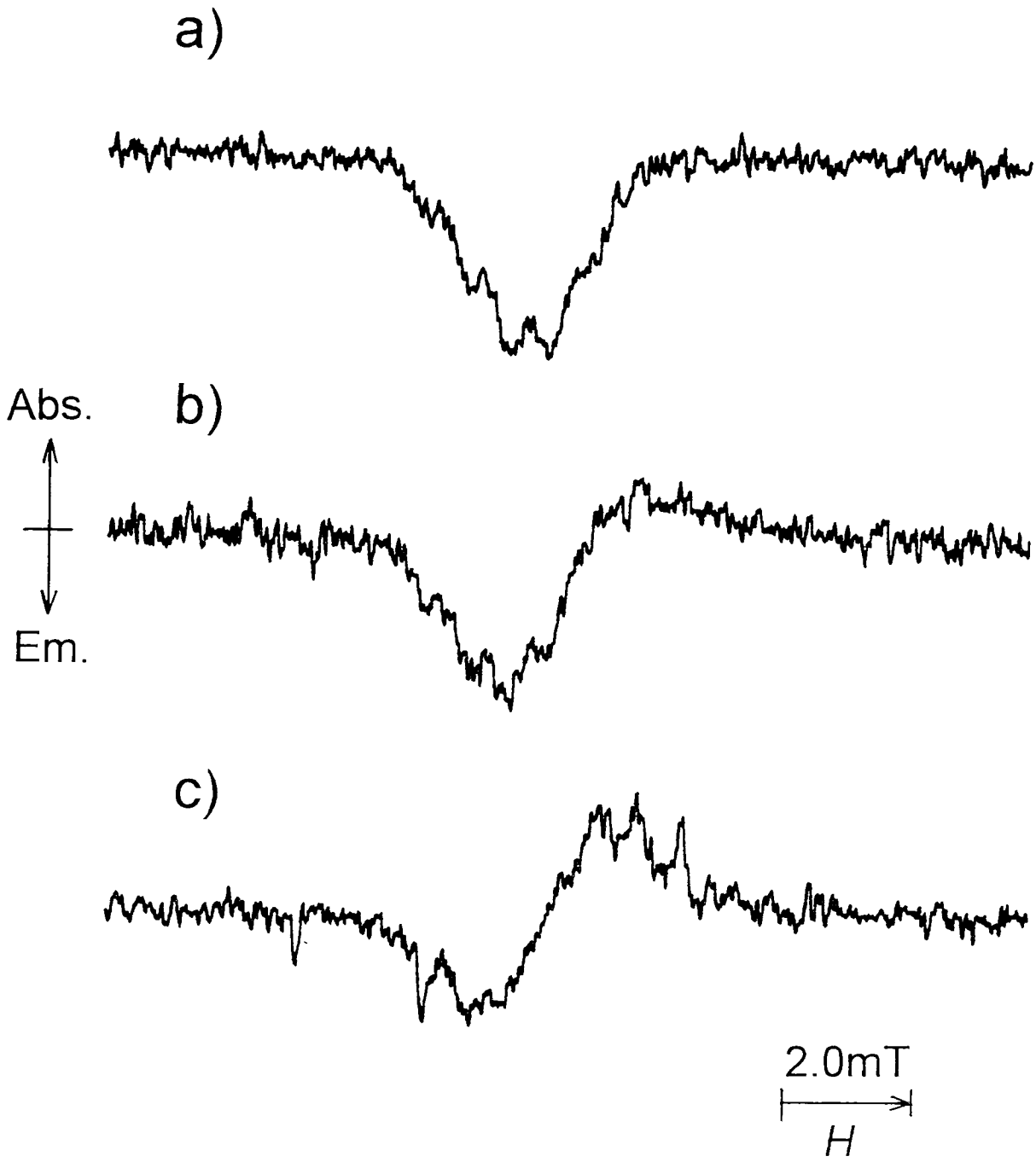


Figure 8-1 Concentration dependence of the CIDEP spectrum observed in the photolysis of quinoxaline in 2-propanol at 0°C. (a) 0.022 M, (b) 0.010 M, (c) 0.0027 M.

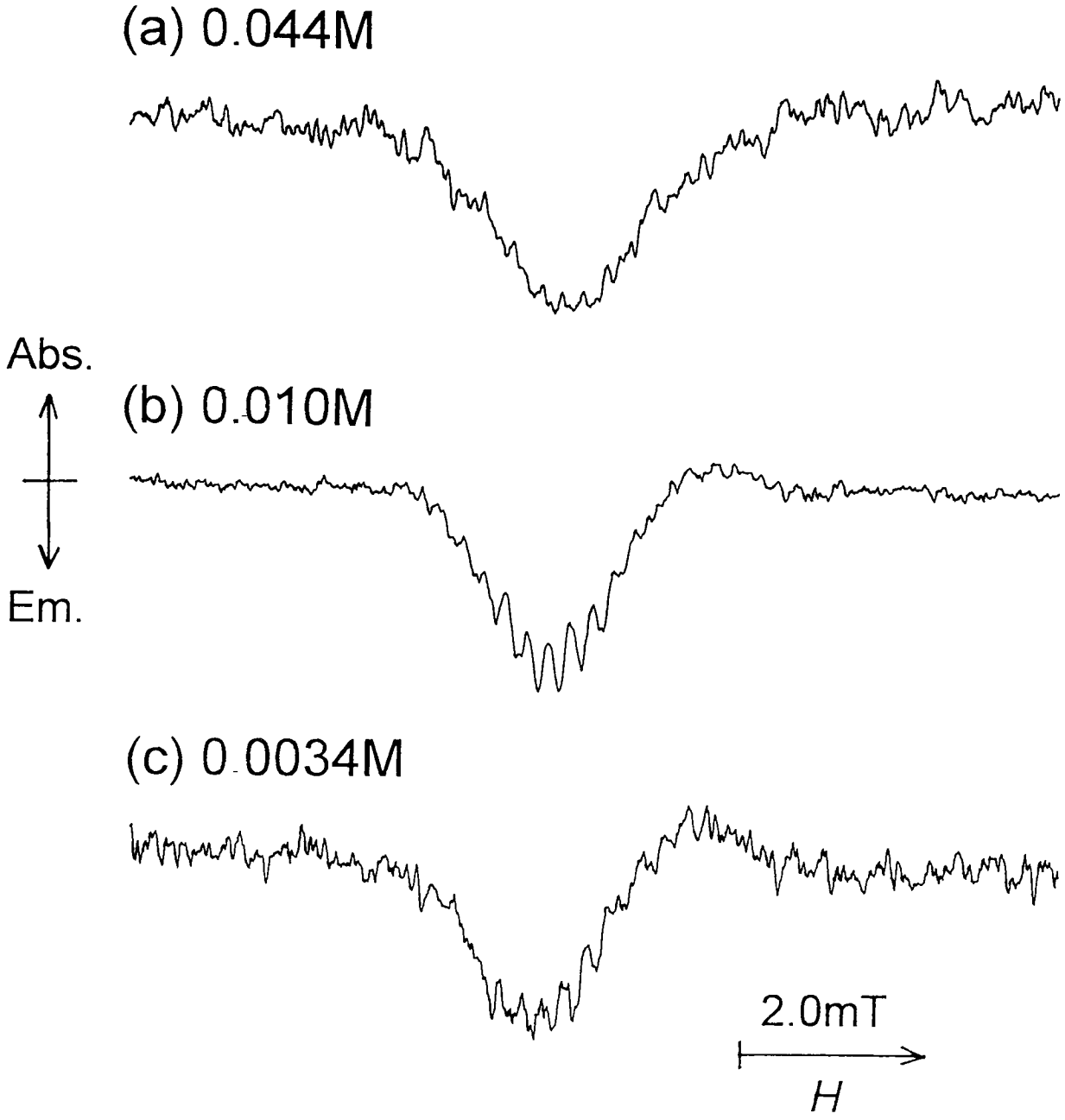


Figure 8-2 Concentration dependence of the CIDEP spectrum observed in the photolysis of phenazine in 2-propanol at 0°C. (a) 0.044 M, (b) 0.010 M, (c) 0.0034 M.

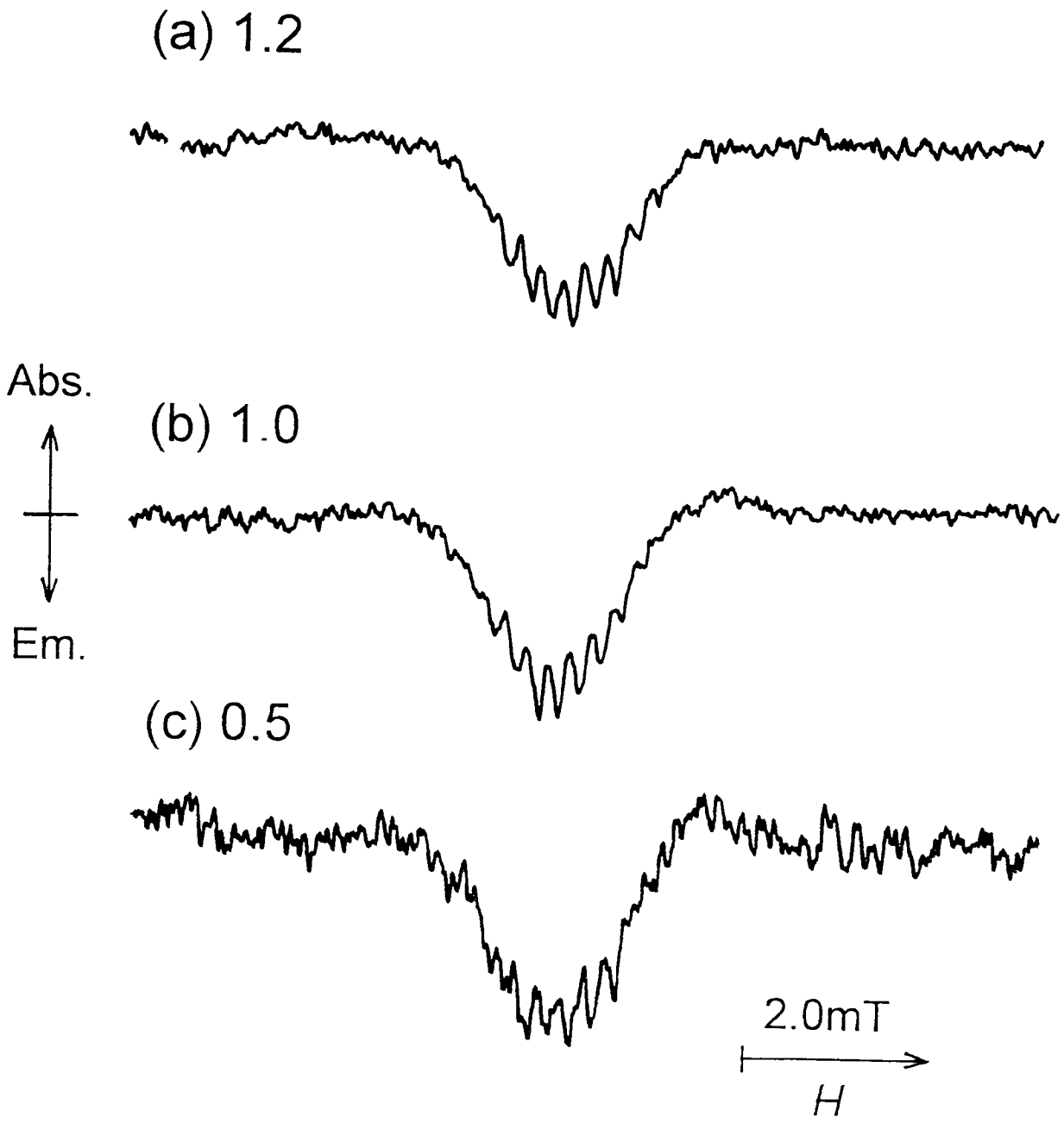


Figure 8-3 Excitation laser power dependence of the CIDEP spectrum of phenazine (0.0010M) in 2-propanol at 0°C. Relative power: (a) 1.2, (b) 1.0, (c) 0.5.

of the excited state and/or radical affect the amount of the net polarization.

8.3.2. Mechanism producing the net emission CIDEP

The relative contribution of the net E polarization is enhanced by the increases of the radical concentrations produced by the increases of the initial concentrations of parent molecules and the increase of the excitation light intensity.

The TM and ST$_-$ mixing RPM cannot explain the above result. On the other hand, the RTPM or the spin polarization transfer mechanism [31,58,59] may be able to explain it. The spin polarization transfer to radicals is known to occur in two situations; one is the case when the spin polarized radical reacts quickly and produces the secondary radical,[31,58,59] and the other is the case when the spin polarized triplet interact with the radical through the spin exchange or the chemical exchange.[63] For this mechanism to be effective the primary species must have an effective net polarization and the transfer process must take place in a time comparable to the spin-lattice relaxation time. The net spin polarization of the primary species is usually generated by TM and/or ST$_-$M. In the present case, the secondary reaction represented by reaction (II) produces the quinoxalinyl (or phenazinyl) radical, but the primary reaction rate is far too slow. The spin polarization transfer from the triplet parent molecule is not likely to occur unless the radical concentration is very high and the spin polarization of the triplet state is conserved before the transfer. Therefore, the RTPM is considered to be the most probable mechanism.

The prerequisite for the RTPM to be effective is that both triplet molecules and radicals are sufficiently long-lived to interact together. It is shown here that the lifetimes of the triplet state and the produced radical are long enough to cause the RTPM interaction. Figure 8-4 shows the transient absorption spectrum obtained by the photolysis of quinoxaline (0.0012M) in 2-propanol at room temperature. The absorption bands of the quinoxaline triplet and the quinoxalinyl radical are located around 420nm. In

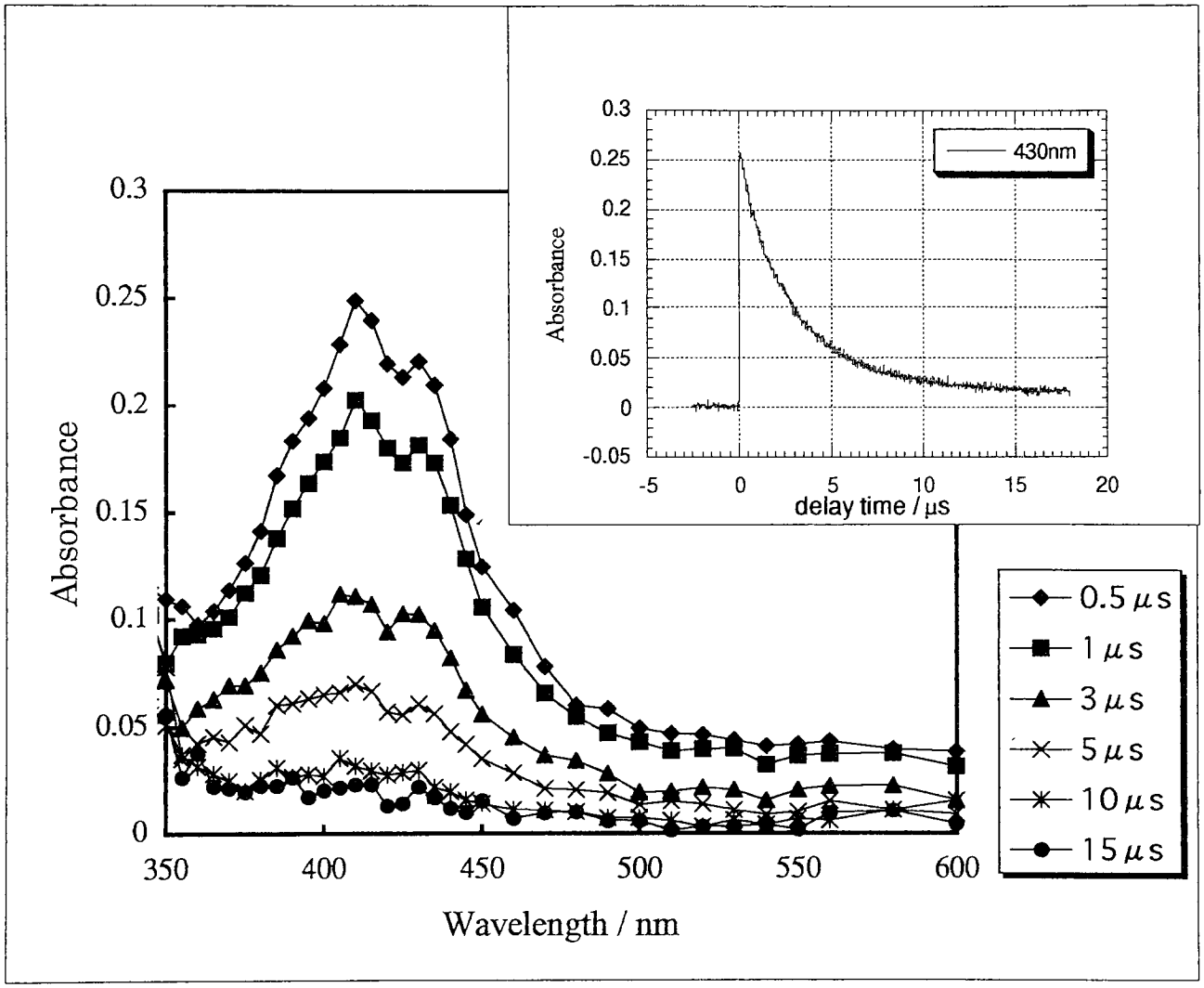


Figure 8-4 Transient absorption spectra observed in the photolysis of quionoxaline (0.0010M) in 2-propanol at room temperature. The time development of the transient absorption at 430nm is superimposed in the figure.

an early time region within 1μs, the spectrum is nearly given by the absorption of triplet quinoxaline, but in a later time region it shows the absorption of the quinoxalinyl radical which perfectly agrees with that reported in literature.[26,53] The absorption of 2-hydroxypropan-2-yl is located around 350nm, but it is too weak to be observed. The decay of the transient absorption at 430nm is also shown in Figure 8-4. The decay curve consists of a fast decay of quinoxaline triplet and a slow one of the quinoxalinyl radical, and could be analyzed by two exponential decays. The lifetimes of the quinoxaline triplet determined by the least squares fits of the data are 3.0μs at R.T. and 4.7μs at -30°C. The lifetime at R.T. is in reasonable agreement with the lifetime estimated from the reported quenching rate constant of triplet quinoxaline. The lifetime of the quinoxalinyl radical was more than 20μs at both R.T. and -30°C.

Similarly, the transient absorption spectrum obtained by the photolysis of phenazine (0.0011M) in 2-propanol at room temperature shows absorption bands of the phenazine triplet and the phenazinyl radical around 420nm, which agree with the literature.[26] The lifetime of the phenazine triplet determined by a least squares fit of the time evolution data are 3.6μs at R.T. The phenazinyl radical is also quite long-lived.

The results of the transient absorption experiments thus indicate that the condition for the RTPM to be important is satisfied.

### 8.3.3. Qualitative features of the time dependence of the CIDEP spectra

In this section, we first discuss time dependent changes of the CIDEP spectra qualitatively. Figure 8-5 shows the time dependent changes of the CIDEP spectra observed in the photolysis of quinoxaline (0.0036M) / 2-propanol at 0°C, -30°C and 60°C. The CIDEP spectra show different time dependence depending on the temperature. At 0°C the spectral pattern is E/A in all the time regions of observation. The net component is very weak. On the other hand, at -30°C the spectrum initially shows an A/E* pattern within 0.5μs, then changes quickly to an opposite phase, i.e., E/A( 1.0 to

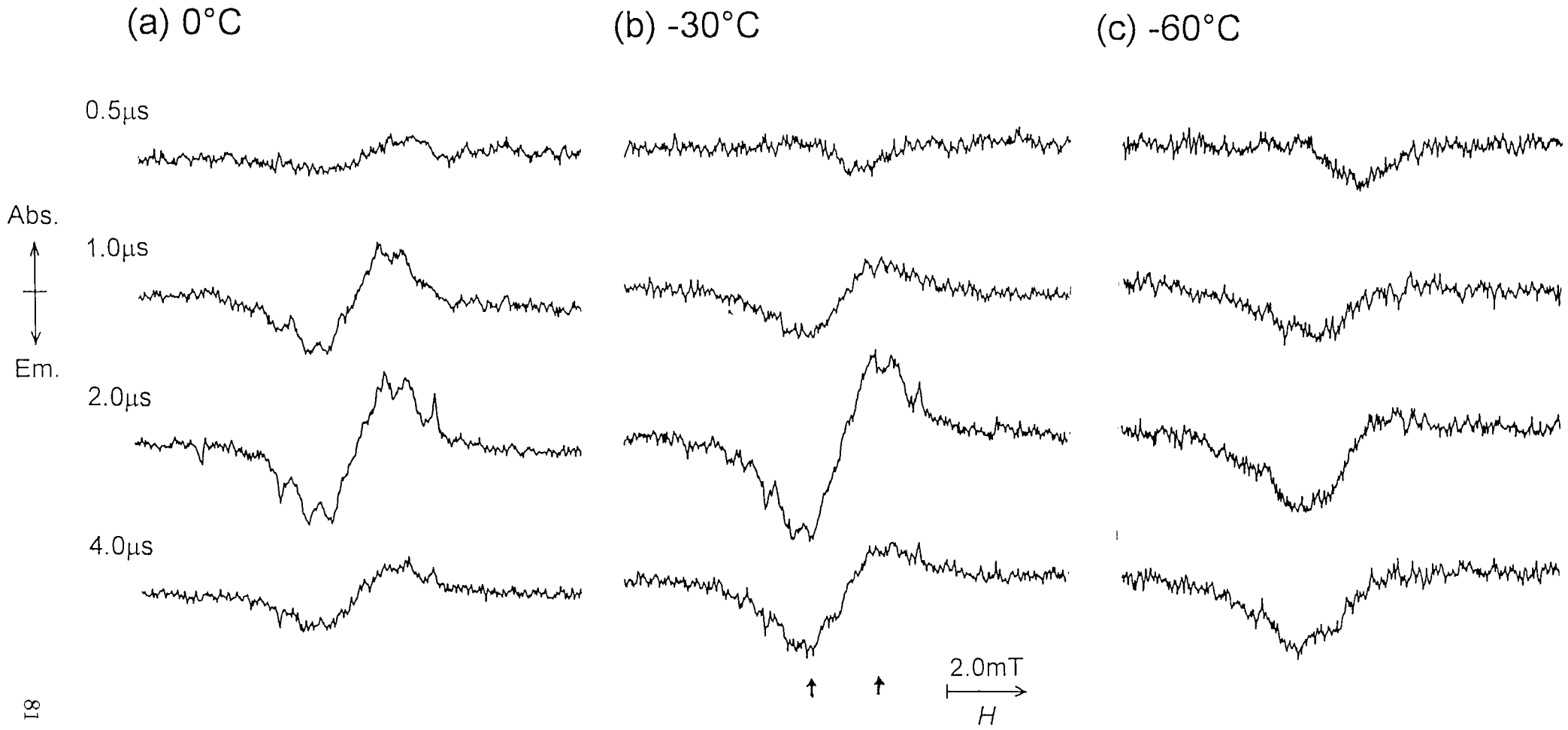


Figure 8-5 Time evolution of the CIDEP spectra observed in the photolysis of quinoxaline (0.0036M) in 2-propanol at (a) 0°C, (b) -30°C and (c) -60°C. Arrows in (b) indicate the positions at which time evolution of the signal was measured. (see Figure 8- 7)

2.0μs), and then decays slowly, changing the phase to E*/A character (≥4.0μs) at last. The contribution of the net E polarization is increased in a later time region. The spectral change at -60°C is similar to that at -30°C, but the contribution of the net E polarization is considerably larger compared with that at higher temperatures. These results are qualitatively explained in the following way.

The A/E polarization observed in the early time region is explained in terms of the $ST_0$ mixing RPM of the singlet precursor provided that the exchange integral $J$ is negative. The E/A polarization observed in the following time region is generated by the $ST_0$ mixing RPM of the triplet precursor. The results suggest that both the excited singlet and triplet states reacts competitively. This situation is similar to that found previously in the CIDEP of acetone in triethylamine.[51,57] The minor singlet reaction is hidden by the major triplet reaction at higher temperatures, but at lower temperatures (≤-30°C), the singlet reaction apparently becomes dominant in an early time region. The triplet reaction increases with time and becomes dominant in a later time region, changing the A/E polarization of the singlet geminate pair RPM to the E/A polarization of the triplet RPM. The E/A polarization persists for a long time. The E/A polarization observed in a later time region (>10μs) is considered to be due to the F-pair RPM, which should rise with the spin-lattice relaxation rate and decay with a time constant determined by the second order decay of the radical.[57] The net E polarization increases with decreasing the temperature. This is because the lifetime of the triplet state of quinoxaline increases with decreasing the temperature as confirmed by the transient absorption experiments. Then the RTPM polarization is enhanced, because the chance of the interaction between the triplet and radical is enhanced. Furthermore, the increased viscosity at lower temperatures prolongs the correlation time of the RTPM interaction, enhancing the polarization. The results support the suggestion that the net polarization is caused by the RTPM.

Figure 8-6a shows the time evolution of the CIDEP spectrum observed in the photolysis of quinoline ( 0.0125M ) in 2-propanol at -15°C. The spectra are assigned to

the quinolinyl radical. The CIDEP spectrum changes with time from A/E* to net E. Here the contribution of the E/A polarization appears to be very weak. The result is explained mainly by the A/E polarization due to the singlet precursor $ST_0$ mixing RPM and the net E polarization due to the RTPM. Long-lived character of triplet quinoline and the quinolinyl radical were also confirmed by the transient absorption experiment. The reaction scheme and the CIDEP generation mechanism are believed to be similar to the case of quinoxaline, though the signals were much weaker in quinoline.

The photoreaction and the CIDEP development mechanisms of the phenazine / 2-propanol system are considered to be similar to the quinoxaline system except that the singlet reaction was not observed. Figure 8-6b shows the time evolution of the CIDEP spectrum observed in the photolysis of phenazine ( 0.0034M ) in 2-propanol at 0°C. The spectra shows E*/A character at all times, in contrast to quinoxaline which shows almost symmetric E/A character at the same concentration. Stronger emissive components are also ascribed to the RTPM.

### 8.3.4. Time evolution of the polarization

In this section, we try to analyze the time evolution of the CIDEP signals more quantitatively. As the discussion of the previous section indicates, several different polarization mechanisms are involved. Complete quantitative treatments are quite difficult and accurate analytical expressions cannot be obtained. Therefore several simplifications are taken. Firstly the hyperfine dependent RTPM polarization is neglected. The reason is that it is very difficult to separate the hyperfine dependent RTPM from the RPM polarization. This is probably a good approximation in the present case. We first consider various processes involved in the present systems and give approximate expressions for various concentrations and polarizations.

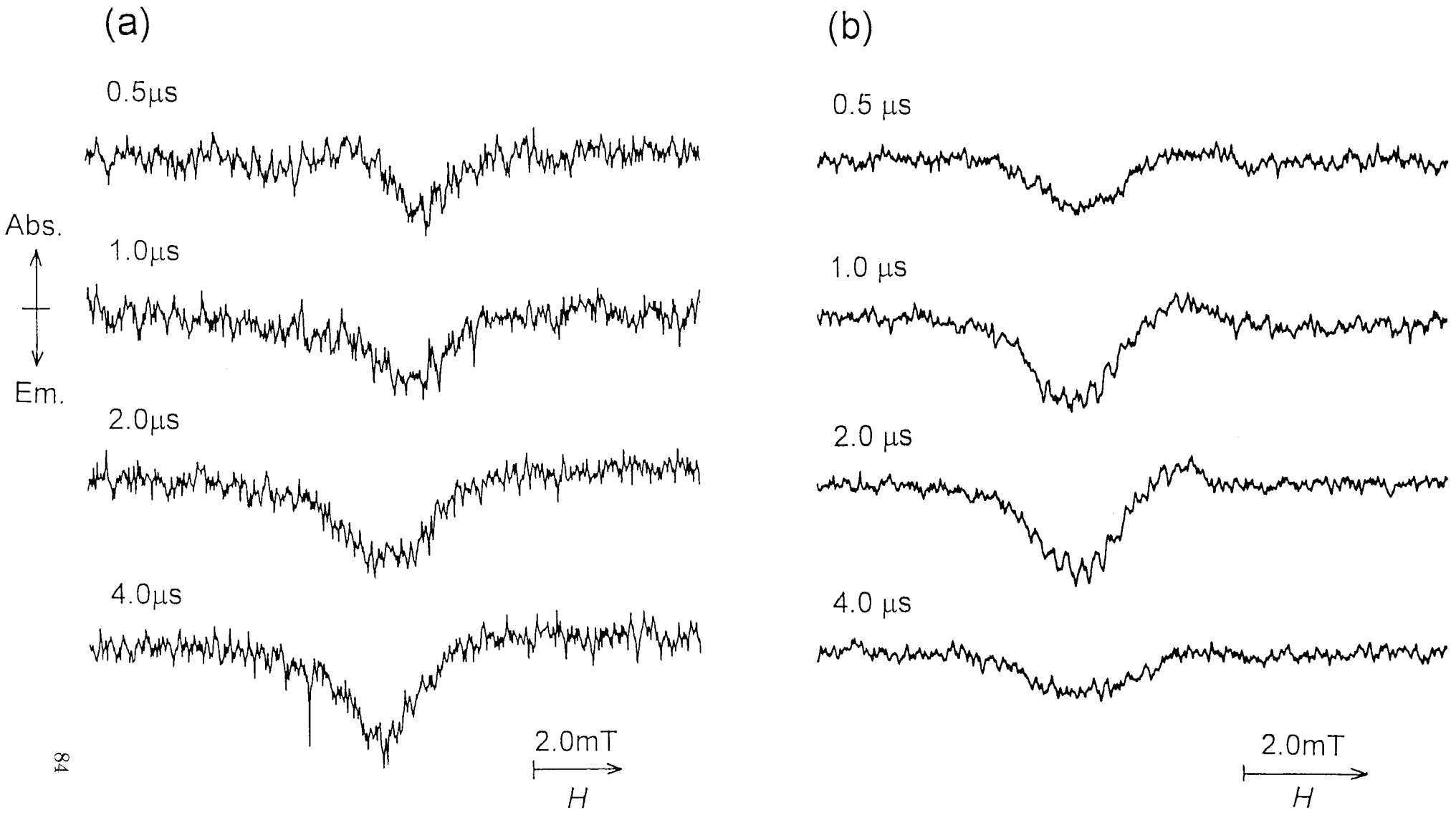


Figure 8-6 Time evolution of the CIDEP spectra observed in the photolysis of (a) quinoline (0.013M) in 2-propanol at -15°C and (b) phenazine (0.0034M) in 2-propanol at 0°C.

(1) Triplet concentration

The processes involved in the production and decay of the triplet state is considered to be the following.

$$S_1 \xrightarrow{ISC} T$$
$$T \xrightarrow{k_p} S_0$$
$$T + ROH \xrightarrow{k_T} R + \cdot ROH$$
$$T + Q \xrightarrow{k_q^{TS}} \text{quench}$$
$$T + \cdot R \xrightarrow{k_q^{TR}} \text{quench}$$
$$T + T \xrightarrow{k_q^{TT}} \text{quench}$$

Here, $k_p$ is the natural decay rate constant, $k_T$ is the triplet reaction rate constant, $k_q^{TS}$, $k_q^{TR}$ and $k_q^{TT}$ are the quenching reaction rate constants by the ground state parent molecule, the radical, and the triplet state itself, respectively. The production process is considered to be much faster than our observation time. When the triplet concentration is low, the second order term may be neglected. Then the triplet concentration is given by a simple form:

$$[T] = [T]_0 \exp(-k_T' t) \qquad (8\text{-}1)$$

with

$$k_T' = k_p + k_T + k_q^{TS}[Q] + k_q^{TR}[R]$$

Here, $[T]_0$ represents initial triplet concentration.

(2) Radical concentration

The radical is considered to be produced mainly by the reaction of the triplet state, but it is suggested that the reaction of the singlet excited state also produces the radical as described in the previous section. There are several possible processes of radical quenching which include the second order chemical decay and the RTPM interaction itself. Then the radical produce and decay is represented by;

$$\frac{d[\mathrm{R}]}{dt} = k_T[\mathrm{T}] - k_q^{TR}[\mathrm{T}][\mathrm{R}] - k_{2r}[\mathrm{R}]^2 \qquad (8\text{-}2)$$

Here, $k_T$ is the apparent rate constant of the radical producing reaction from the excited triplet state. $k_{2r}$ is the second order decay rate constant. Since the lifetime of the singlet state is very short, probably less than 20ns, the concentration of the radical produced from the singlet precursor is treated as an initial radical concentration. When the second and third terms are neglected in eq(2), the solution is given by;

$$[\mathrm{R}] = [\mathrm{R}]_0 + \frac{k_T}{k_T'}[\mathrm{T}]_0\left\{1 - \exp\left(-k_T' t\right)\right\} \qquad (8\text{-}3)$$

where $[\mathrm{R}]_0$ is the initial radical concentration which is given by the singlet reaction and the steady state concentration.

(3) Polarizations due to geminate pair and F-pair RPM

Spin polarization due to the geminate and F-pair RPM have been discussed in detail in the previous report.[57)]

(a) Geminate pair RPM polarization

Spin polarization due to the geminate pair RPM is given by;

$$P_{RPM} = P^0_{RPM}\left\{\exp(-t/T_1^R) - \exp(-k_f t)\right\} + P^\infty_{RPM}\left\{1 - \exp(-t/T_1^R)\right\} \qquad (8\text{-}4)$$

Here, $P^0_{RPM}$ and $P^\infty_{RPM}$ are the initial polarization and the polarization at thermal equilibrium of the geminate-pair RPM, respectively. $T_1^R$ is the spin-lattice relaxation time of the radical. $kf$ is the growth rate constant of the polarization due to the geminate-pair RPM.

(b) F-pair RPM polarization

When the initial the radical concentration is high and its decay is determined by

the second order radical decay, the magnitude of the F-pair polarization is approximately given by,[57]

$$P_{FRPM} = ak_F[\mathrm{R}]_0^2 \; T_1^R \left\{ \frac{1}{(k_{2r}[\mathrm{R}]_0 t + 1)^2} - \exp(-t / T_1^R) \right\} \qquad (8\text{-}5)$$

(4) RTPM polarization

The RTPM polarization is generated when a triplet state and a radical make a collision and interacts each other. The polarization decays with the spin-lattice relaxation time. Then, when we can neglect the second order radical decay, the RTPM polarization ($P_{\mathrm{RTPM}}$) is obtained by solving the following differential equation.[64-66]

$$\frac{dP_{RTPM}}{dt} = k_{RTPM}[\mathrm{T}][\mathrm{R}] - \frac{P_{RTPM}}{T_1^R} \qquad (8\text{-}6)$$

Here, $k_{\mathrm{RTPM}}$ is the rate constant of the RTPM and $T_1^{\mathrm{R}}$ is the spin-lattice relaxation time of the radical. Assuming that [T] and [R] are given by eq.8-1 and 8-3, respectively, the solution of eq.8-6 is given by the following equation;

$$P_{RTPM} = \alpha \exp(-2k_T' t) - \beta \exp\left(-k_T' t\right) + \gamma \exp(-t/T_1^R) \qquad (8\text{-}7)$$

$$\alpha = \frac{k_{RTPM} \dfrac{k_T}{k_T'}[T]_0^2}{2k_T' - 1/T_1^R}, \quad \beta = \frac{k_{RTPM}[T]_0 \left( [R]_0 + \dfrac{k_T}{k_T'}[T]_0 \right)}{k_T' - 1/T_1^R}, \quad \gamma = \beta - \alpha$$

The solution represented by eq.8-7 is meaningful under the condition of $1/T_1^{\mathrm{R}} \neq k_{\mathrm{T}}'$ and $1/T_1^{\mathrm{R}} \neq 2k_{\mathrm{T}}'$ which is usually valid. Then, the time evolution of the RTPM polarization is represented by three exponential components. The time development always consists of one rise and two decay components. In this case, the rate of one decay component is much larger than the rate of the rise component, and another decay component is much smaller. Here, we consider two typical cases. One is $2k_{\mathrm{T}}' > k_{\mathrm{T}}' > 1/T_1^{\mathrm{R}}$,

and another is $2k_T' > 1/T_1^R > k_T'$ In the former case the rise constant is determined by $k_T'$ and the decay constant is by $1/T_1^R$ In the latter case the rise constant is determined by $1/T_1^R$ and the decay constant is by $k_T'$ In both cases $\alpha$ is positive, and the $2k_T'$ term represents a quick decay component which may not appear clearly in the time evolution of the signal. Therefore, the time development of the RTPM polarization should look like one rise and one decay.

8.3.5. Time evolution of CIDEP signals

The exact time evolution of the CIDEP signal observed in a CW time-resolved EPR experiment is in general complicated because of the constant interaction of the spin system with the microwave. It should be described by the solution of a modified Bloch equation, but such a solution cannot be obtained easily without making simplifications in the present case. In a CW time-resolved EPR experiment, we observe a time dependence of the transverse magnetization $M_y$, but for simplicity here we assume that $M_y$ is approximately proportional to $M_z$ whose time evolution is described by the time evolution of various polarizations discussed in the previous section.

Figure 8-7a shows the time evolution of the CIDEP signals at a low field position from the center of the spectrum and the corresponding high field position observed in the quinoxaline (0.0036M)/ 2-propanol system at -30°C. The signals shows a strange change with time. This is because the time developments of the net component and the antiphase ( E/A or A/E ) component are quite different. A quantitative analysis requires the separation of the each component. The time evolutions of the E/A (or A/E) component and the net component of the polarization can be separated by taking the difference ($\Delta S$ ) and the sum ($\Sigma S$ ) of the signal intensities at the low field and the corresponding high field positions, shown by arrows in Figure 8-5b. The $\Delta S$ component is considered to include three $ST_0$ mixing RPM components, singlet geminate pair, triplet geminate pair and F-pair. The $\Delta S$ component due to the geminate pair RPM rises quickly

to A/E ( singlet precursor ) followed by E/A ( triplet precursor ) with the apparent reaction rate of the triplet and decays with the spin-lattice relaxation rate. The E/A component which remains at longer times (over 10μs) is presumably due to the F-pair RPM. This is possible because of a large initial concentration of the radical produced by the singlet reaction. The F-pair RPM polarization should decay with the second order decay rate constant of the radical as represented by eq.8-4. The spin-lattice relaxation time of the radical is determined to be 3.4μs by the fits of the decay curve of the E/A component. On the other hand, the $\Sigma S$ component rises to net E much more slowly than the $\Delta S$ component, and decays more slowly to a small absorption which is presumably due to the thermal equilibrium signal. The rise time of the $\Sigma S$ agrees with the spin-lattice relaxation time of about 3.4μs. The decay rate was determined to be about 8μs, which is somewhat larger than the triplet lifetime of 4.7μs determined by the transient absorption experiment. The time evolution of the net polarization can be rationalized by the RTPM dynamics represented by eq.8-7 in the case of $2k_T' > 1/T_1^R > k_T'$, except for a small discrepancy between the decay rate of the net polarization and the measured lifetime of triplet quinoxaline.

There is one puzzling observation about the time evolution of the $\Delta S$ component. The time evolution of $\Delta S$ is interpreted on the basis of the contributions of the singlet and triplet geminate pair RPM. The E/A component due to the triplet geminate pair rises rapidly within 1μs. However, the triplet lifetime is too long to explain this rise. Therefore, there may be another process to give a rise to a fast rising E/A polarization.

Figure 8-8 shows the time evolution of the E/A polarization and the net polarization of the quinoxaline (0.0036M)/ 2-propanol system at 0 and -60°C. Comparing the temperature dependencies, it is seen that the relative intensity of the net E polarization increases drastically with decreasing the temperature. The E/A polarization at -60°C also shows a very slow decay due to the F-pair polarization dynamics represented by eq.8-4. The spin-lattice relaxation times estimated by the fits of the decay of the E/A polarization

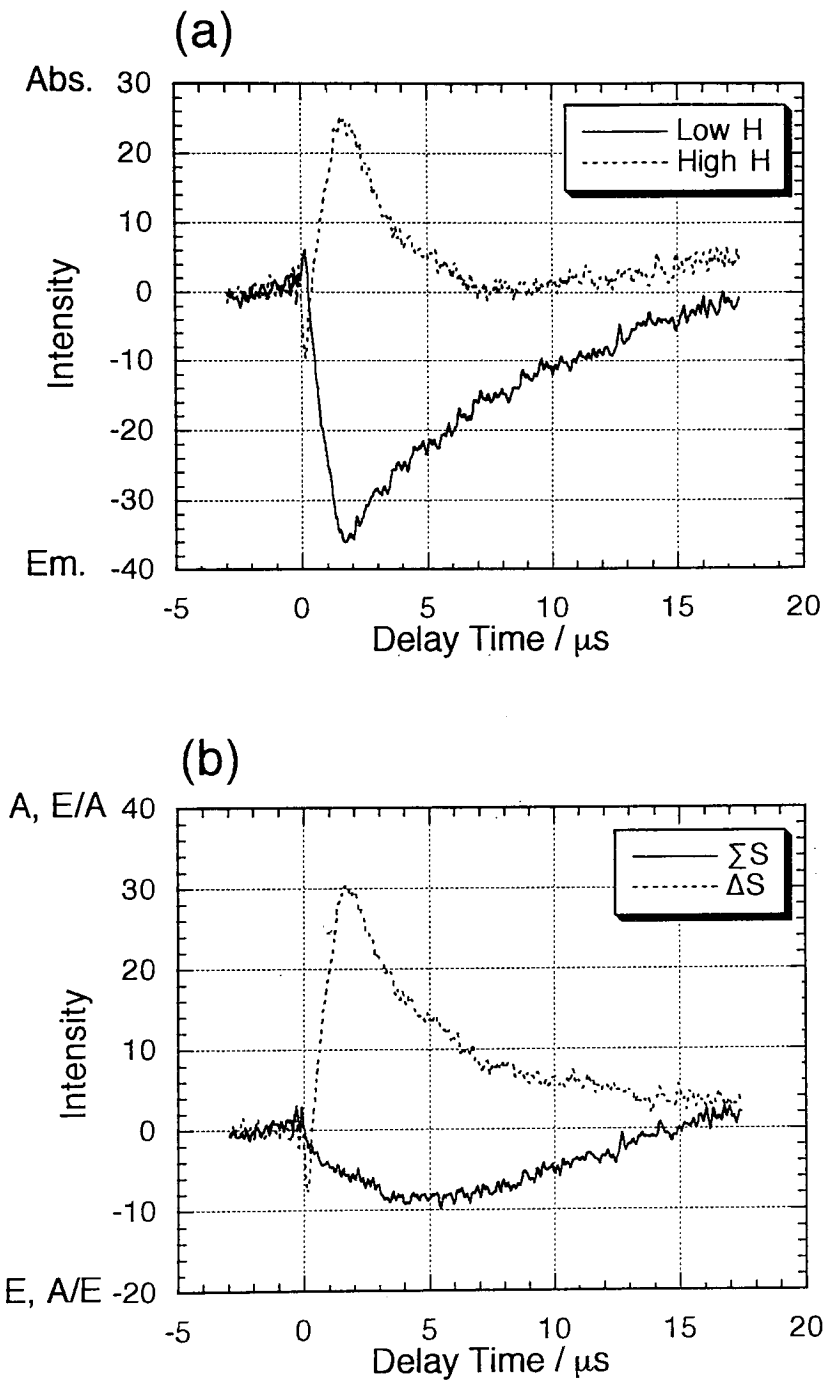


Figure 8-7 Time evolution of the transient EPR signals obtained in the photolysis of quinoxaline (0.0036M) in 2-propanol at -30°C. (a) Intensities of signals at a low field position ( — ) and the corresponding high field position ( ... ), (b) Intensities of the net component ($\Sigma S$ ) and the antiphase component ($\Delta S$ ).

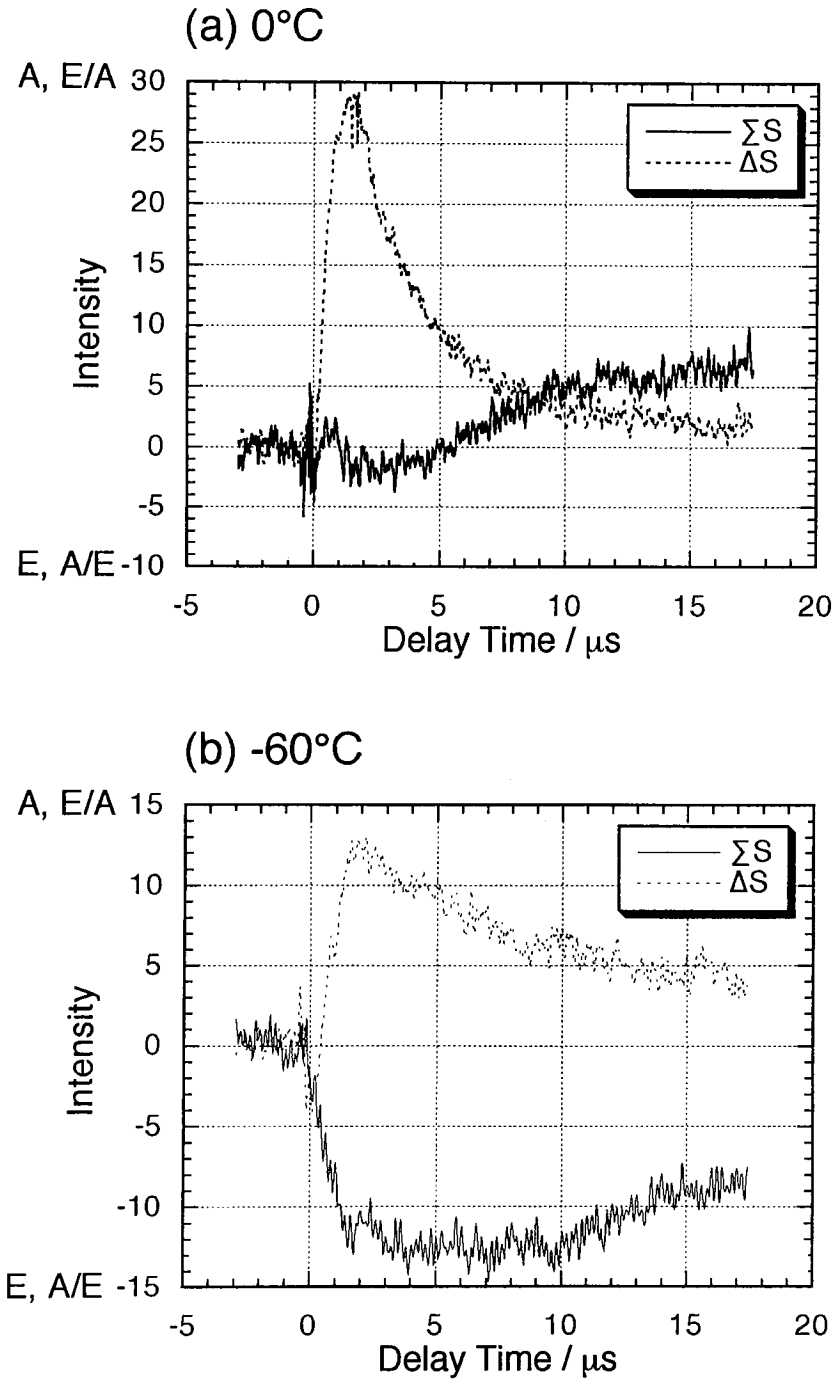


Figure 8-8 Time evolution of the net component ($\Sigma S$) and the antiphase component ($\Delta S$) of the transient EPR signal of the quinoxaline (0.0036M)/ 2-propanol system at (a) 0°C and (b) -60°C.

as described before are 2.5μs at 0 °C and 7.5μs at -60°C. At 0 °C, the time constants of the rise and the decay of the net polarization are about 2.5μs and 3.5μs which are in good agreement with the spin-lattice relaxation time and the triplet lifetime, respectively. The results can be explained by the RTPM dynamics model represented by eq.8-7 On the other hand, at -60°C the rise time was around 2μs which is shorter than both the spin-lattice relaxation time and the triplet lifetime. The decay rate at -60°C was around 20μs, which is considered to be determined by the triplet lifetime at this temperature. Therefore, the time development at -60°C is considered to be mainly due to the RTPM dynamics, but the quantitative agreement with the prediction of eq.8-7 is not good in the early time region.

Figure 8-9 shows the time evolution of the EPR signal at the center position of the spectrum observed in more concentrated quinoxaline ( 0.010M and 0.051M ) solutions at different temperatures. At these concentrations, the CIDEP spectra show almost total emission with a slight E/A distortion. Therefore, we can consider the center signal to represent the net polarization. The rise times of the signals are much shorter compared with those at a low concentration (0.0036M). The time constants of the decays at 0.010M are 3.3μs, 5μs, and 10-20μs at 0, -30, and -60°C, which agree with those at 0.0036M, and indicate the triplet lifetimes. Then the time developments in later time regions are explained by the RTPM dynamics, but the cause for the fast rise components must be found. A possible explanation is the involvement of the triplet-triplet annihilation at higher concentrations of the triplet state. This process reduces the triplet lifetimes drastically in the early time region and increases the rise of the net polarization. Another possibility is the polarization transfer from the triplet state to the radical. This mechanism was recently shown to be important in systems consisting of metalloporphyrins and nitroxide radicals.[63] The relaxation times of the triplet porphyrins are exceptionally long because of their small zero field splitting constants and large molecular volumes. In the cases of ordinary organic molecules, the triplet relaxation times are less than 10ns and the

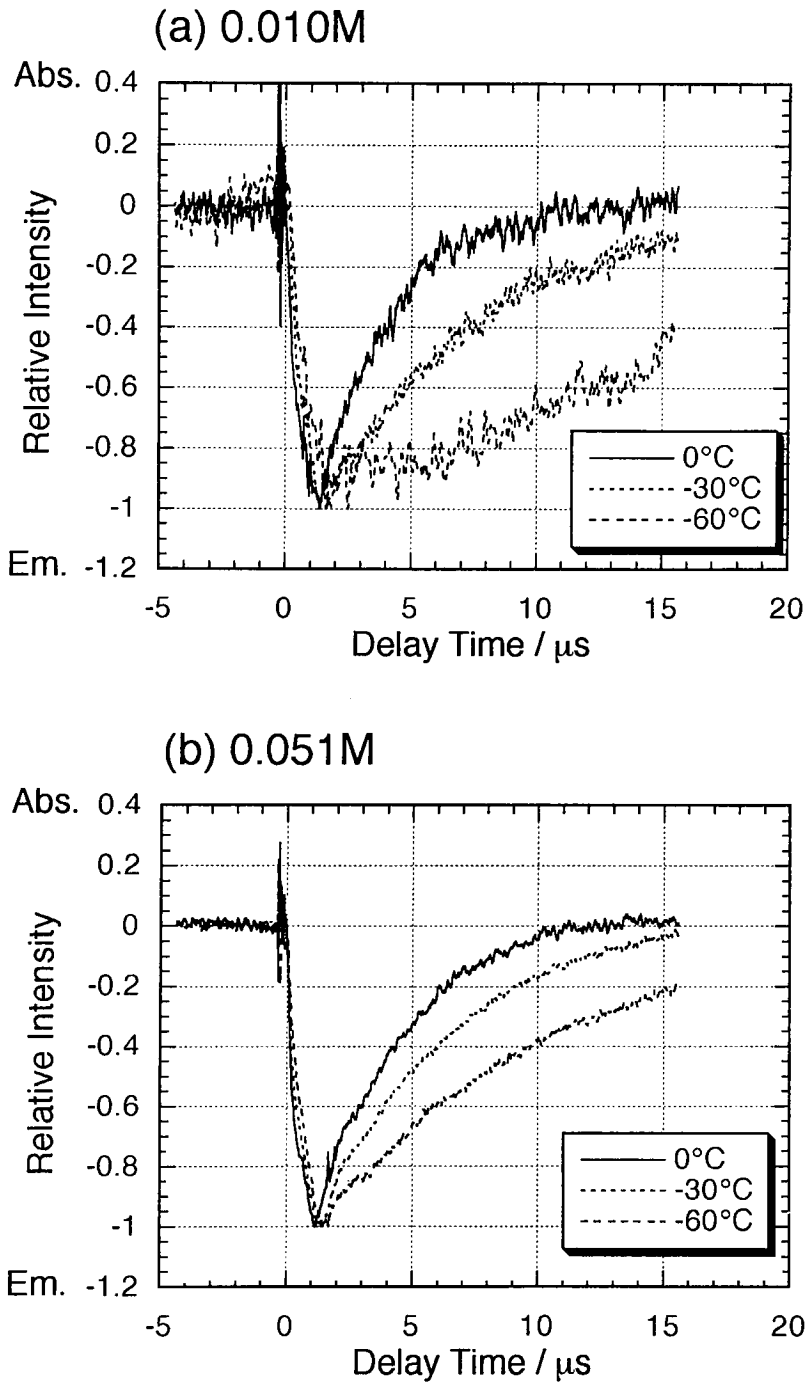


Figure 8-9 Time evolution of the transient EPR signals at the center of the spectra obtained in the photolysis of quinoxaline in 2-propanol at (a) 0.010M and (b) 0.051M.

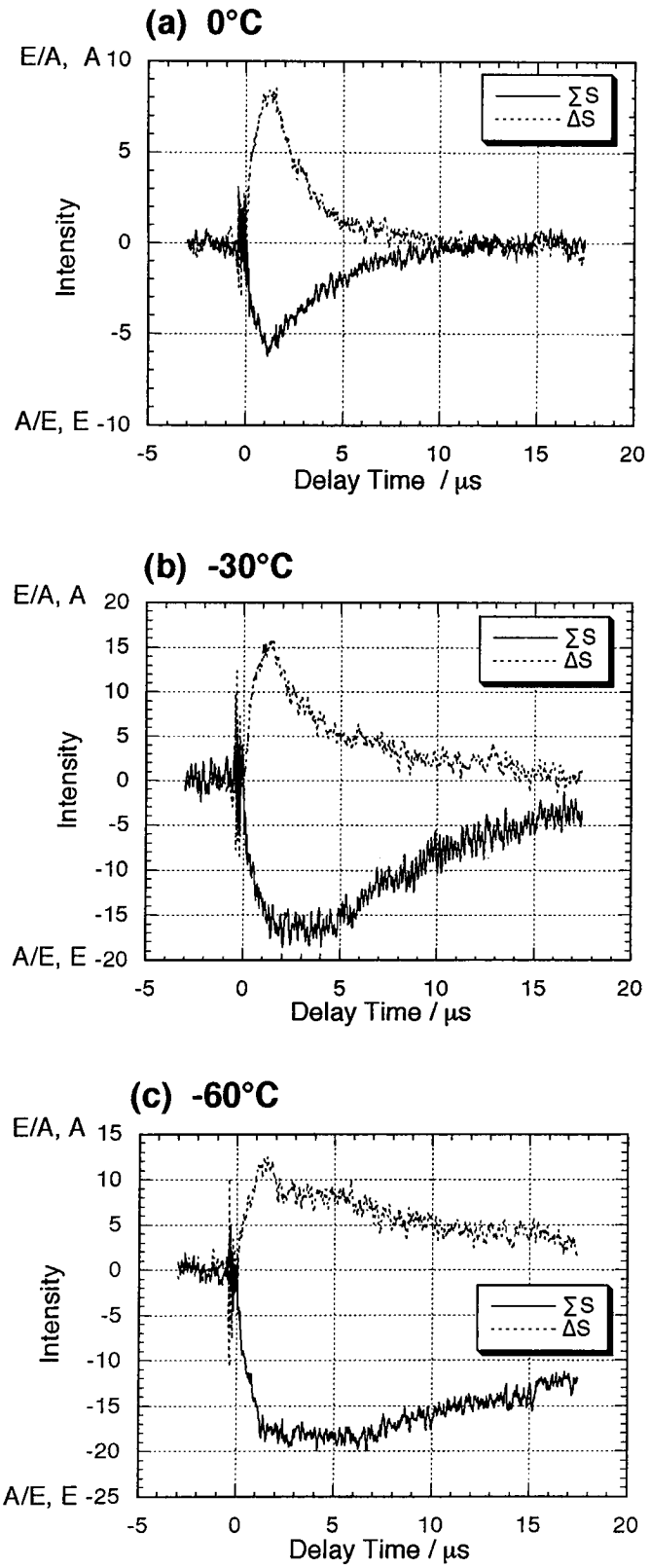


Figure 8-10 Time evolution of the net component ($\Sigma S$) and the antiphase component ($\Delta S$) of the transient EPR signal of the phenazine (0.0034M)/ 2-propanol system at (a) 0°C, (b) -30°C, and (c) -60°C.

spin polarization transfer is unlikely to be important unless the radical concentration is very high.

Figure 8-10 shows the time evolutions of the net and the E/A components of the EPR signals observed in phenazine (0.0036M ) in 2-propanol at 0, -30, and -60°C. The net polarization rises quickly with almost the same rate of the E/A component, which is close to the response time of our apparatus. The decay rate of the net component is slower than that of the E/A component. The rise rates of both components are almost the same at all temperatures, whereas the decay rates decrease with decreasing temperature. The slow decay of the net component is considered to be determined by the triplet lifetime, which drastically increases with the decrease of temperature. The time evolution of the net component in a later time region ( >3μs ) can be explained by the RTPM dynamics represented by eq.8-7. The rise of the net polarization at -60°C consists of a fast and a slow component. The slow rise component is explained by the RTPM dynamics as the rise constant is determined by the spin-lattice relaxation time, but the fast rising net component in the early time region cannot be explained clearly. A fast decrease of the triplet concentration by the triplet-triplet annihilation can give rise to a fast rise of the RTPM polarization, if the triplet production is very efficient and triplet-triplet annihilation takes place with a diffusion controlled rate. Another possibility is that a reaction from a higher excited triplet state takes place via a two photon process and the produced radical has the net E polarization of TM. This situation resembles the benzil case.[16,67] On the other hand, the decay of the E/A component is determined mainly by the spin-lattice relaxation of the radical. At lower temperatures, the contribution of the F-pair polarization increases. The decay is not single exponential because it is determined by a combination of the decays of the geminate pair and the F-pair RPM.

## 8-4. Conclusion

The CIDEP development mechanisms of the azaaromatic compounds,

quinoxaline, phenazine and quinoline are investigated in detail. It is shown that several polarization mechanism are involved and the dominant mechanism is strongly dependent on the concentration and temperature. The net emissive polarization is explained mainly by the RTPM between the produced radical and the precursor triplet. At a low concentration, the time evolution of the net component agrees with the prediction of the RTPM model, which indicates that the rise is determined by the spin-lattice relaxation rate and the decay is by the triplet lifetime. The RTPM usually gives a net E polarization of a slow rise and a slower decay compared with those of the TM and the geminate pair RPM, but at high concentrations the emissive polarizations are found to show fast rises. This may be due to triplet-triplet annihilation. For a more complete understanding of the polarization mechanisms, more precise analysis of the time developments of the polarizations are needed. The RTPM polarization plays an important role generally, when the concentrations of triplet states and radicals are high and triplet states are relatively long-lived.

# Summary

In the present thesis, the magnetic field dependencies of the TM and SCRP CIDEP were investigated in detail using three deferent frequency TREPR. The experimental results on the magnetic field dependence of the TM are explained well the prediction of the theory. The magnetic field dependence of the TM is very sensitive to the several conditions, therefore, its detailed studies are very useful for studying the environments and the reaction process of the radicals. The E/A line shape of the SCRP CIDEP signals is not influenced by the magnetic field. However the relaxation time of the SCRP depends on the magnetic field. The detailed analyses of the magnetic field dependence of the SCRP CIDEP would be useful to understand the relaxation process and the interaction of the SCRP.

The CW and FT TREPR studies of the spin and reaction dynamics were also presented. The photoreaction system of acetone with triethylamine, the quenching reaction of the 2-hydroxypropan-2-yl radical, and the CIDEP mechanisms observed in the photolysis of quinoxaline, phenazine, and quinoline in 2-propanol were discussed. These systems include the complicated processes of CIDEP mechanisms and reactions, which were analyzed qualitatively, and the spin and reaction dynamics are clarified.

# Acknowledgment

The author acknowledges Professor N.Hirota and Dr. M.Terazima. The author thanks Professor H.van Willigen and Dr. C.A.Steren ( University of Massachusetts at Boston ) for experiments and discussion of FT-EPR studies. The author thanks Dr. H. Murai ( Tohoku Univesity ).

# References


(1) Steiner, U. E.; Ulrich, T. *Chem. Rev.* **1989,** *89*, 51.

(2) Hayashi, H.; Nagakura, S. *Bull.Chem.Soc.Jpn.* **1984,** *57*, 322.

(3) Tanimoto, Y.; Fujiwara, Y.; Takamatsu, S.; Kita, A.; Itoh, M., Okazaki, M. *J.Phys.Chem.* **1992,** *96*, 9844.

(4) *Spin Polarization and Magnetic Field Effects in Radical Reactions*; Molin, Y. N., Ed.; Elsevier: Amsterdam, 1984.

(5) *Chemically Induced Magnetic Polarization*; Muus, L. M.; Atkins, P. W.; McLauchlan, K. A., Pedersen, J. B., Eds.; Reidel: Dordrecht, 1977.

(6) van Willigen, H.; Levstein, P. R.; Ebersole, M. H. *Chem.Rev.*, **1993** *93*, 173.

(7) Adrian, F. J. *J.Chem.Phys.* **1971,** *54* 3918; **1972,** *57*, 5107.

(8) Pedersen, J. B.; Freed, J. H. *J.Chem.Phys.* **1973,** *58* 2746; **1973,** *59*, 2869.

(9) Wong, S. K., Huchinson, D. A., Wan, J. K. S. *J.Amer.Chem.Soc.* **1973**, *95*, 622.

(10) Atkins, P. W., Evans, G. T. *Mol.Phys.* **1974,** *27*, 1633.

(11) Pedersen, J. B.; Freed, J. H. *J.Chem.Phys.* **1975,** *62*, 1706.

(12) Adrian, F. J.; Monchick, L. *J.Chem.Phys.* **1979,** *71*, 2600.

(13) Buckley, C. D., McLauchlan, K. A. *Chem.Phys.Lett.* **1987,** *137*, 86.

(14) Buckley, C. D.; Hunter, D. A., Hore, P. J.; McLauchlan, K. A. *Chem.Phys.Lett.* **1987,** *135*, 307.

(15) Closs, G. L.; Forbes, M. D. E.; Norris, J. R. *J.Phys.Chem.* **1987,** *91*, 3592.

(16) Blättler, C., Jent, F., Paul, H. *Chem.Phys.Lett.* **1990,** *166*, 375.

(17) Kawai, A.; Okutsu, T., Obi, K. *J.Phys.Chem.* **1991,** *95*, 9130.

(18) Kawai, A.; Obi, K. *J.Phys.Chem.* **1992,** *96*, 5701; *Res.Chem.Intermed.* **1993,** *19*, 866.

(19) Forbes, M. D. E. *J.Phys.Chem.* **1992,** *96*, 7836.

(20) Forbes, M. D. E.; Ruberu, S. R. *J.Phys.Chem.* **1993,** *97*, 13223.

(21) Terazima, M.; Hayakashi, S.; Azumi, T. *J.Phys.Chem.* **1991,** *95*, 4297.

(22) Terazima, M.; Miura, Y.; Ohara, K.; Hirota, N. *Chem.Phys.Lett.* **1994,** *224*, 95.

(23) Yamauchi, S., Hirota, N. *J. Phys. Chem.* **1984** *88*, 4631.

(24) Ohara, K., Terazima, M., Hirota, N. *J.Phys.Chem.* **1995**, in press.

(25) Levstein, P. R.; van Willigen, H. *J. Chem. Phys.* **1991** *95*, 900.

(26) Bent, D. V.; Hayon, E.; Moorthy, P N. *Chem.Phys.Lett.* **1974,** *27*, 544; *J.Am.Chem.Soc.* **1975,** *97*, 5065.

(27) Basu, S.; McLauchlan, K. A., Sealy, G. *Chem. Phys. Lett.* **1982** *88*, 84.

(28) Plüschau, M.; Zahl, A., Dinse, K. P.; van Willigen, H. *J.Chem.Phys.* **1989,** *90*, 3153.

(29) Ebersole, M.; Levstein, P. R.; van Willigen, H. *J.Phys.Chem.* **1992,** *96*, 9310.

(30) Yamauchi, S., Ueda, T.; Satoh, M.; Akiyama, K.; Tero-Kubota, S.; Ikegami, Y.; Iwaizumi, M. *J.Photochem.Photobiol.A:Chem.* **1992,** *65*, 177.

(31) Ohara, K.; Murai, H.; Kuwata, K. *Bull.Chem.Soc.Jpn.* **1992,** *65*, 1672.

(32) Scherz, A.; Levanon, H. *J.Phys.Chem.* **1980,** *84*, 324.

(33) Iwaizumi, M.; Yamamoto, K., Ohba, Y.; Yamauchi, S. *Coord.Chem.Rev.* **1994**, *132*, 29; unpublished data(private communication).

(34) Burland, D. M.; Schmidt, J. *Mol.Phys.* **1971,** *22*, 19.

(35) Yamauchi, S.; Pratt, D. W. *Mol.Phys.* **1979,** *37*, 541.

(36) Ishiwata, N.; Murai H.; Kuwata, K. *Res.Chem.Intermed.* **1993,** *19*, 59.

(37) Pedersen, J. B., Shushin, A. I., Jorgensen, J. S. *Chem.Phys.* **1994,** *189*, 479.

(38) Shushin, A. I., Pedersen J. B., Lolle, L. I. *Chem.Phys.* **1994,** *188*, 1.

(39) Terazima, M.; Maeda, K.; Azumi, T., Tanimoto, Y.; Okada, N.; Itoh, M. *Chem.Phys.Lett.* **1989,** *164*, 562.

(40) Murai, H.; Honma, H.; Kuwata, K. *Res.Chem.Intermed.* **1993,** *19*, 103.

(41) Yamauchi, S., Tominaga, K., Hirota, N. *J. Phys. Chem.* **1986**, *90*, 2367.

(42) Tominaga, K.; Yamauchi, S.; Hirota, N. *Chem.Phys.Lett.* **1988**, *149*, 32.

(43) Levstein, P R., van Willigen, H. *Chem.Phys.Lett.* **1991**, *187*,415.

(44) Paul, H. *Chem. Phys.* **1979**, *40*, 265; **1979**, *43*, 294.

(45) Wong, S. K., Chui, T. M.; Bolton, J. R. *J. Phys. Chem.* **1981**, *85*, 12.

(46) Basu, S., Grant, A. J., McLauchlan, K. A. *Chem. Phys. Lett.* **1983**, *94*, 517.

(47) Tominaga, K., Yamauchi, S.; Hirota, N. *J. Chem. Phys.* **1988**, *88*, 553; **1990**, *92*, 5175.

(48) McLauchlan, K. A.; Simpson, N. J. K., Smith, P D. *Res. Chem. Intermed.* **1991**, *17*, 141.

(49) I. A. Shkrob and J. K. S.Wan, *Res. Chem. Intermed.* **1992**, *17*, 77

(50) Batchelor, S. N., Kay, C. W. M.; McLauchlan, K. A., Smith, P. D.; Yeung, M. T. *Mol. Phys.* **1994**, *82*, 325.

(51) Tominaga, K.; Yamauchi, S.; Hirota, N. *J. Phys. Chem.* **1988**, *92*, 5160.

(52) Tominaga, K.; Yamauchi, S., Hirota, N. *J. Phys. Chem.* **1990**, *94*, 4425.

(53) Moorthy, P.N.; Hayon, E. *J.Phys.Chem.* **1974**, *78*, 2615.

(54) Terazima, M., Hirota, N. *J.Chem.Phys.* **1993**, *98*, 6257.

(55) Terazima, M., Okamoto, K.; Hirota, N. *J.Phys.Chem.* **1993**, *97*, 5188.

(56) McLauchlan, K. A. Chapt.7, "*Modern Pulsed and Continuous-Wave Electron Spin Resonance*", Kevan, L.; Bowman, M. K., Eds. John Wiley & Sons, New York **1990**.

(57) Ohara, K.; Hirota, N., Steren, C. A., van Willigen, H. *Chem.Phys.Lett.* **1995**, *232*, 169.

(58) McLauchlan, K. A.; Simpson, N. J. K. *Chem.Phys.Lett.* **1989**, *154*, 550.

(59) Akiyama, K.; Depew, M.C.; Wan, J. K. S. *Res.Chem.Intermed.* **1989**, *11*, 25.

(60) de Groot, M. S.; Hesselmann, I. A. M.; Schmidt, J.; van der Waals, J. H. *Mol.Phys.* **1968**, *15*, 19.

(61) Schmidt, J., Artheunis, D. A.; van der Waals, J. H. *Mol.Phys.* **1971**, *22*, 1.

(62) Ohara, K.; Hirota, N.; Steren, C. A., van Willigen, H. *J.Phys.Chem.* in press.

(63) Fujisawa, J.; Ishii, K.; Oba, H.; Iwaizumi, M., Yamauchi, S. *J.Phys.Chem.* in press.

(64) Goudsmit, G. -H.; Paul, H. *Chem.Phys.Lett.* **1993**, *208*, 73.

(65) Shushin, A. I. *Chem.Phys.Lett.* **1993,** *208*, 173.

(66) Goudsmit, G. -H.; Paul, H.; Shushin, A. I. *J.Phys.Chem.* **1993,** *97*, 13243.

(67) Mukai, M., Yamauchi, S.; Hirota, N. *J.Phys.Chem.* **1992** *93*, 4411; **1992** *96*, 2179.